NASA CONTRACTOR REPORT

NASA CR-334

INVESTIGATIONS OF ELECTRON INTERACTIONS WITH MATTER

PART 1. BREMSSTRAHLUNG PRODUCTION IN ALUMINUM AND IRON

by William E. Dance and Leo L. Baggerly

PART 2. ELECTRON SCATTERING IN ALUMINUM

by David H. Rester and Walter J. Rainwater, Jr.

INVESTIGATIONS OF ELECTRON INTERACTIONS WITH MATTER

PART 1.   BREMSSTRAHLUNG PRODUCTION

IN ALUMINUM AND IRON

By William E. Dance and Leo L. Baggerly

PART 2.   ELECTRON SCATTERING IN ALUMINUM

By David H. Rester and Walter J. Rainwater, Jr.

TABLE OF CONTENTS

Part 1.

BREMSSTRAHLUNG PRODUCTION IN ALUMINUM AND IRON

by William F. Dance and Leo L. Baggerly

BREMSSTRAHLUNG PRODUCTION IN ALUMINUM AND IRON

INTRODUCTION

Experimental studies at LTV under Contract NASw-948 are concerned with measurements of the bremsstrahlung produced and the electrons scattered when various materials are bombarded with monoenergetic electrons. This work was initiated under Contract NASw-647, during which data were obtained which describe pertinent characteristics of the bremsstrahlung: spectral distribution and angular distribution. Bremsstrahlung intensities differential in photon energy and angle were measured from thick targets of aluminum, and differential cross section measurements were initiated for thin targets of aluminum under that contract. The electron bombarding energy ranged from 0.5 MeV to 3.0 MeV. Work during the past year has been an extension of these studies to include bremsstrahlung measurements for targets of other materials.

During the first two quarters of this period the bremsstrahlung work included measurement of thick target intensities from targets of aluminum and iron at photon angles from 0 to 150 deg in the electron energy range 0.5 to 3.0 MeV. During the third quarter the study consisted of further analysis of the thick target data and resumption of the experimental measurement of thin target differential cross sections. The thick target data analysis included partial correction for photon absorption in targets with thicknesses greater than the electron range, and empirical curve fitting to the experimental intensities. Thin target differential cross sections were determined for aluminum at two bombarding energies and three angles, for comparison with past measurements at the National Bureau of Standards. In

the last quarter, measurements were made at photon angles from 0 through
20 deg at 5 deg intervals, and earlier measurements were repeated at 30, 45,
and 60 deg for aluminum, for incident electron energies 0.5, 1.0, and 2.0
MeV. Analysis of intensity data taken for iron and gold at the above-men-
tioned angles for incident electron energies 1.0 and 2.0 MeV is currently
in progress.

Efforts during the past year to improve the characteristics of the
electron beam from the Van de Graaff accelerator have resulted in a well-
collimated beam which can be focused to a spot size less than 2 mm in di-
ameter. Mapping of the region around the bremsstrahlung target holder by
means of a solid state detector, which is a highly sensitive method for
observing any electrons which might possibly be scattered from the holder,
indicated that the amount of "halo" around the beam, if any, was negligible.
The improvement in this property of the beam made possible the resumption
of the thin target differential cross section measurements initiated earlier
in this laboratory.

EXPERIMENTAL PROCEDURE

The experimental arrangement for the bremsstrahlung measurements of the present study is shown schematically in Figure 1. The electron beam from the LTV Van de Graaff accelerator impinges at normal incidence on the target positioned at the center of an evacuated cylindrical chamber, 12 inches in diameter and approximately 14 inches high. The bremsstrahlung radiation produced at the target and emerging at an angle θ to the incident beam direction passes through a thin window in the chamber wall, through a lead collimator, and then through a defining aperture in a three-inch thick lead sheath which encloses the scintillation spectrometer. In front of the detector a permanent magnet is provided for the purpose of sweeping out any electrons which are scattered into the solid angle of acceptance of the detector.

Targets are mounted on a vertical shaft which can be driven remotely for positioning of either the target or a zinc sulfide viewer into the beam. The positions of the target and electron beam spot are observed by a television monitor. Windows in the cylindrical chamber are of .005 inch mylar, bonded to the outside of the chamber wall. With these windows, absorption of the bremsstrahlung is less than one percent at photon energies above 20 keV. The electron beam enters the chamber through a 1/4" carbon aperture.

The early thick target data were taken with the targets placed in the evacuated cylindrical chamber as previously described. To increase the number of small angles which are accessible to the detector the system was modified to allow the target discs to terminate the evacuated electron
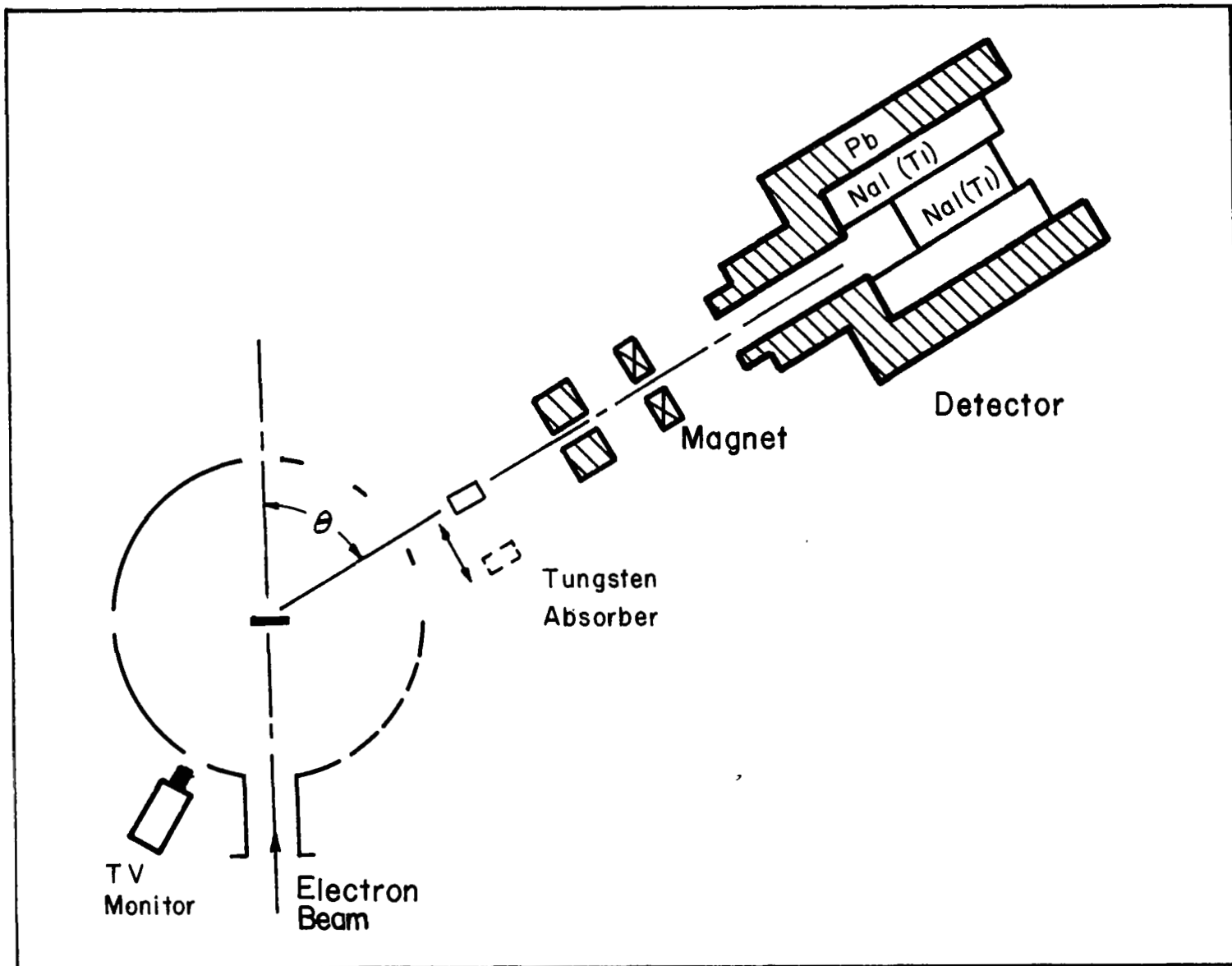
Figure 1.   Schematic of the experimental arrangement.

drift tube. This procedure leaves a continuous range of angles from 0 deg to 60 deg accessible for bremsstrahlung observation. In the case of the thinner targets, suitable adaptors were fabricated to allow use of small diameter targets which support the atmospheric pressure. Target thicknesses in each case were chosen so as to present to the electron beam a thickness of material equal to or greater than the maximum range of the electrons.

The target chamber is isolated electrically from the electron beam tube and from the chamber support stand, to enable one to integrate the total electron current delivered to the target and the chamber, and thus to determine the number of electrons incident on the target during a run. Currents in the range 10^{-9} to 10^{-7} ampere in this experiment were measured with a current integrator. In the range from below 10^{-11} to 10^{-9} ampere, currents were measured with an electrometer, the output of which was fed into the integrator. A third method of current integration used was to charge a known capacitance to a specified voltage measured by the electrometer.

The target-to-detector distance is 98.1 cm, so that with a 1/2 inch-defining aperture the detector subtends a solid angle of 1.31×10^{-4} steradian. The spectrometer carriage can be rotated through angles ranging from 0 deg to 150 deg with the target as center. Figure 2 shows schematically the spectrometer and its output arrangement. The scintillation detector is a 2.32-inch diameter by 6 inch long NaI(Tl) crystal surrounded by an annulus of NaI(Tl), the annulus being operated in anticoincidence with the center crystal. Thus only those pulses from the center crystal which are not accompanied by coincident pulses in the surrounding annulus are accepted for analysis. This dual crystal arrangement effectively removes a substantial portion of the low-energy part of the detector line shape which is due
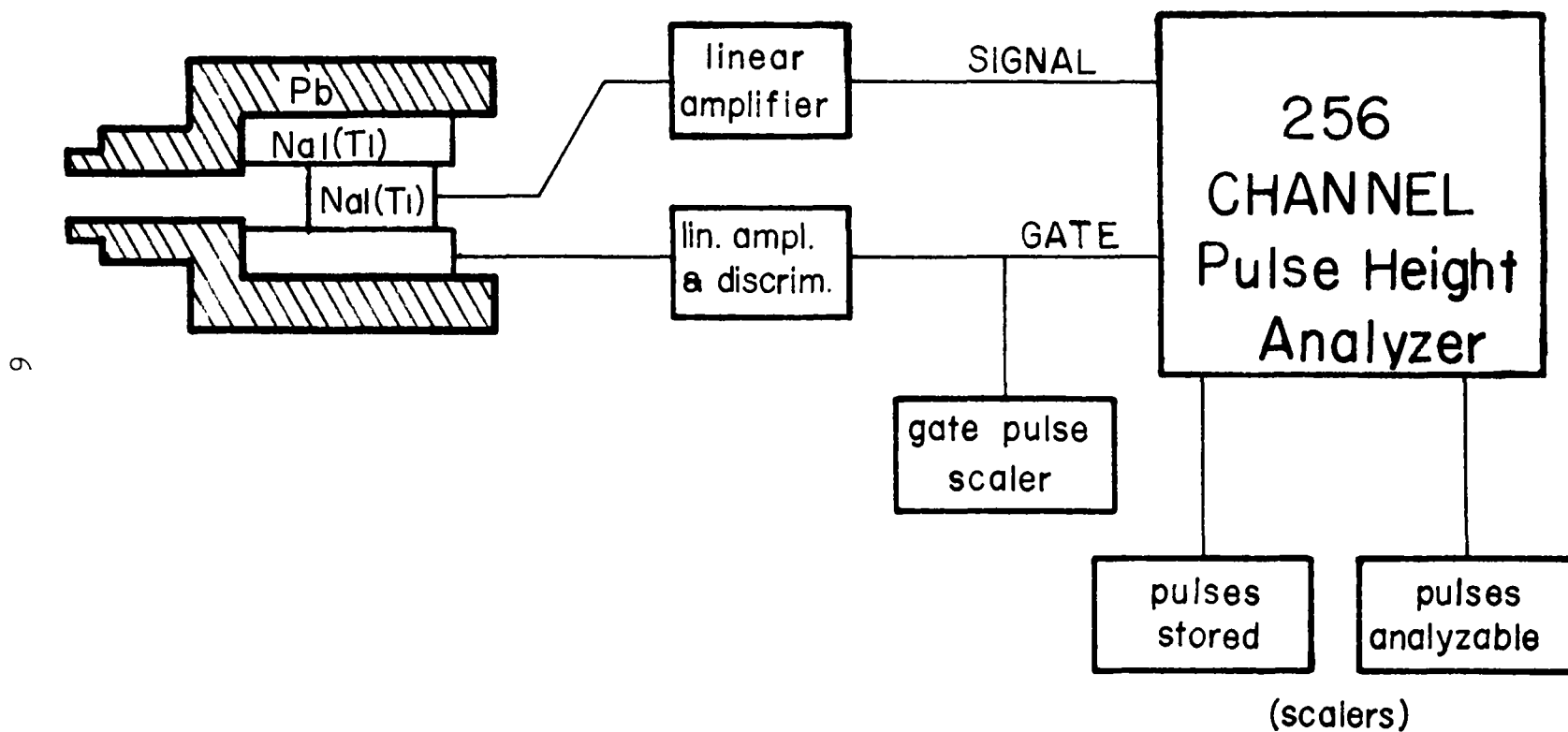
5

Figure 2. Block diagram of spectrometer and associated circuitry.

to Compton scattering and other partial absorption processes in the center crystal. The response of the detector to monoenergetic gamma rays in the energy range of interest is well approximated by a Gaussian photopeak and a trapezoidal low-energy tail. A 7090 computer program was written to remove this response from the pulse height distributions to yield the final spectra. The energy calibration and the efficiency of the detector were determined experimentally using various standard gamma ray sources having energies ranging from .279 MeV (Hg^{203}) to 2.754 MeV (Na^{24}). The photopeak efficiency is about .94 at 200 keV and decreases to approximately .25 at 3.00 MeV.

Energy calibration of the electron beam from the accelerator was performed using lithium drift silicon detectors prepared in this laboratory. These detectors were used to count the electrons scattered by thin foils inserted into the electron beam. Energy calibration of the detectors was achieved by reference to the 625 keV internal conversion electron line from Cs^{137} and the 482 keV, 972 keV and 1.68 MeV lines of Bi^{207}. The accelerator potential was measured with a generating voltmeter and read by a vacuum tube voltmeter. The accuracy of the beam energy determination is estimated to be ± 15 keV.

The procedure used in making a typical data run to obtain a bremsstrahlung spectrum for a given electron energy T_o and photon angle θ involves the following steps:

1. Accumulation of the main pulse height distribution: Pulses corresponding to photons absorbed in the center crystal are amplified and fed to a 256-channel pulse height analyzer (Figure 2). The amplified signal from the

7

annulus serves to gate off the analyzer for maximum reduction in background. The analyzer live time is determined by the ratio of the number of pulses stored in the memory to the number arriving at the analyzer with pulse height between the lower and upper level discriminator levels, as counted by two fast scalers. In each run counts are accumulated for a fixed total charge of electrons on target, consistent with reasonable counting statistics.

2. Background run: A background spectrum is accumulated by inserting a remotely operated tungsten absorber between the target and the detector and observing the counts for one-half the total fixed charge of the main spectrum. The diameter of the absorber was chosen so as to shield only the target from the detector, leaving exposed to the detector all background producing areas within its acceptance angle.

3. Background subtraction: The background data are subtracted from the main pulse height data after correcting each group of data for analyzer live time and normalizing the background run to the total charge of the main spectrum.

Several times during each day of runs a detector energy calibration spectrum is accumulated and recorded as a part of each run in order to allow a correction for gain shift in the spectrometer during the day. This calibration spectrum, along with the main spectrum, the background spectrum, the total charge, and the live time correction factor, are input data peculiar to each individual run, for the 7090 computer program used to calculate the spectral intensities.

The 7090 computer program was used to compute the following quantities:

1. Bremsstrahlung spectral intensities differential in photon energy

and solid angle, k dn/dkdΩ, for each value of Θ and each electron energy T_o.

2. Differential yields, dn/dkdΩ.

3. For thin targets, differential cross sections (k/Z^2) (dσ/dkdΩ).

4. Spectral intensities integrated over photon angle Θ, giving k dn/dk, for each energy T_o, with or without correction for absorption in the thickness of material in excess of the mean electron range.

5. Total intensities (integrated over photon angle and energy) ∫ k dn/dk, for each electron energy T_o.

EXPERIMENTAL RESULTS

The experimental intensity spectra, differential in photon energy and angle, for thick targets of aluminum and iron in the electron energy range 0.5 MeV to 3.0 MeV are presented in Figures 3 through 20.

For every case except the 90 deg spectra, the electron beam was incident normally on the target. The 90 deg spectra were taken with the beam at 45 deg incidence on the target, with the spectrometer viewing the target from the same side as the incoming beam. Target thicknesses were as specified in the figures. The differential spectra presented here are those observed from the specified thickness of material without correction for photon absorption in the target. The first group of curves, Figures 3 through 12, shows the energy dependence of the bremsstrahlung production, while the second group, Figures 13 through 20, exhibits the angular dependence of the spectra at the specified incident electron energies. In all cases the intensity spectra are smoothly decreasing functions of the photon energy.

The spectra integrated over photon angle are given for aluminum and iron in Figures 21 and 22, respectively, as a function of incident electron energy T_o. These curves were obtained by integrating the spectra for 0, 2.5, 15, 20, 30, 45, 60, 90, 120, and 150 deg. The integration was carried out over the photon energy range 0 to T_o. The low energy portion of the spectrum was determined in each case by extrapolating the differential spectra to zero below the detector cut-off energy. The integrated intensities are corrected for photon absorption in that portion of the target material which is in excess of one mean range. Inasmuch as the bremsstrahlung production is peaked at small angles, recent spectra taken in the modified
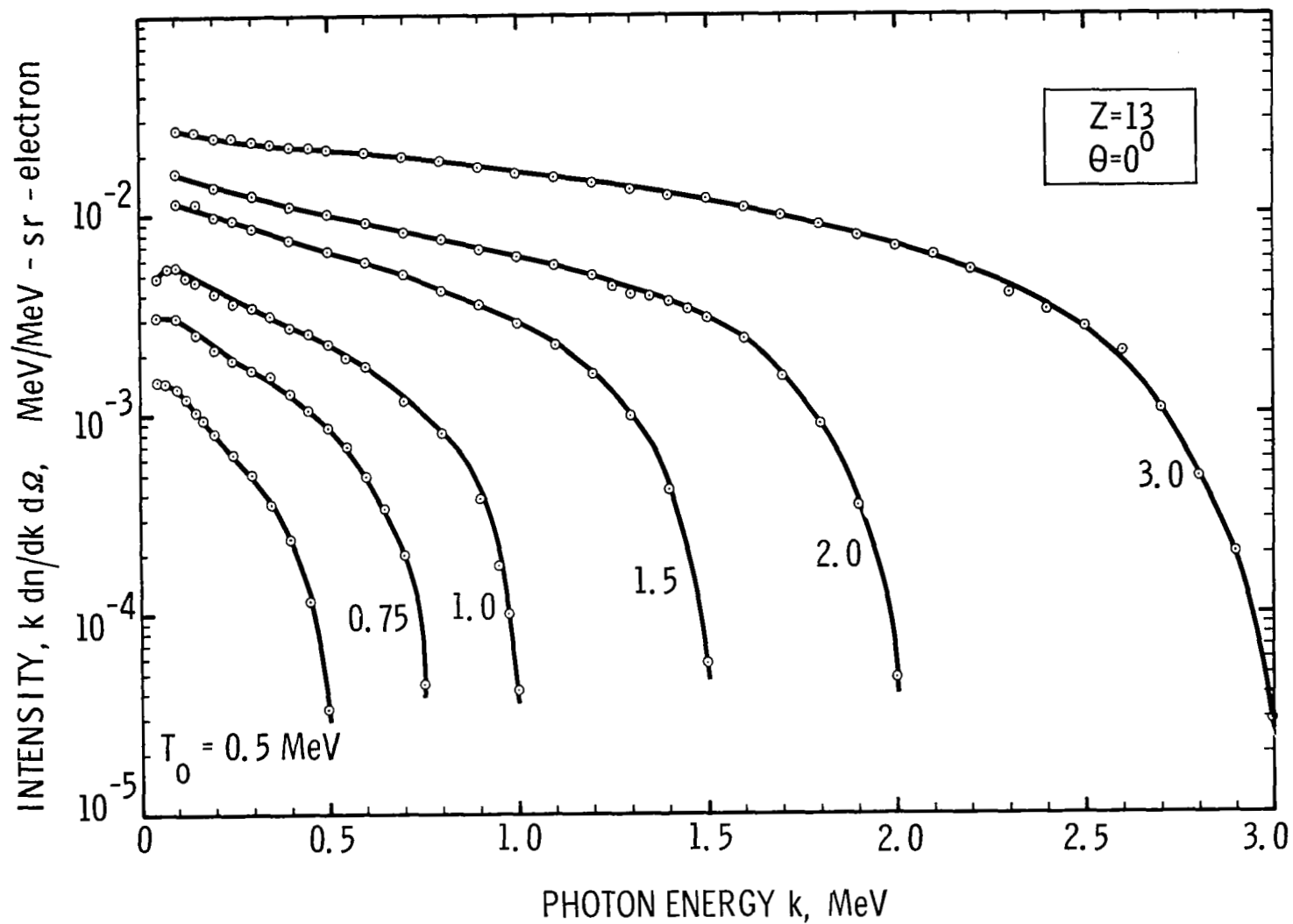
Figure 3. Bremsstrahlung intensity at 0 deg from thick aluminum targets, for incident electron energies ranging from 0.5 to 3.0 MeV.
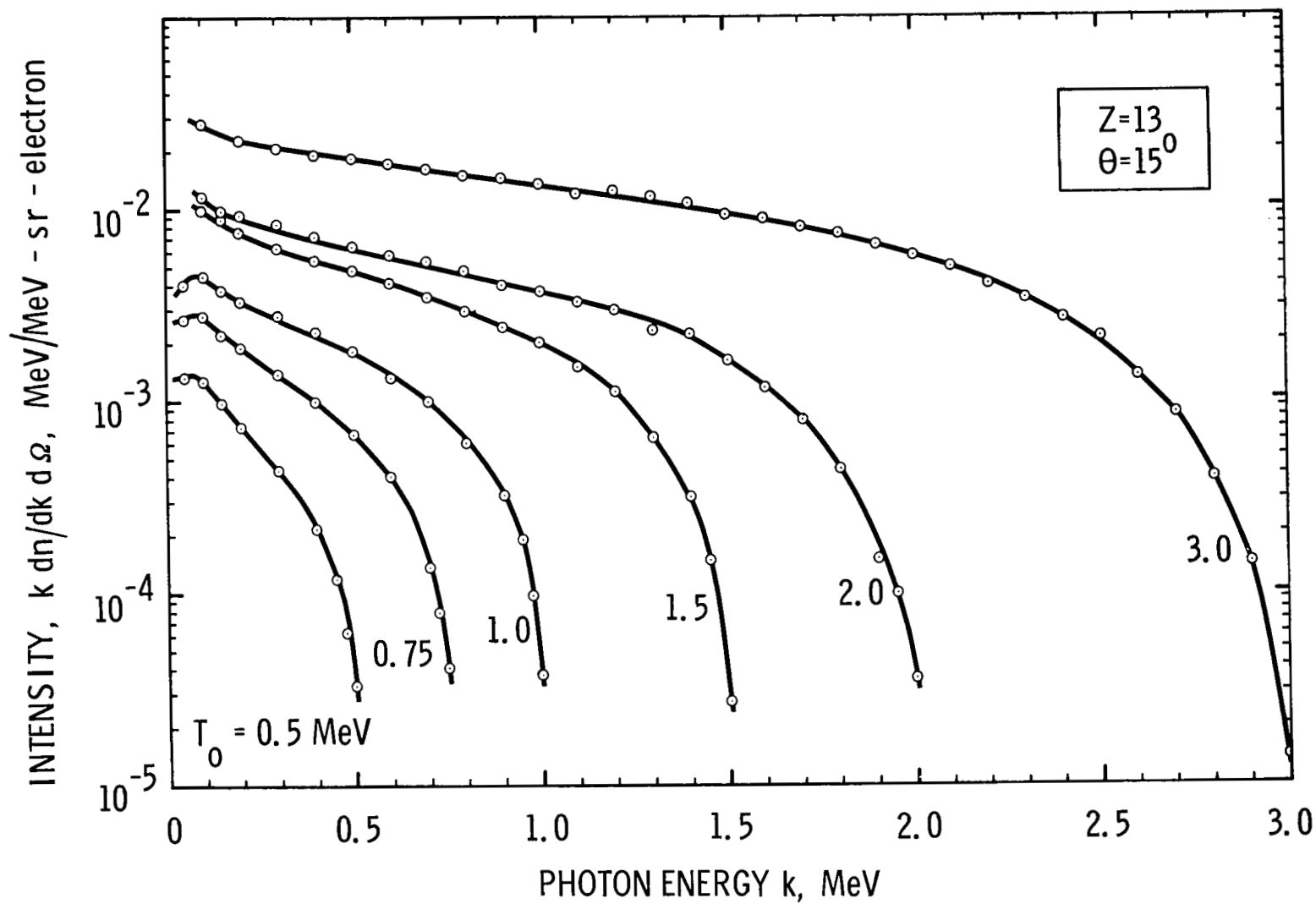
Figure 4. Bremsstrahlung intensity at 15 deg from thick aluminum targets, for incident electron energies ranging from 0.5 to 3.0 MeV.
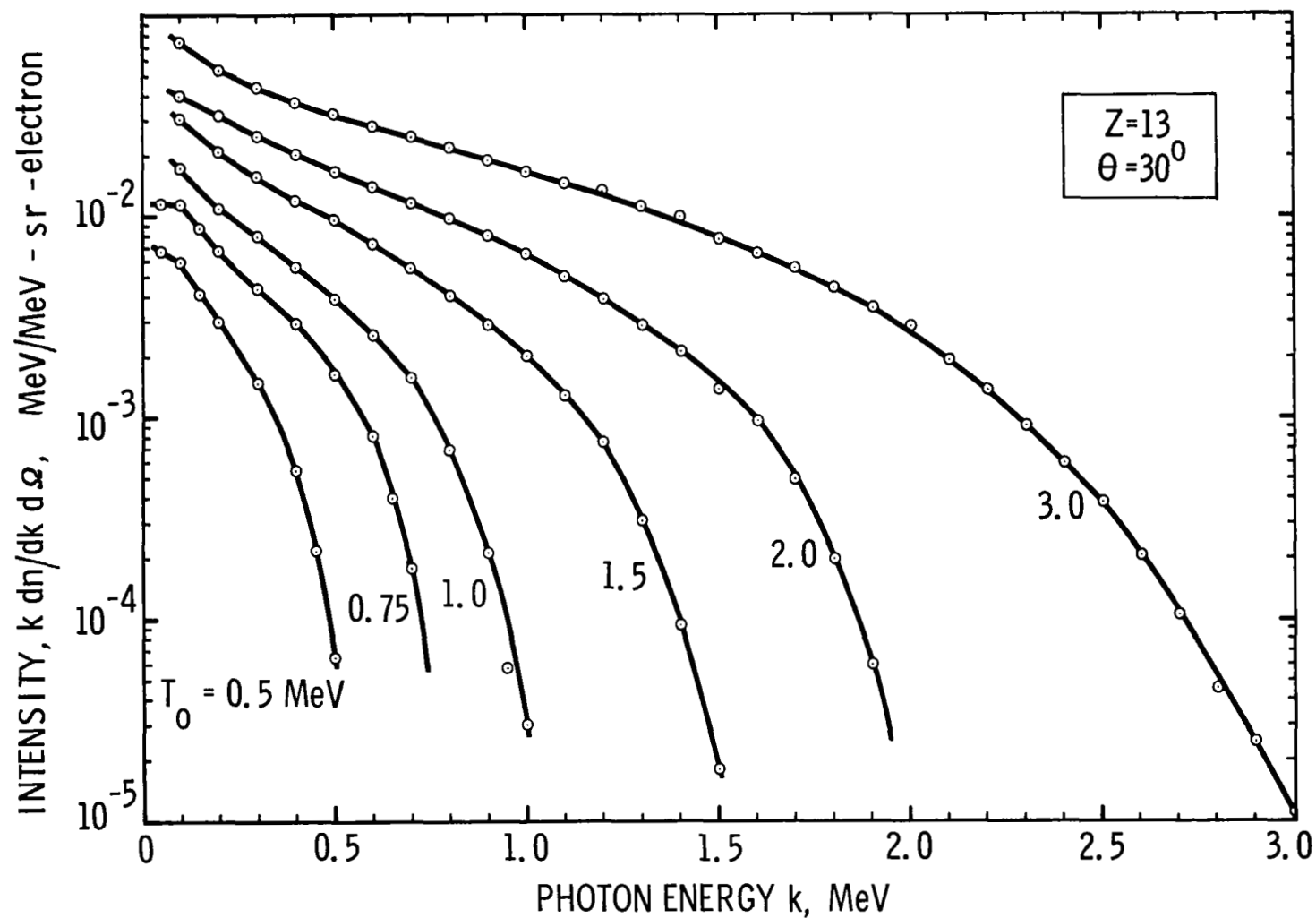
Figure 5. Bremsstrahlung intensity at 30 deg from thick aluminum targets, for incident electron energies ranging from 0.5 to 3.0 MeV.
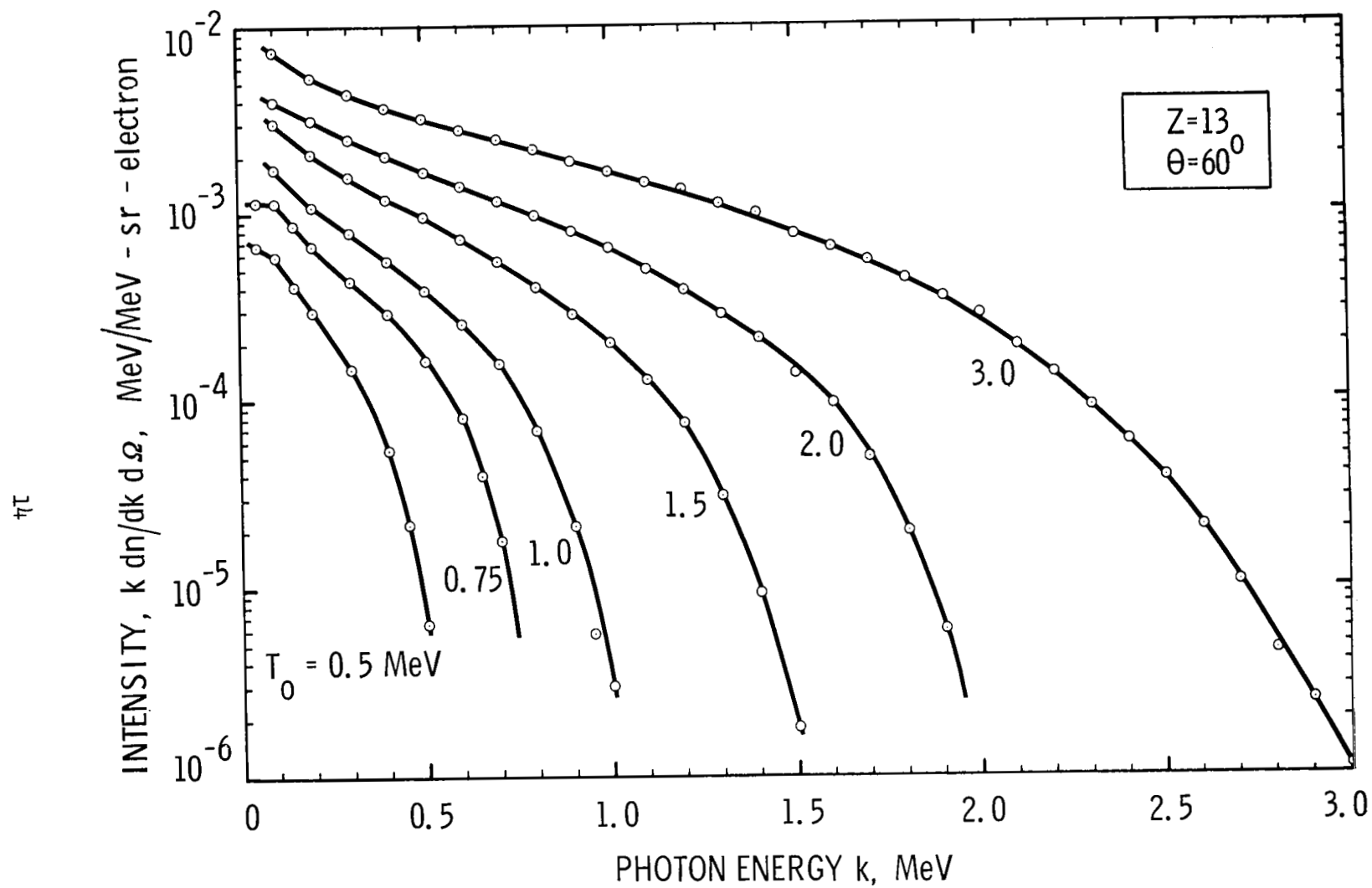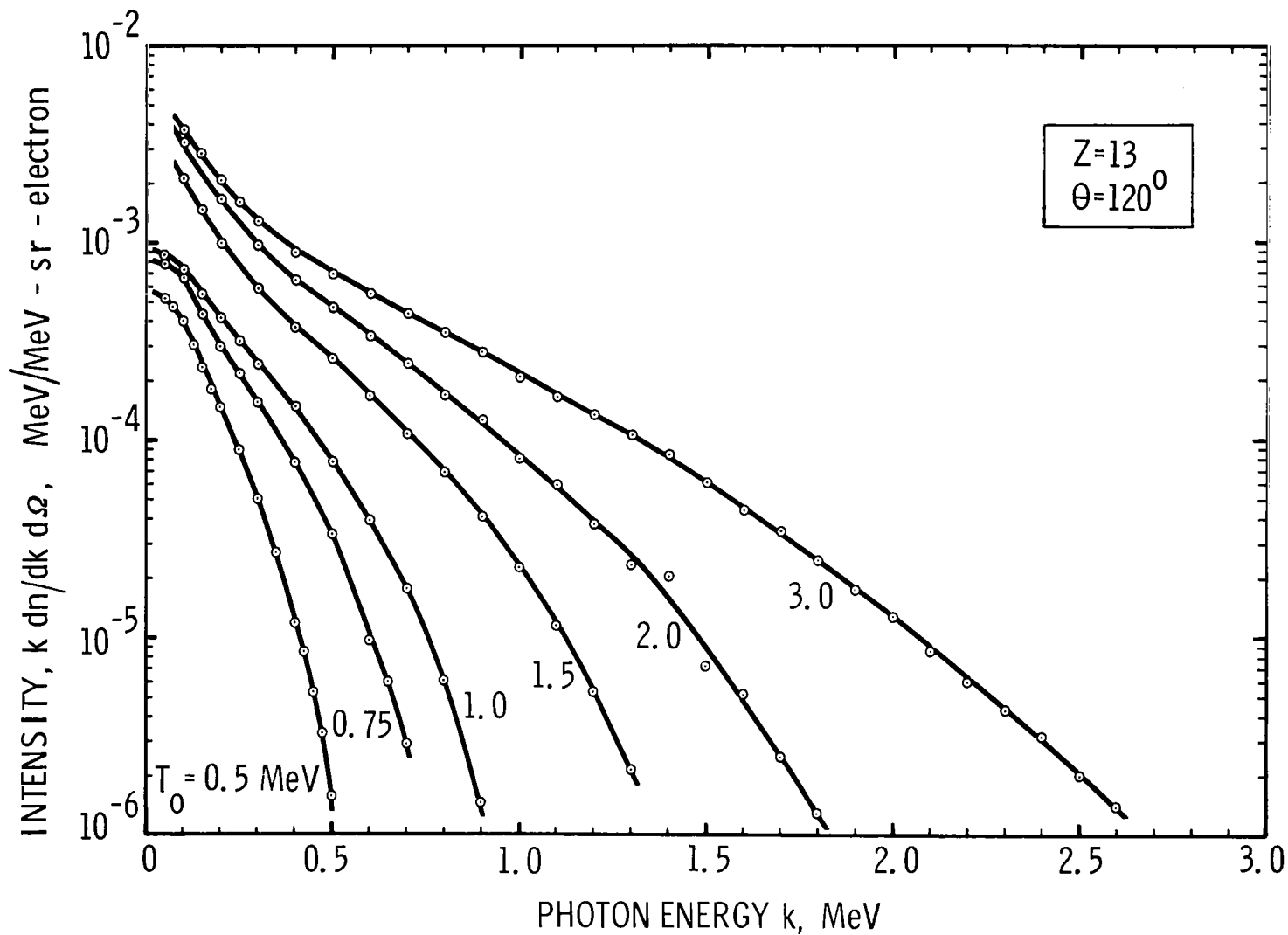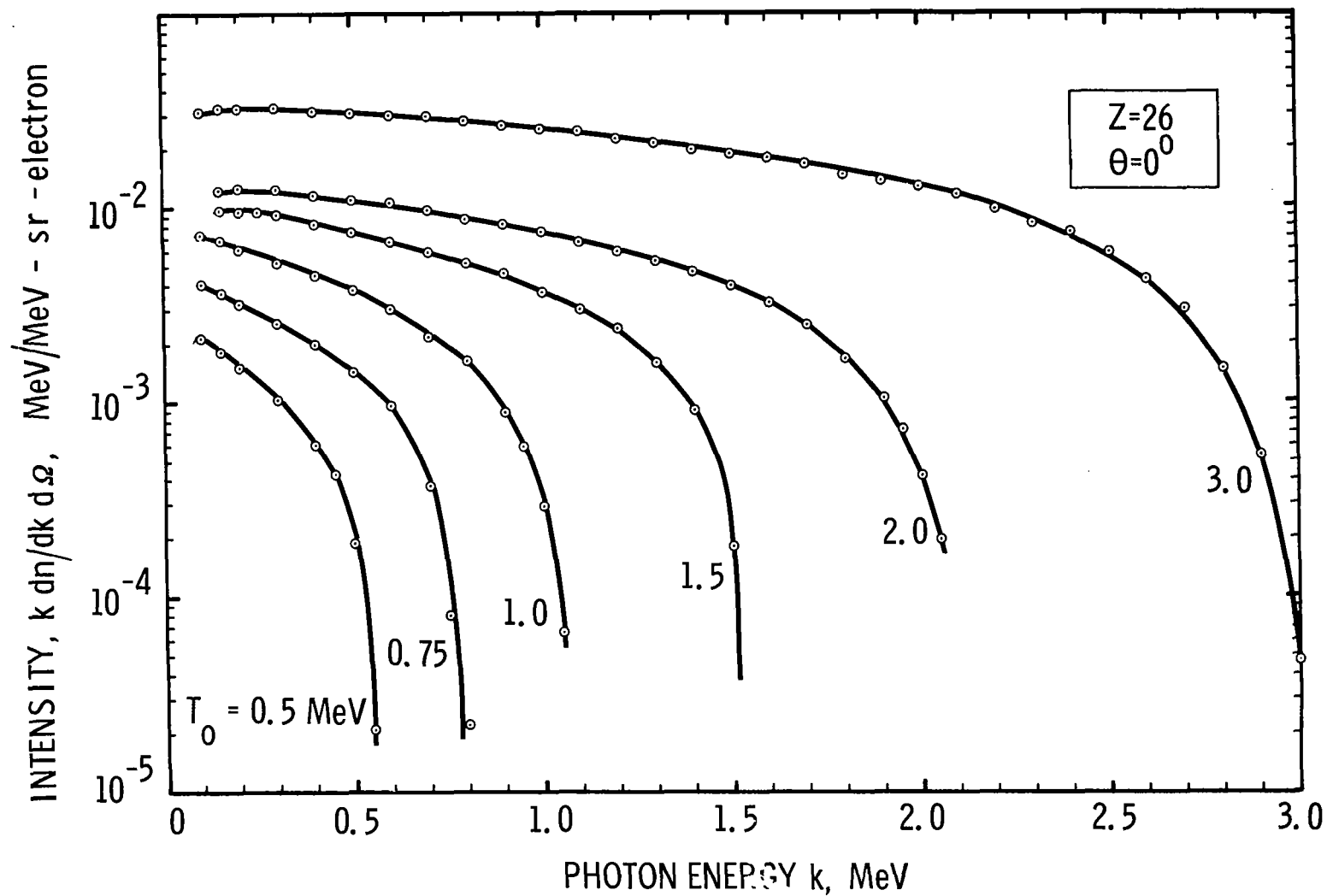
Figure 6. Bremsstrahlung intensity at 60 deg from thick aluminum targets, for incident electron energies ranging from 0.5 to 3.0 MeV.

Figure 7. Bremsstrahlung intensity at 120 deg from thick aluminum targets, for incident electron energies ranging from 0.5 to 3.0 MeV.

Figure 8. Bremsstrahlung intensity at 0 deg from thick iron targets, for incident electron energies ranging from 0.5 to 3.0 MeV.
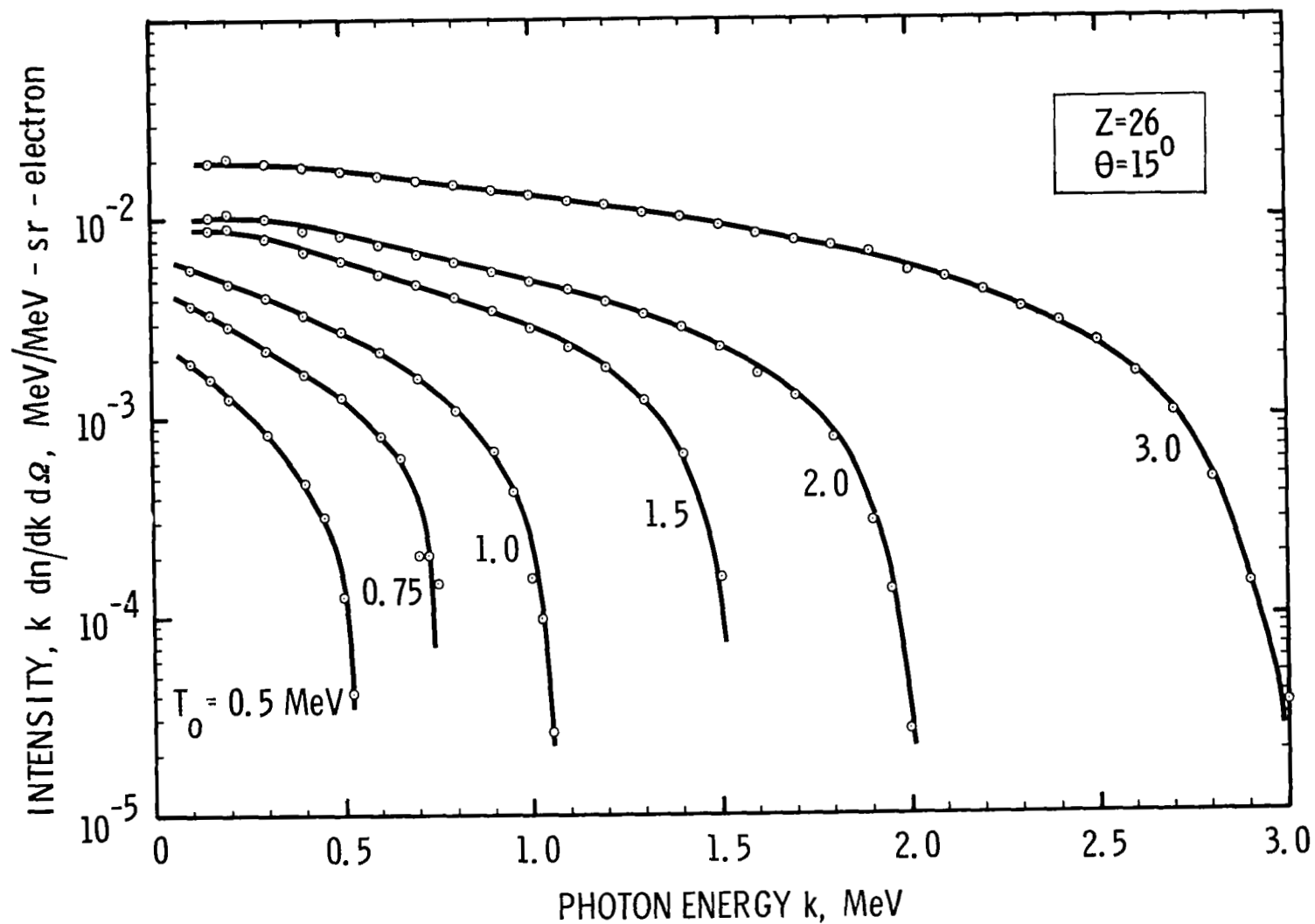
Figure 9. Bremsstrahlung intensity at 15 deg from thick iron targets, for incident electron energies ranging from 0.5 to 3.0 MeV.
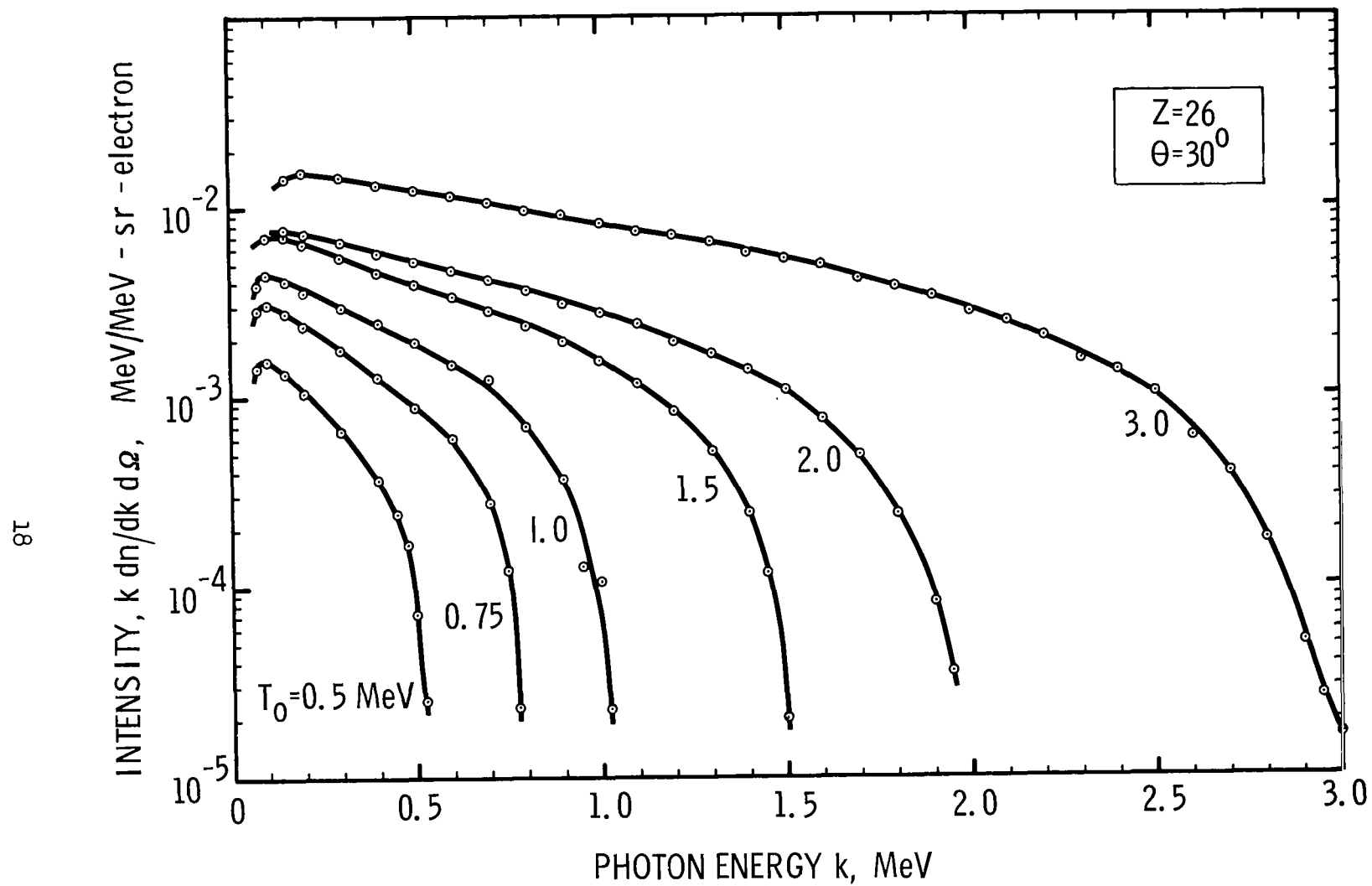
Figure 10. Bremsstrahlung intensity at 30 deg from thick iron targets, for incident electron energies ranging from 0.5 to 3.0 MeV.
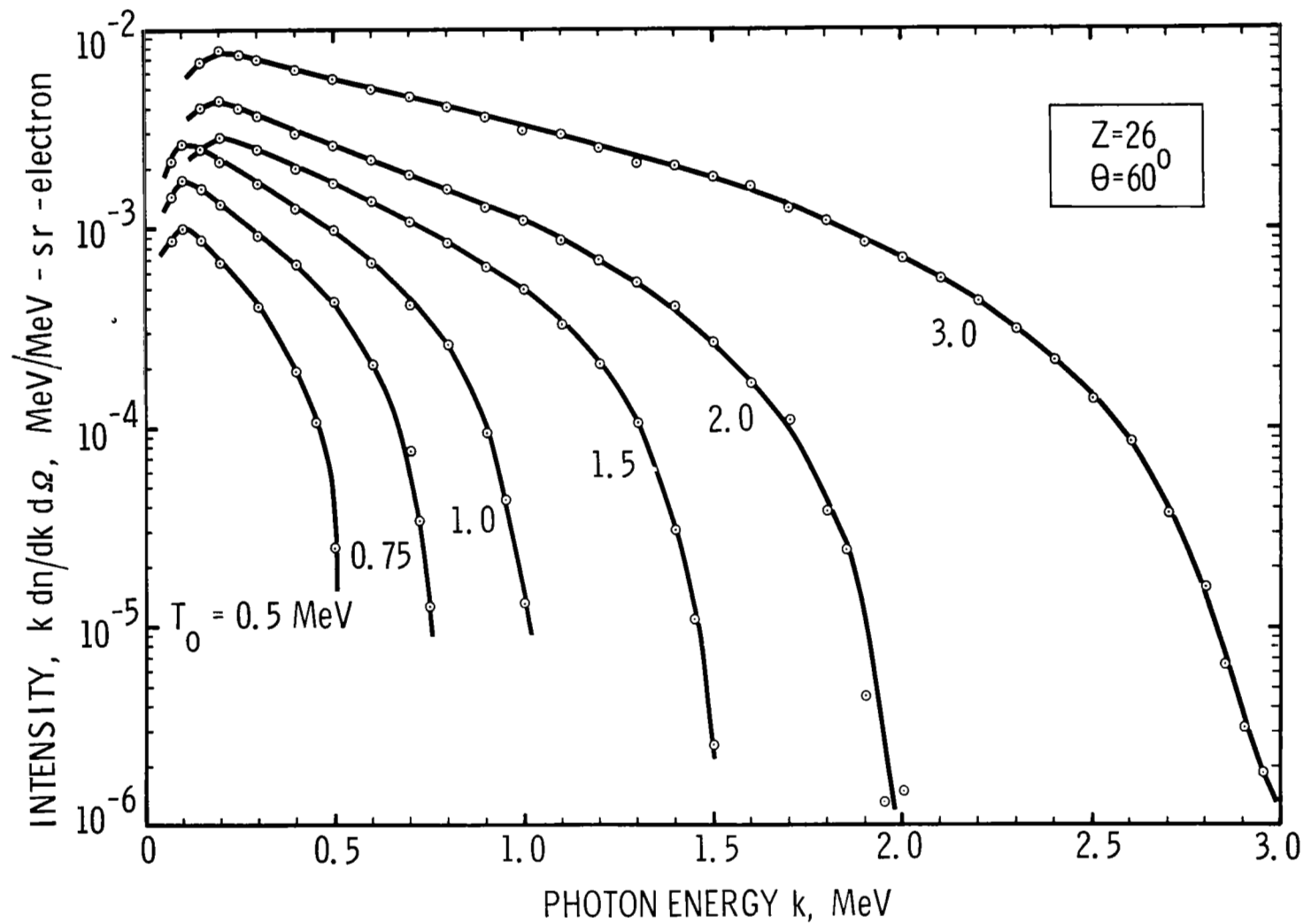
Figure 11. Bremsstrahlung intensity at 60 deg from thick iron targets, for incident electron energies ranging from 0.5 to 3.0 MeV.
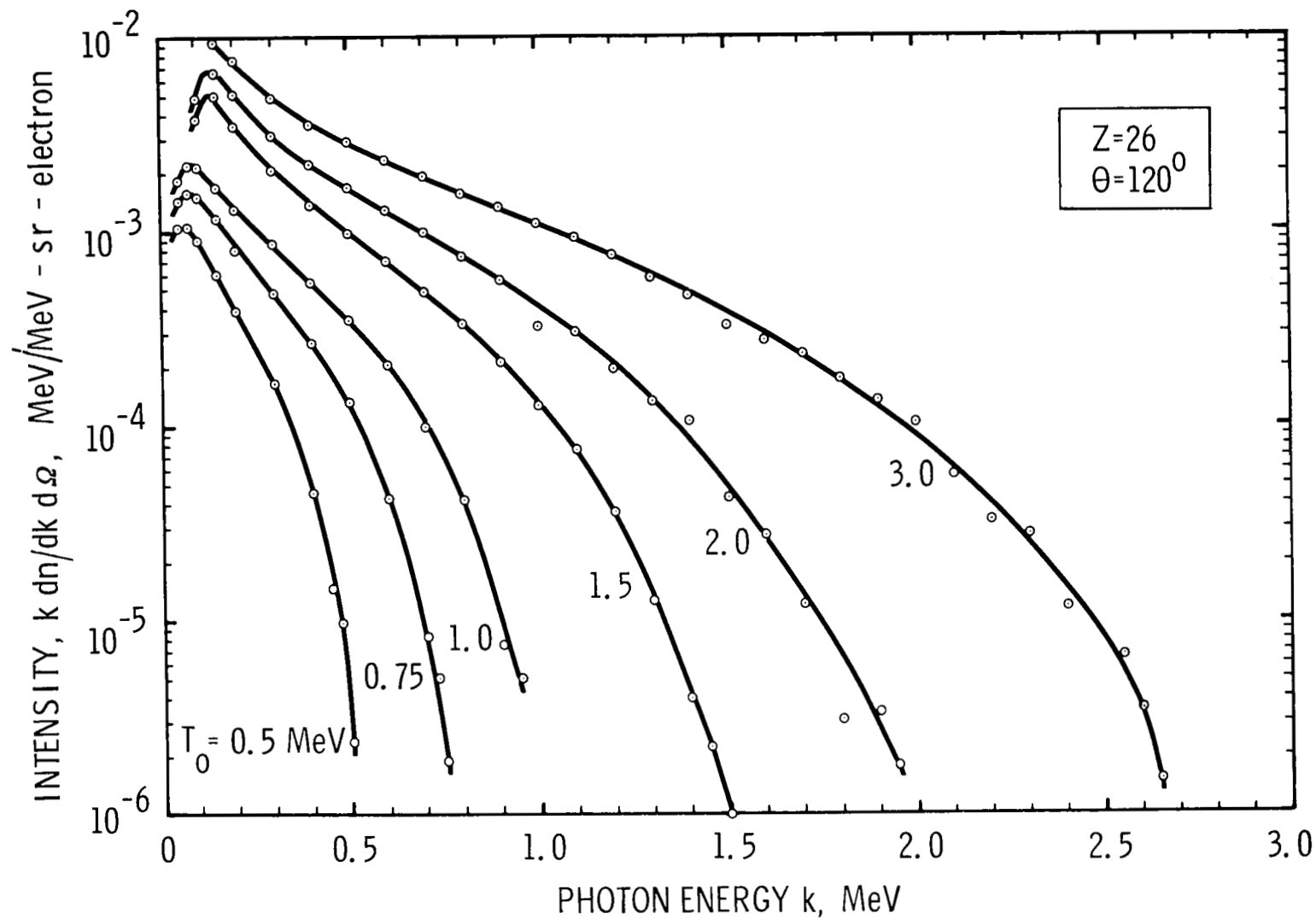
Figure 12. Bremsstrahlung intensity at 120 deg from thick iron targets, for incident electron energies ranging from 0.5 to 3.0 MeV.
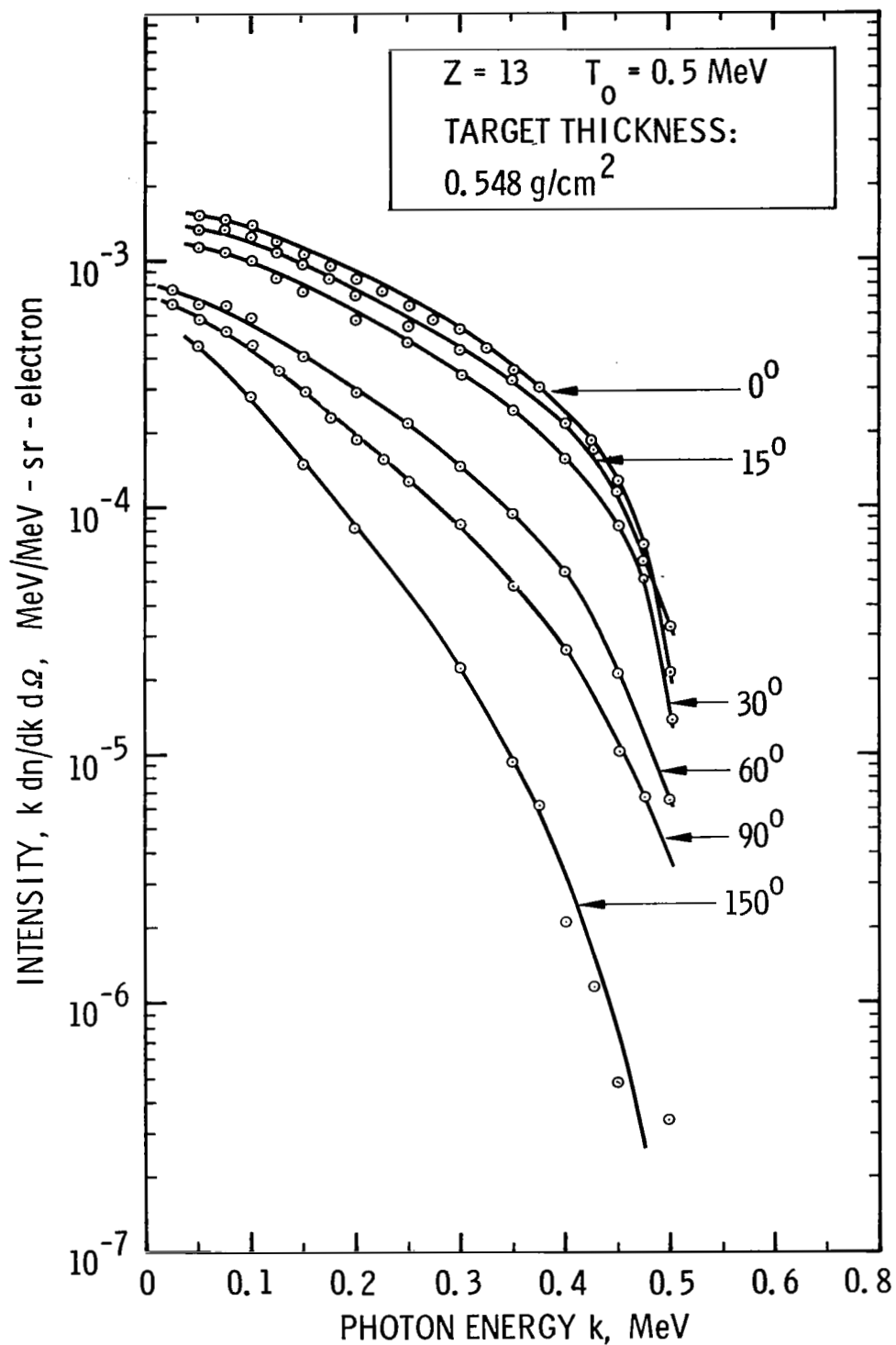
Figure 13. Bremsstrahlung intensity measured at angles ranging from 0 deg to 150 deg, for 0.5 MeV electrons incident on a thick aluminum target.

Figure 14. Bremsstrahlung intensity measured at angles ranging from 0 deg
to 150 deg, for 1.0 MeV electrons incident on a thick aluminum target.

Figure 15. Bremsstrahlung intensity measured at angles ranging from 0 deg to 150 deg, for 2.0 MeV electrons incident on a thick aluminum target.
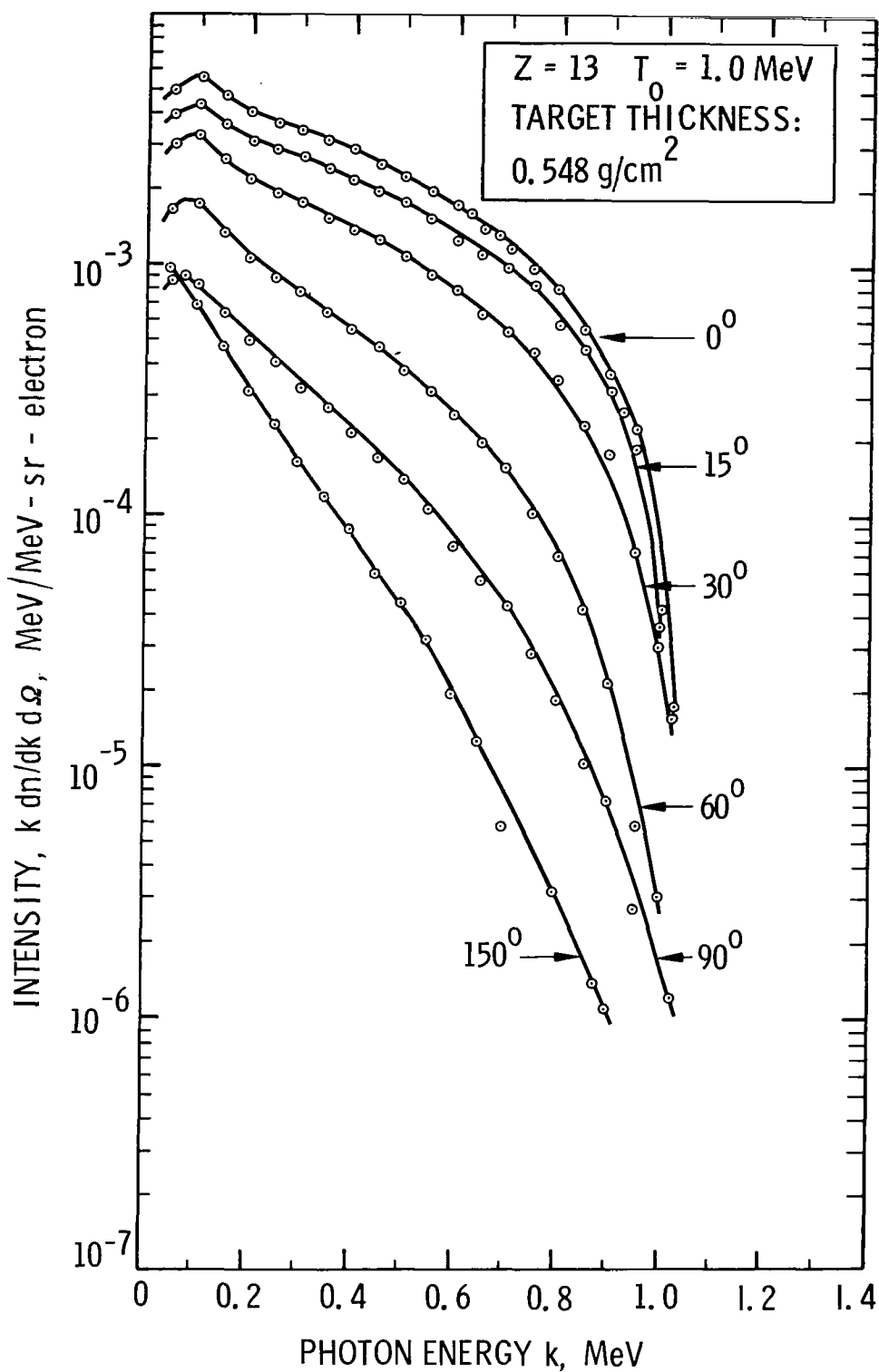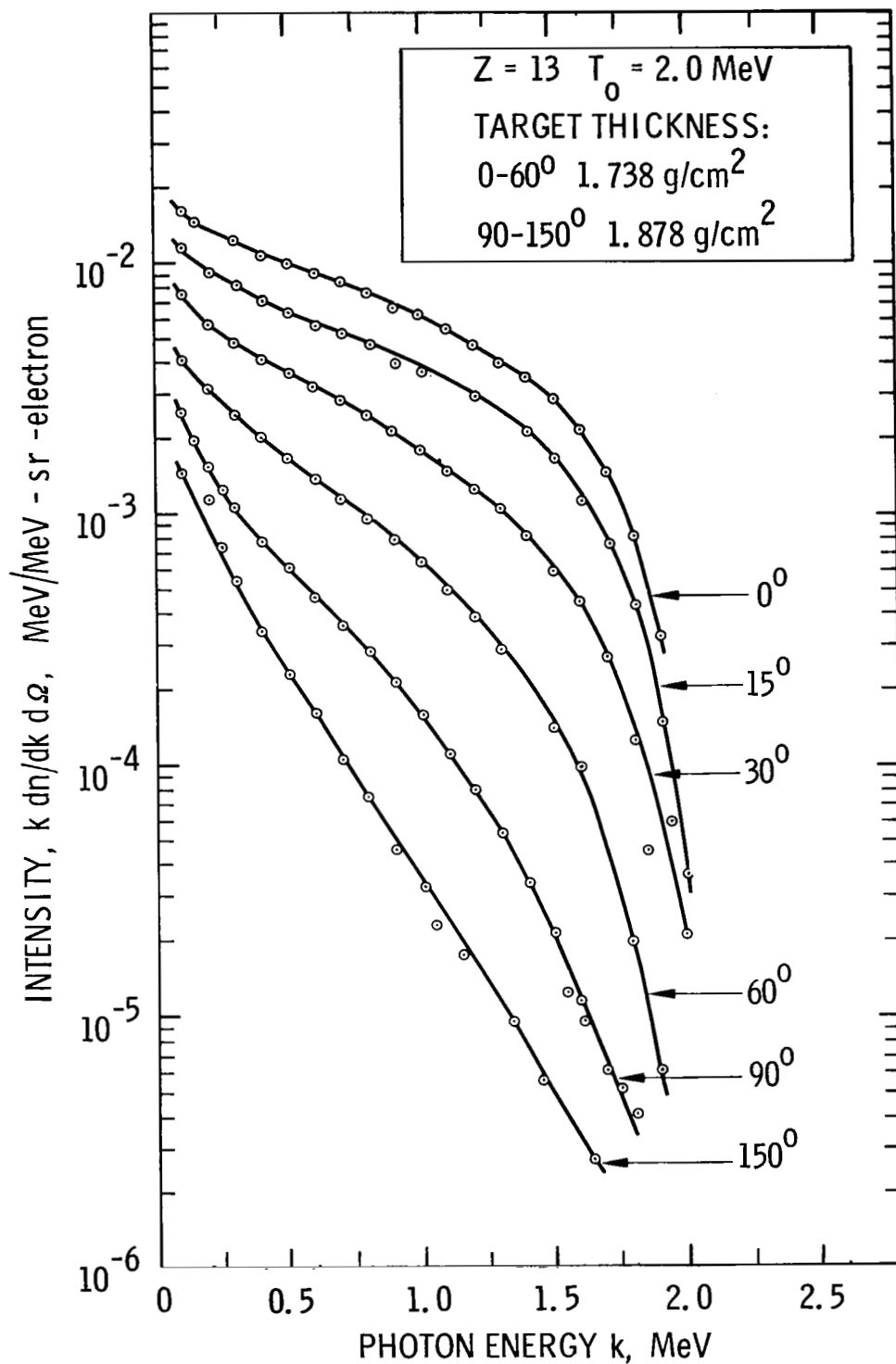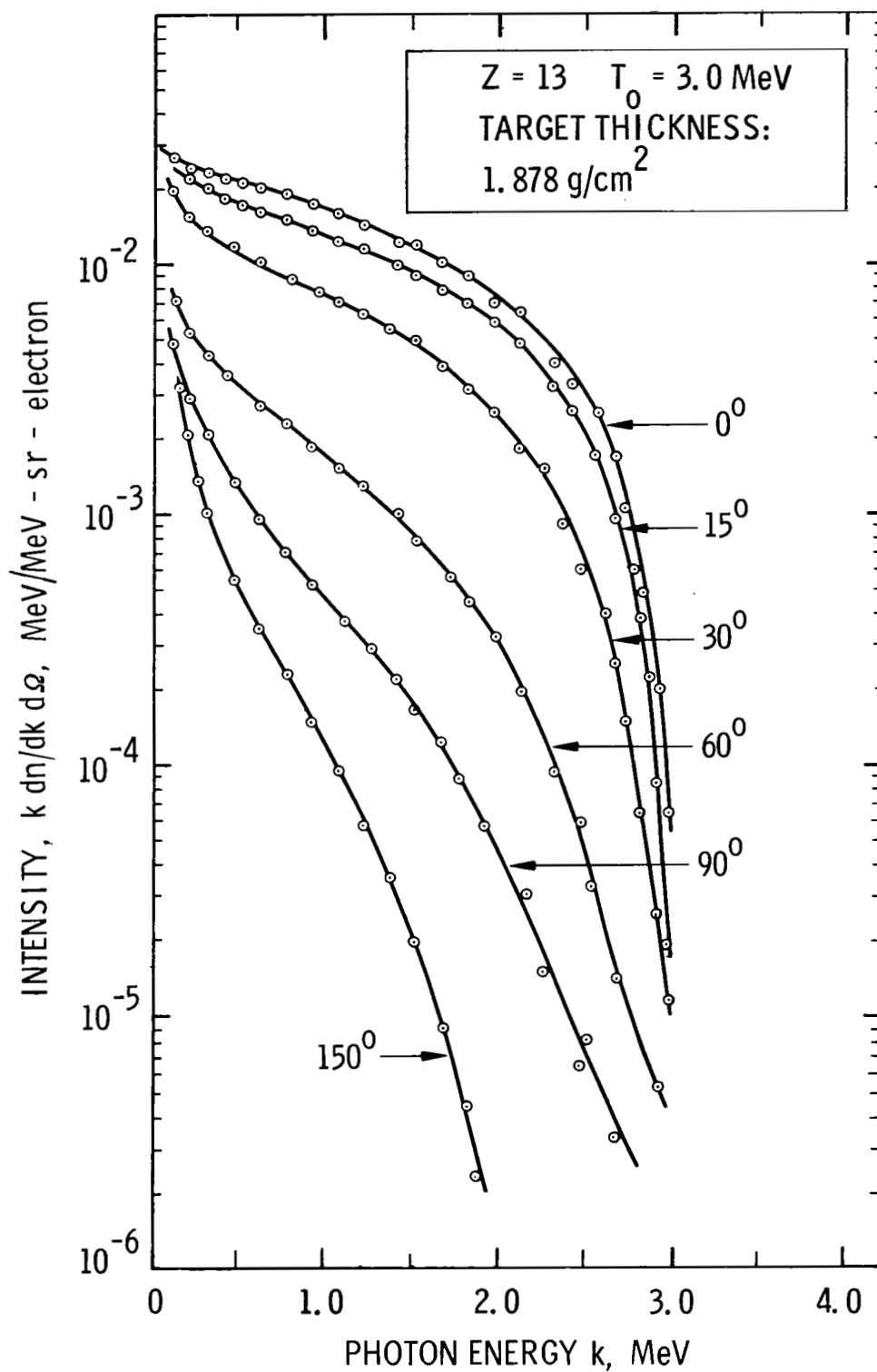
Figure 16. Bremsstrahlung intensity measured at angles ranging from 0 deg to 150 deg, for 3.0 MeV electrons incident on a thick aluminum target.

Figure 17. Bremsstrahlung intensity measured at angles ranging from 0 deg to 150 deg, for 0.5 MeV electrons incident on a thick iron target.

Figure 18. Bremsstrahlung intensity measured at angles ranging from 0 deg to 150 deg, for 1.0 MeV electrons incident on a thick iron target.
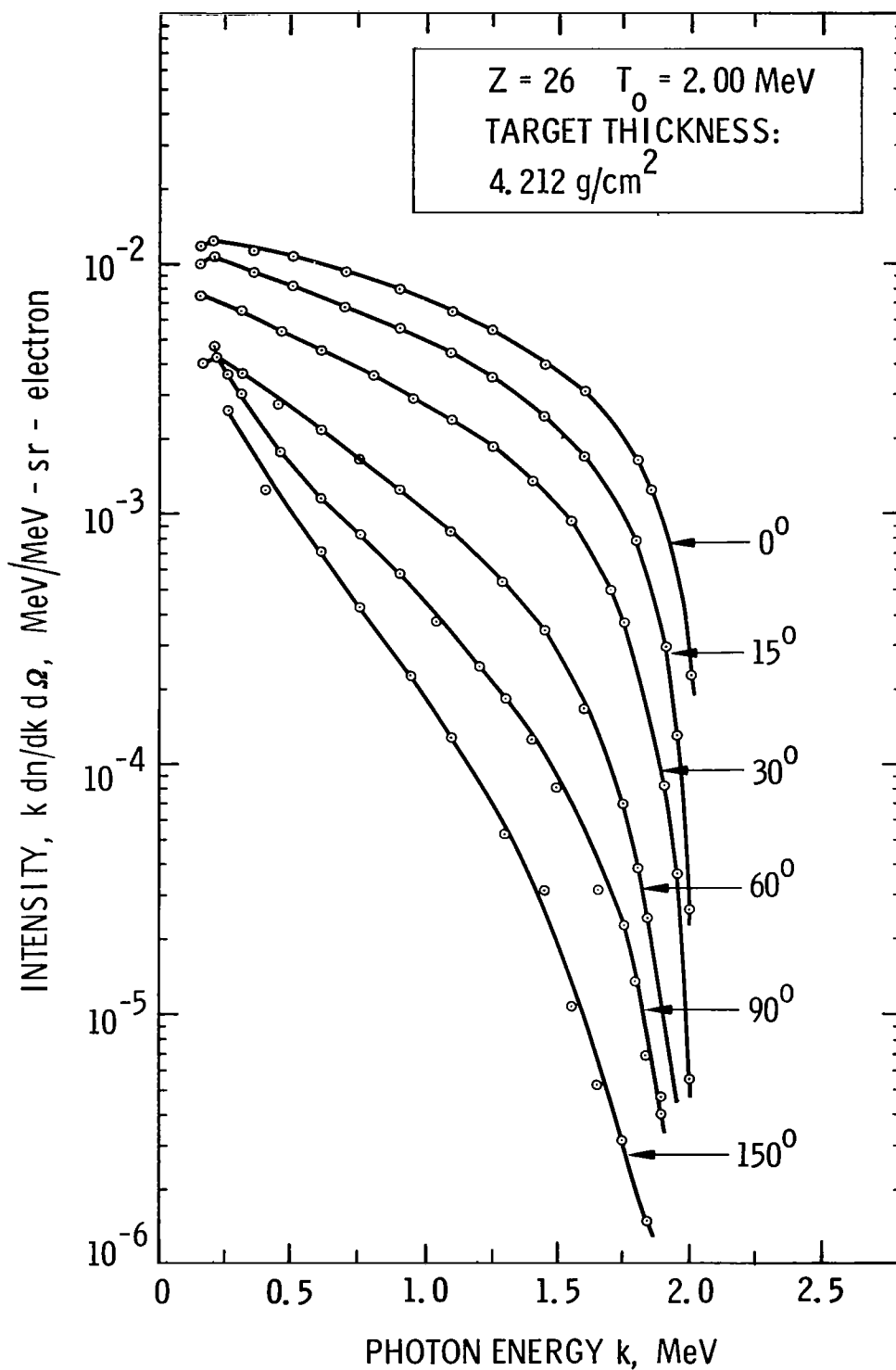
Figure 19. Bremsstrahlung intensity measured at angles ranging from 0 deg to 150 deg, for 2.0 MeV electrons incident on a thick iron target.
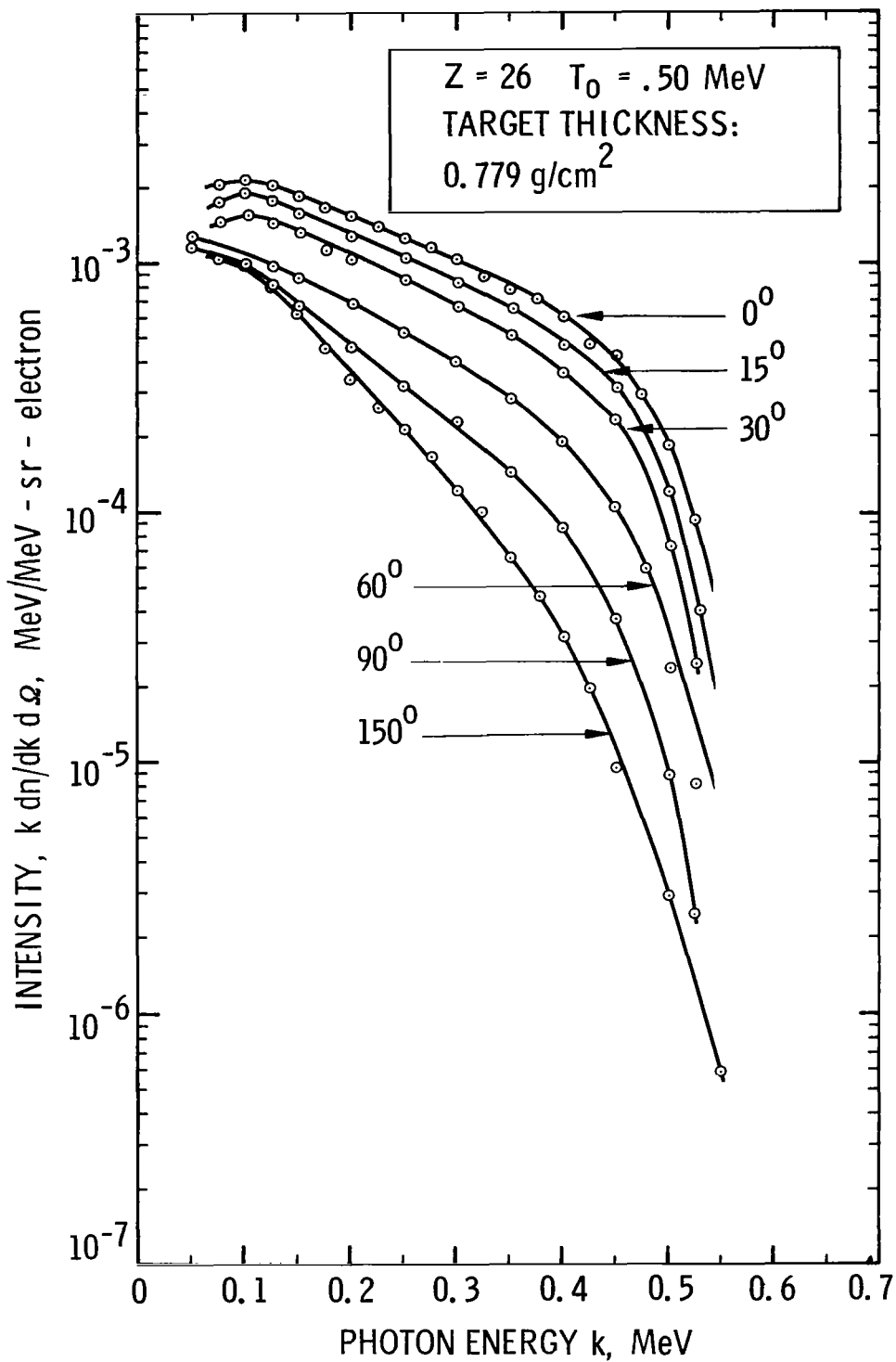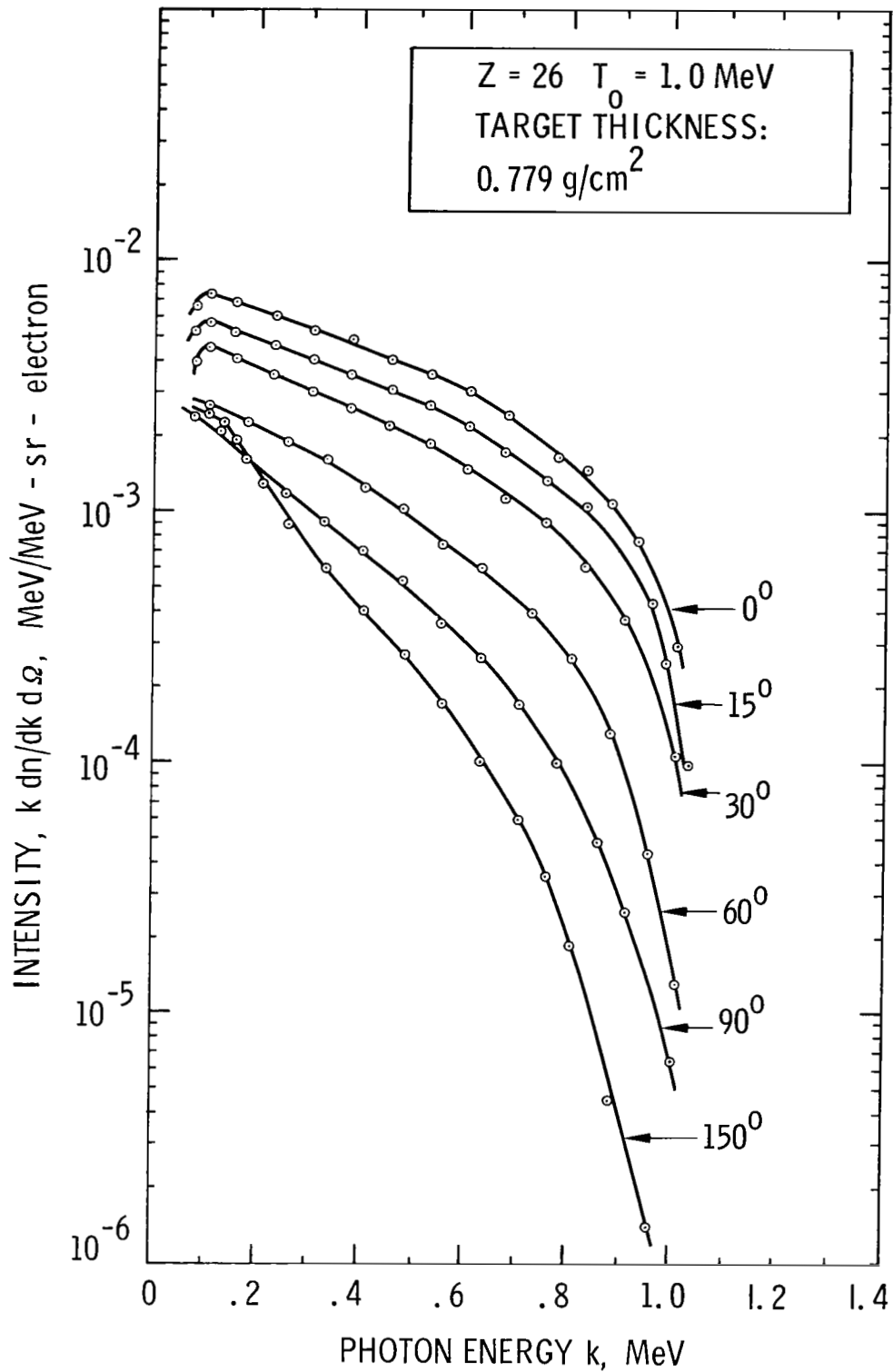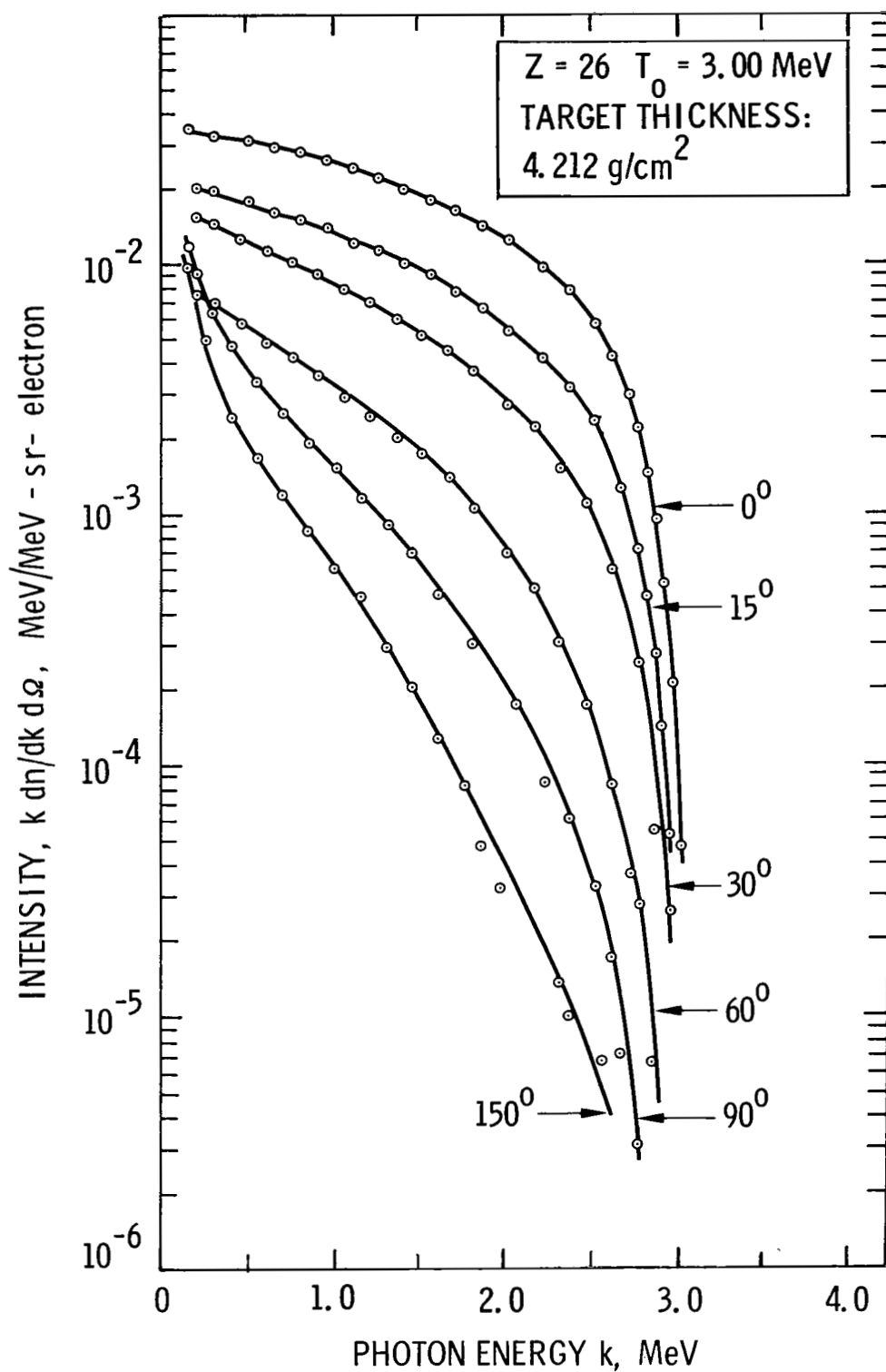
Figure 20. Bremsstrahlung intensity measured at angles ranging from 0 deg to 150 deg, for 3.0 MeV electrons incident on a thick iron target.

Figure 21. Bremsstrahlung intensity spectra from thick aluminum targets, integrated over photon angle θ for incident electron energies 0.5, 1.0, 2.0, and 3.0 MeV.

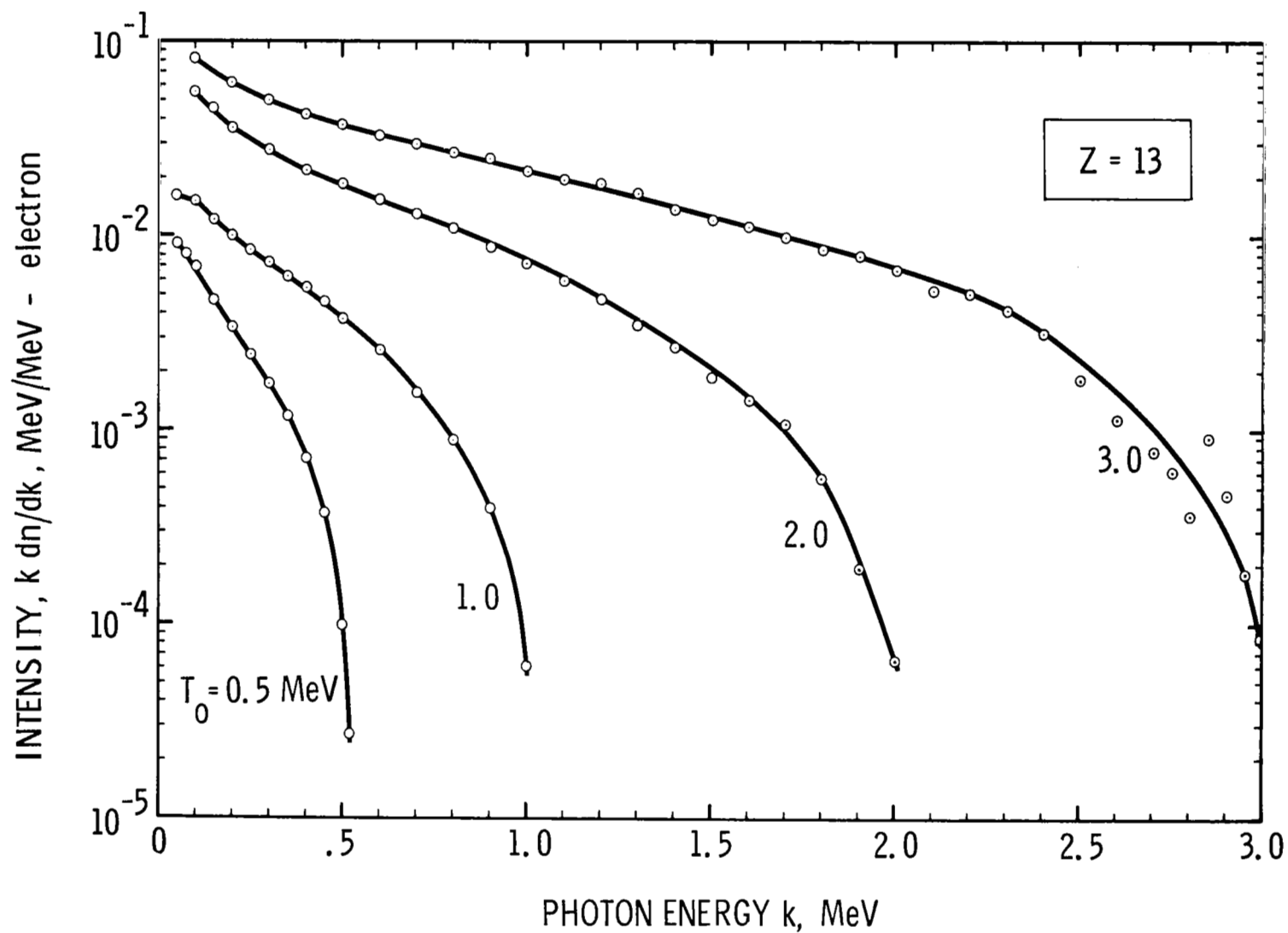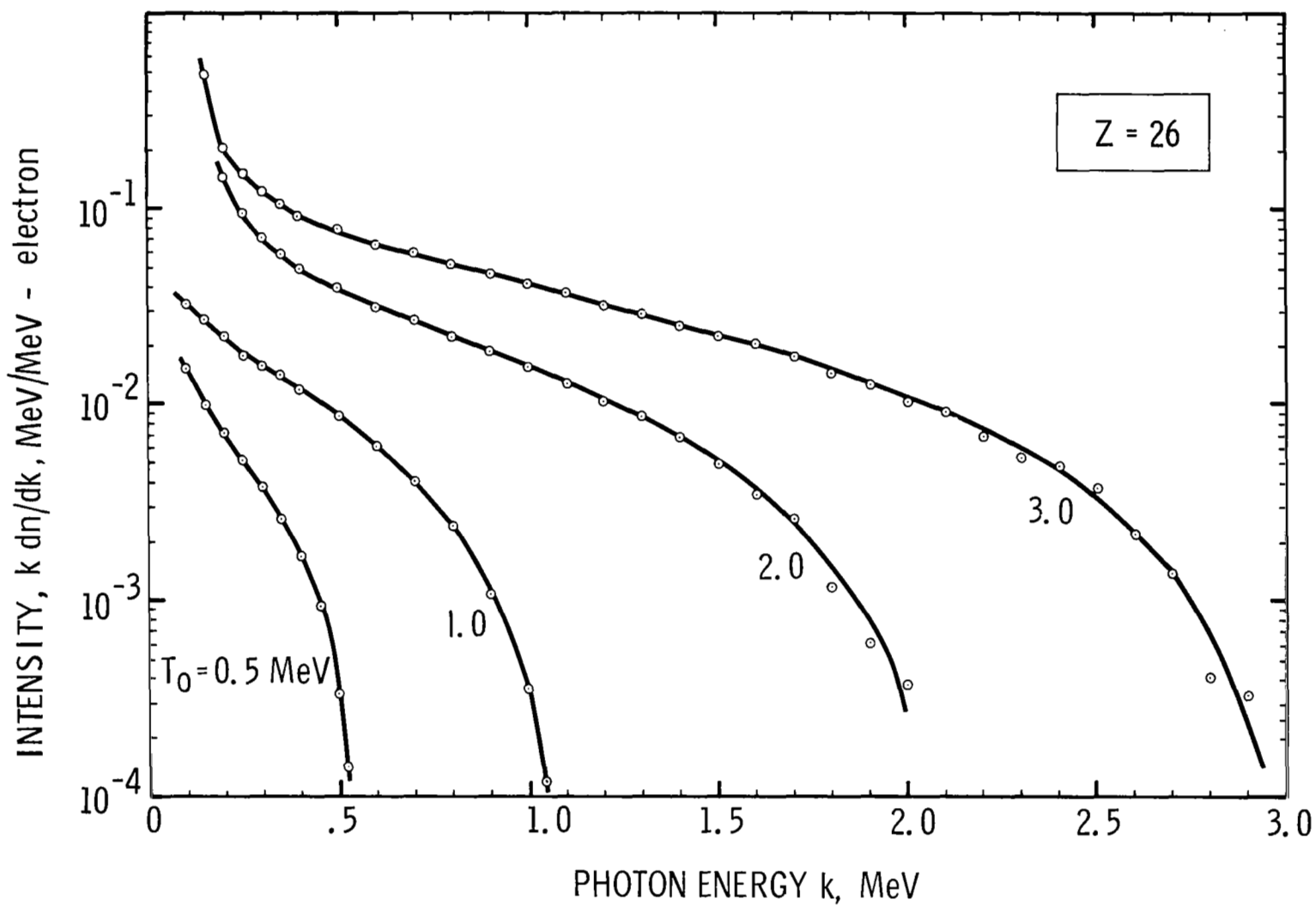Figure 22. Bremsstrahlung intensity spectra from thick iron targets, integrated over photon angle θ for incident electron energies 0.5, 1.0, 2.0, and 3.0 MeV.

forward angle chamber at 0 deg through 20 deg in 5 deg steps will be used to revise this integration. The lower photon energy limit for the revised integration will be chosen so that these results can be compared with the spectra calculated by Berger at NBS.

The experimental data of Edelsack, et al (1) at NRDL provides a comparison of LTV thick target intensities for aluminum in the case of 1.00 MeV electrons, and a photon angle of 0 deg. In that experiment absolute yields were measured using a scintillation spectrometer. Agreement for this spectrum is good. This comparison is shown in Figure 23. The NRDL yields have been converted to intensities for comparison purposes. The LTV spectral yields for various photon angles have also been compared with the theoretical values calculated at NBS by Berger and Seltzer using Monte Carlo methods (2). These comparative data for aluminum are shown in Figures 24 and 25 for 0.5 MeV and 120 deg, and 2.0 MeV and 15 deg, respectively. The curves show good agreement with the theoretical values above approximately .4 T_o. Figures 26 and 27 present LTV preliminary data for spectral intensities from aluminum, integrated over photon angle, compared with calculations by Scott (3) at Langley Research Center, for 1.0 MeV and 3.0 MeV electrons, respectively.

The greatest uncertainty in the experimental spectra presented here lies in the measurement of the integrated electron beam for determination of the number of electrons incident on the target. Throughout the course of the experiment, effort has been directed toward increasing the accuracy of this measurement. During recent runs at 3.0 MeV, fluctuations in the yield were observed, which were possibly attributable to photoionization
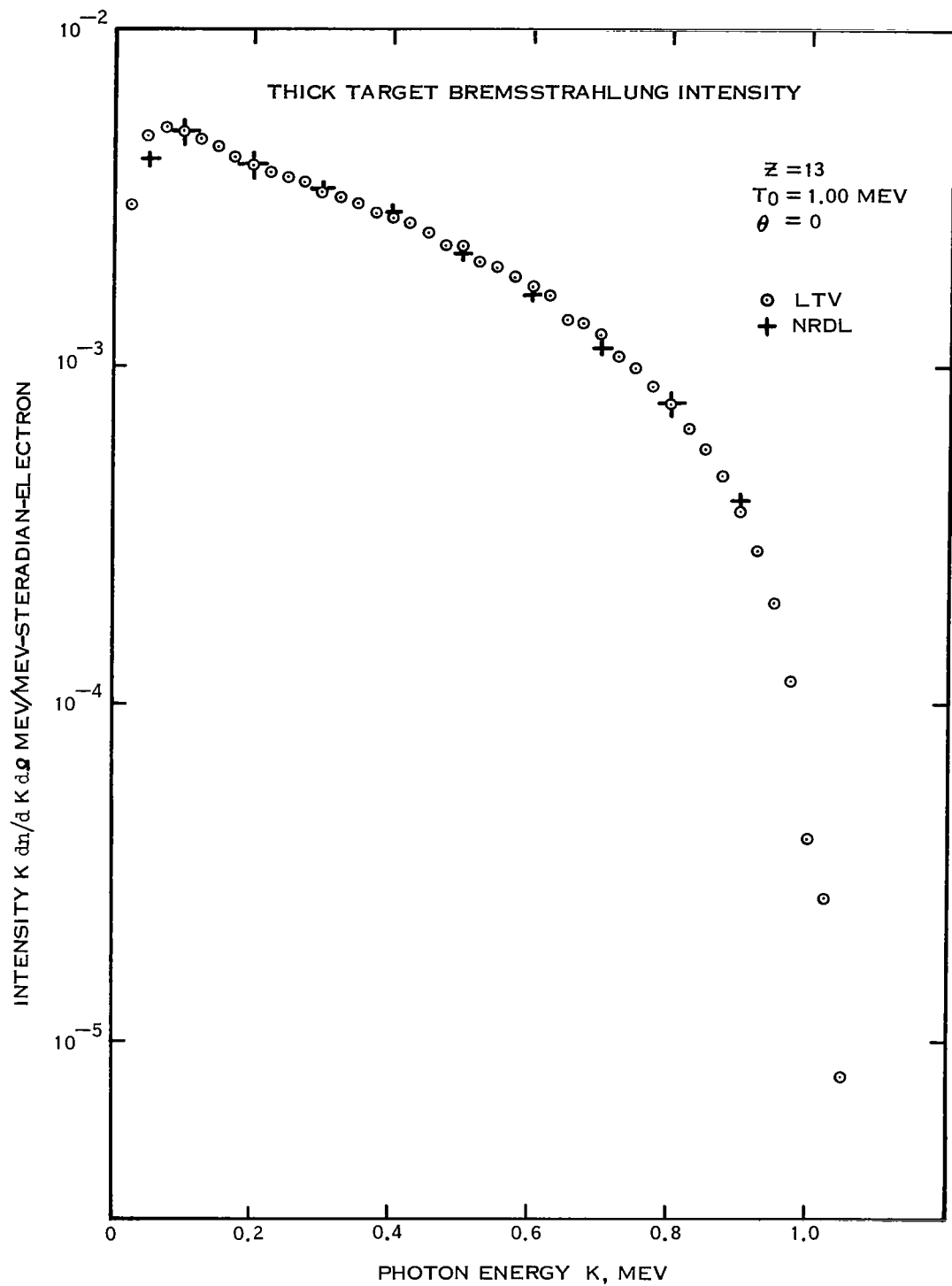
Figure 23. Comparison of LTV measurement of bremsstrahlung intensity at 0 deg from a thick aluminum target bombarded by 1.0 MeV electrons with a spectrum obtained at NRDL.

THICK TARGET BREMSSTRAHLUNG SPECTRUM

$\bar{z} = 13$
$T_0 = 0.5$ MEV
$\theta = 120°$
TARGET THICKNESS: 0.548 G/CM^2
POINTS: LTV, EXPERIMENTAL
HISTOGRAMS: NBS, CALCULATED
SOLID: $115 - 120°$
DASHED: $120 - 125°$

YIELD, PHOTONS/(MEV-STERADIAN)

10^{-1}

10^{-2}

10^{-3}

10^{-4}

10^{-5}

0   0.1   0.2   0.3   0.4   0.5

PHOTON ENERGY K, MEV

Figure 24. Comparison of thick target bremsstrahlung yield from aluminum at 120 deg and a bombarding energy of 0.5 MeV with values calculated at NBS.

33

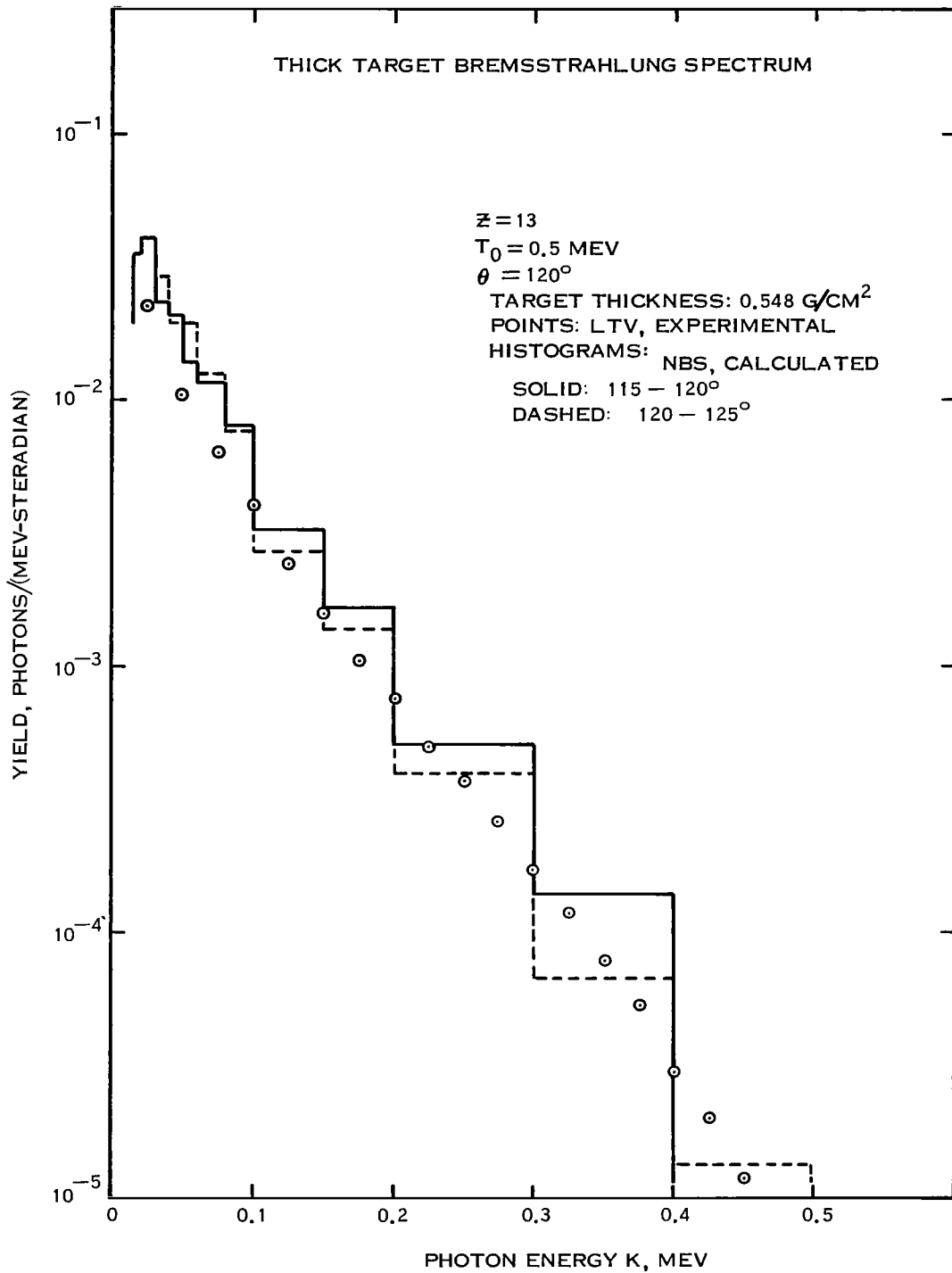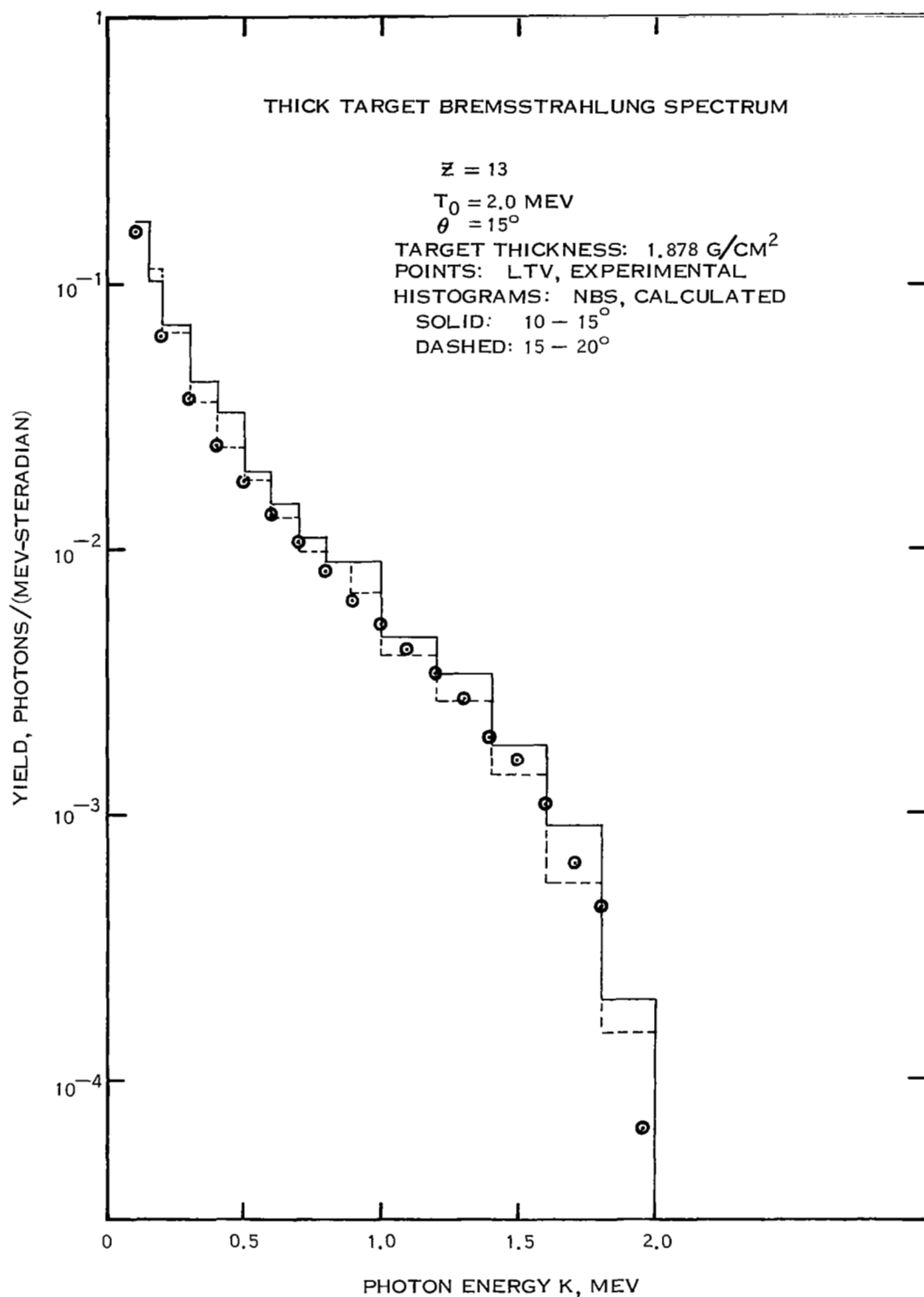Figure 25. Comparison of thick target bremsstrahlung yield from aluminum, at 15 deg and a bombarding energy of 2.0 MeV, with values calculated at NBS.

Figure 26. Integrated intensity of bremsstrahlung from a thick aluminum target bombarded by 1.0 MeV electrons, compared with values calculated at Langley Research Center.

Z = 13
T_0 = 3.0 MEV

○ EXPERIMENTAL - LTV
□ CALCULATED - SCOTT

INTENSITY, K dn/dK, MEV/MEV-ELECTRON

10^{-1}

10^{-2}

10^{-3}

10^{-4}

0   1.0   2.0   3.0

PHOTON ENERGY K, MEV

Figure 27. Integrated intensity of bremsstrahlung from a thick aluminum target bombarded by 3.0 MeV electrons, compared with values calculated at Langley Research Center.

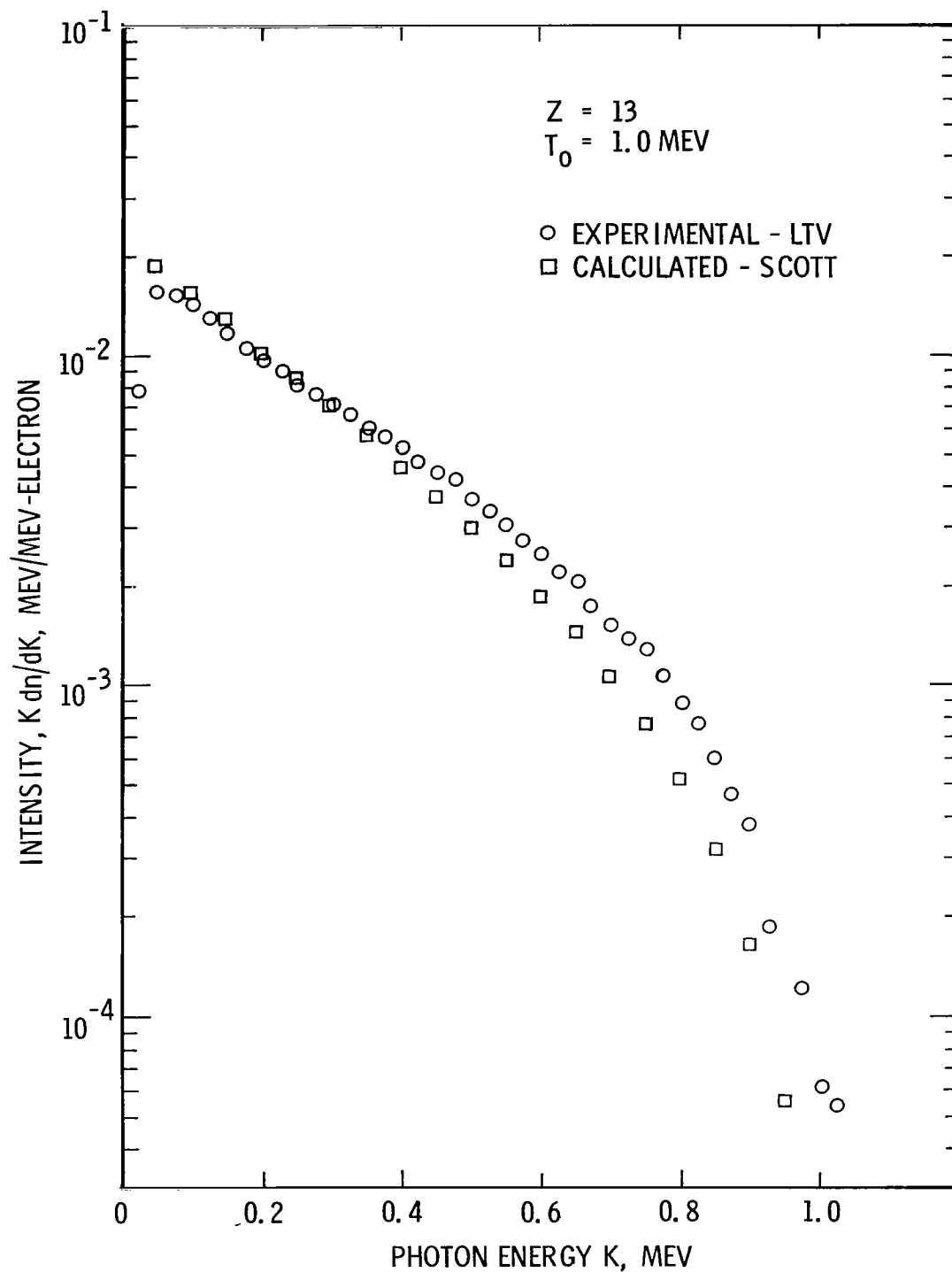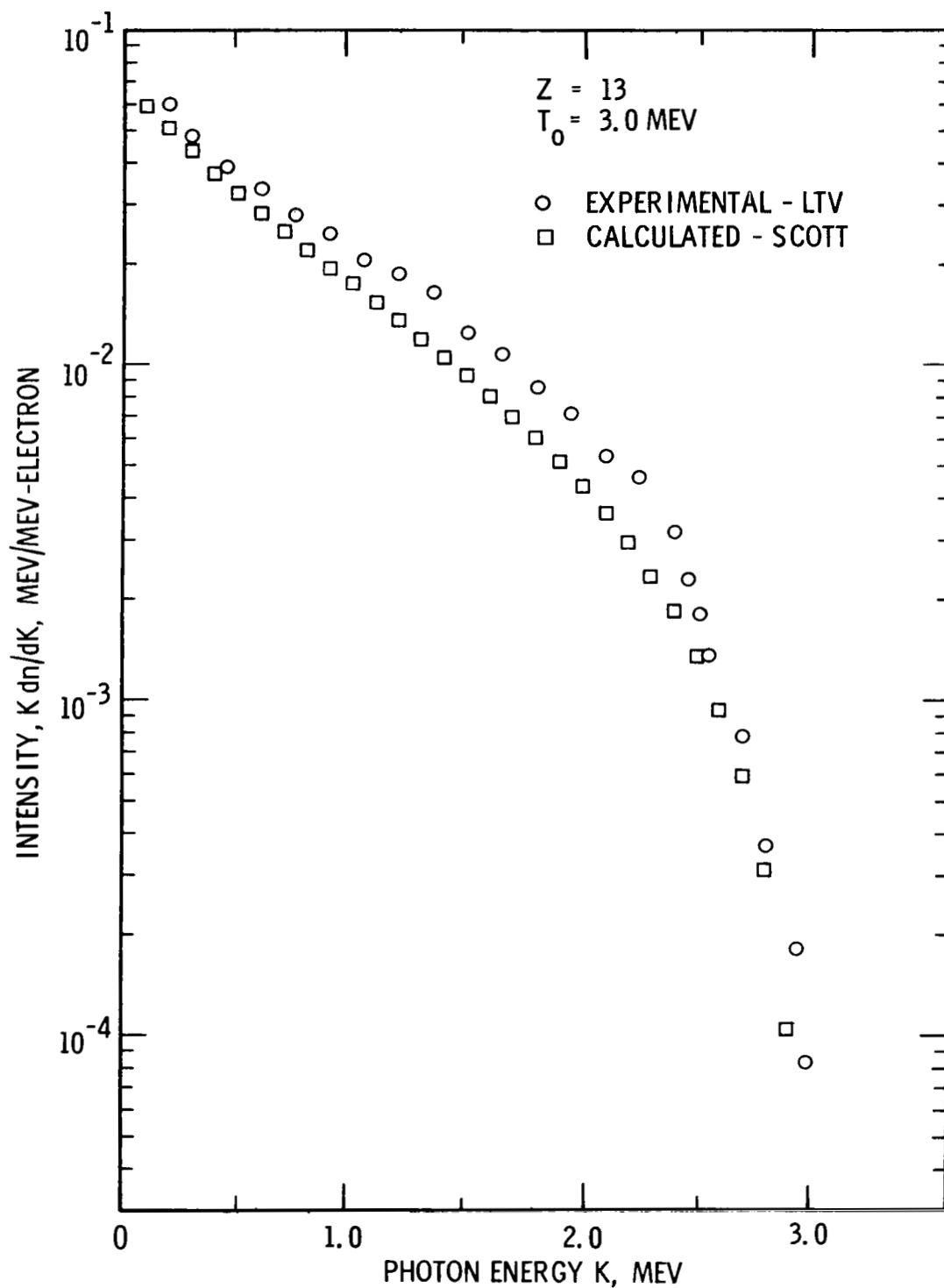of the air surrounding the target, with subsequent integration of spurious currents. This problem is being carefully investigated. An alternate method of beam integration, which will enable one to observe thick target bremsstrahlung with little attenuation at all the desired forward angles, will be utilized as follows: A second chamber containing the target will be placed inside the evacuated chamber and isolated electrically from the latter. Beam current striking the target and the inner chamber can thus be integrated. By grounding the outer chamber it will serve to shield the target and Faraday cage from spurious ionization currents. This method also has the advantage of dispensing with the use of a vacuum gasket to isolate the target assembly from the accelerator.

Throughout the measurements the uncertainty has been less in the spectral shape of the intensity curves than in the absolute value, as the shape has been quite repeatable for different series of runs. The experimental uncertainty in the absolute value of the intensities presented here is estimated to be ± 20%. A continuing effort is being made to increase the accuracy of the measurement.

Some effort has been initiated during the past period toward determining from the thick target intensity data an empirical expression which describes the bremsstrahlung production in the energy range 0.5 to 3.0 MeV. It is apparent that if one could find a simple empirical rule that would adequately approximate the spectral distribution of bremsstrahlung, this would greatly facilitate dose calculations and other engineering applications. The empirical expression which describes the bremsstrahlung produced by nonrelativistic electrons has come to be known as Kramers' rule (4).

37

The spectral intensity is given by

$$I(k) = CZ (T_o - k).$$

At higher energies the data indicates that the spectral distribution is no longer well approximated by Kramers' rule. As a modification to this rule, a spectral distribution was assumed having the form

$$I(k) = AZ (T_o - k) e^{-Bk/T_o},$$

in which the parameters A and B are chosen so as to fit this empirical rule to the observed spectral distributions. This program has met with some measure of success using distributions from aluminum and iron. The analysis is being extended to further test the Z dependence, as intensity measurements from other materials are obtained.

Thin target cross sections differential in photon energy and angle were determined for aluminum for 0.5 MeV and 1.0 MeV electrons and photon emission angles 15, 20, and 30 deg. Thin, self-supporting targets were prepared in this laboratory by vacuum deposition of the aluminum. Measurements were taken using targets of three thicknesses: 122 μg/cm^2, 265 μg/cm^2, and 337 μg/cm^2. The cross section values obtained from these different thicknesses agree to within the error in the experimental determination of the thicknesses ($< 5\%$). Figure 28 shows the results in the case of 0.5 MeV electrons, for 15 and 30 deg. The experimental cross sections are averages for the three target thicknesses. The solid curves represent the Bethe-Heitler theoretical cross sections. Figure 29 presents a comparison of the 1.0 MeV differential cross sections with the Bethe-Heitler theoretical values. The results indicate that this theory underestimates the cross
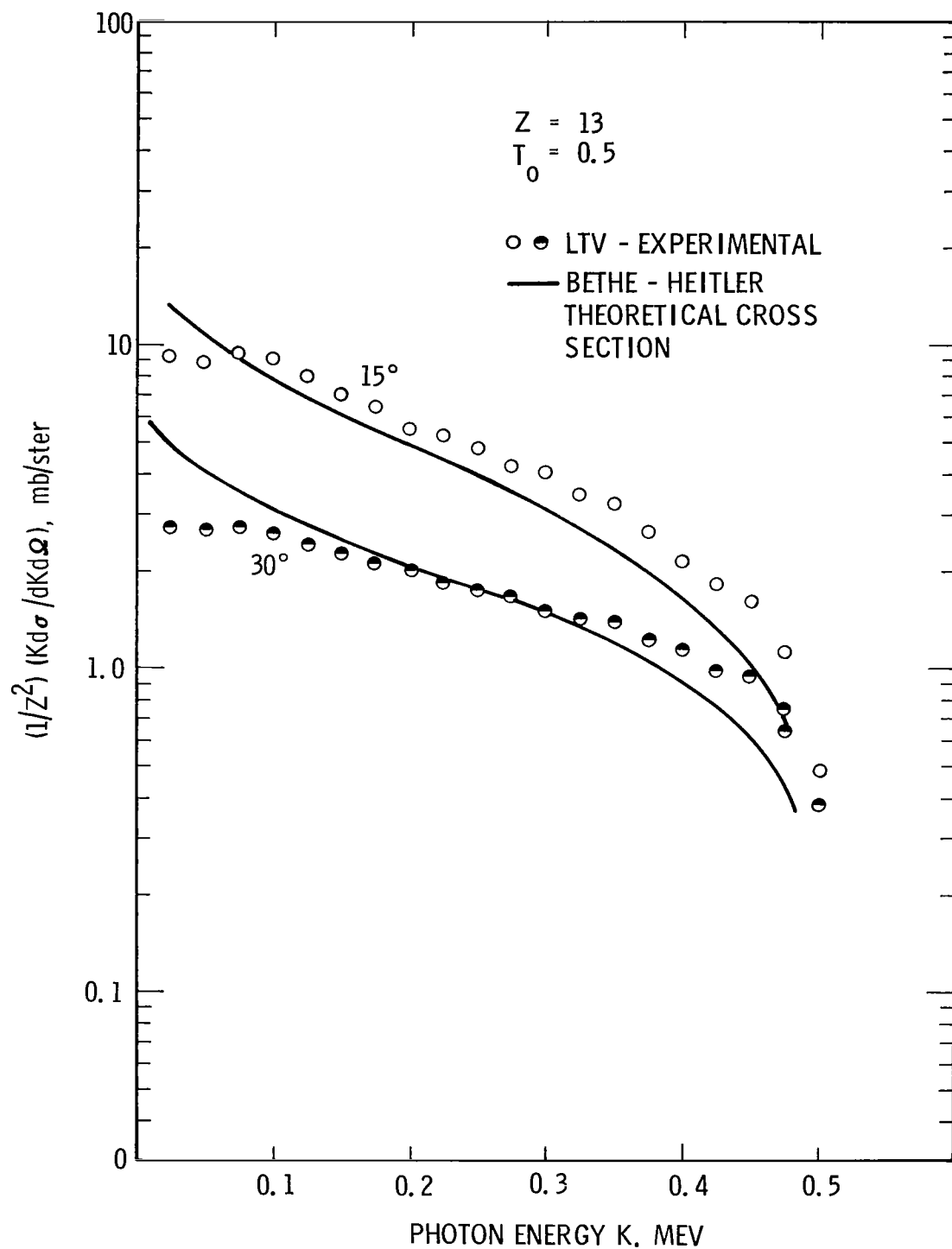
Figure 28. Thin target differential cross sections for 0.5 MeV bremsstrahlung at photon energies k, and photon angles 15 and 30 deg.
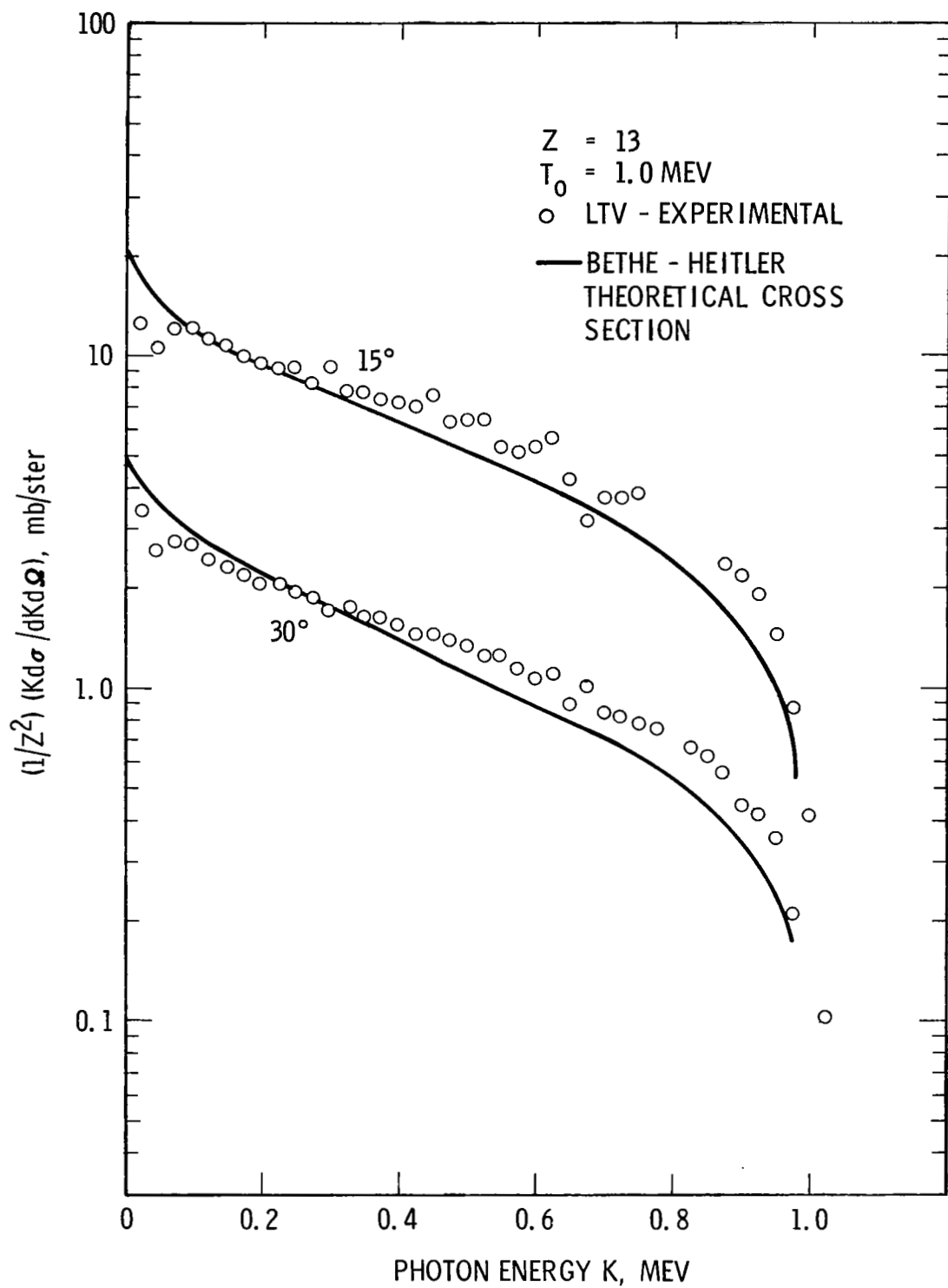
Figure 29. Thin target differential cross sections for 1.0 MeV bremsstrahlung at photon energies k, and photon angles 15 and 30 deg.

sections over most of the 15 deg spectrum and over an appreciable portion of the 30 deg curve. These measurements are compared in Figures 30 and 31 with those of Motz (5) at the National Bureau of Standards.

Cross section measurements at small angular intervals in the forward direction are highly desirable, due to the increased peaking of the bremsstrahlung around zero degrees with increasing electron energy. Measurements at very small angles are experimentally more difficult to obtain, as the scattered electron beam after penetrating the target must be deflected and integrated in the near vicinity of the target without altering the incident angle and focus of the beam on the target. Experimental techniques required to accomplish these measurements are being explored so that such measurements can be obtained.
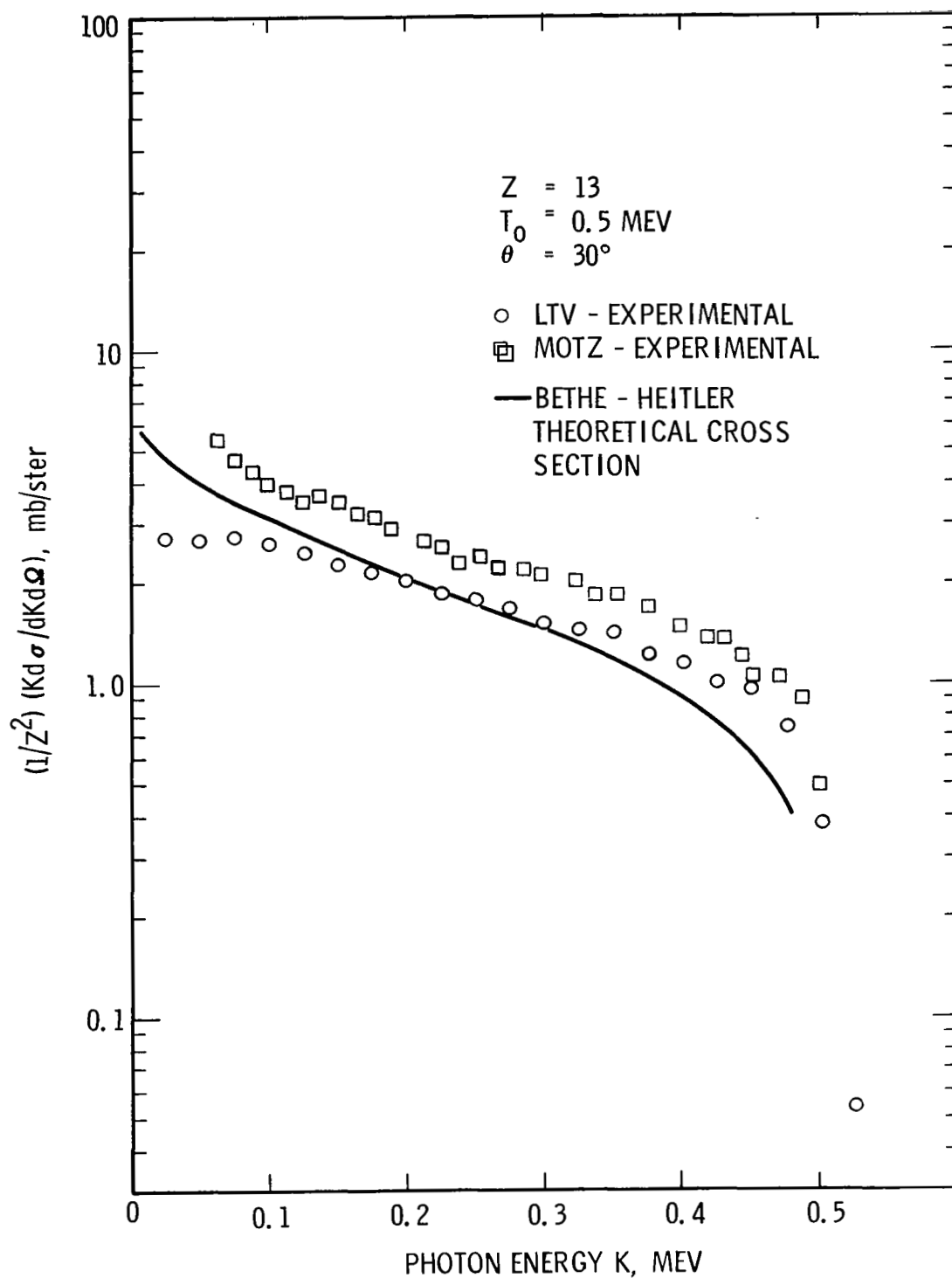
Figure 30. Comparison of LTV experimental cross sections for aluminum at 0.5 MeV and 30 deg with experimental results of Motz.
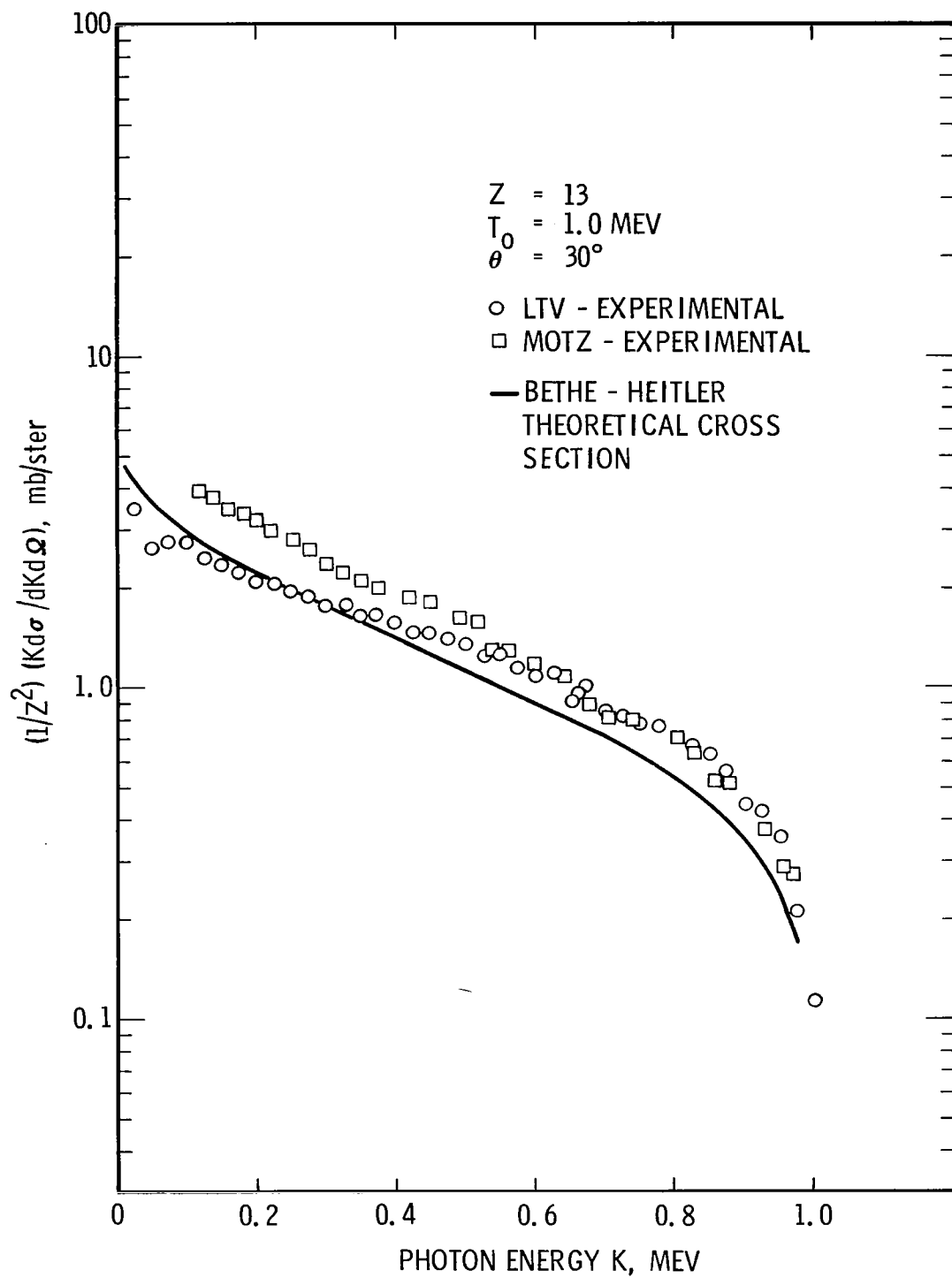
Figure 31. Comparison of LTV experimental cross sections for aluminum at 1.0 MeV and 30 deg with experimental results of Motz.

REFERENCES

1. E. A. Edelsack, W. E. Kreger, W. Mallet, and N. E. Scofield, Health Physics, $\underline{4}$, 1-15 (1960).

2. M. J. Berger and S. M. Seltzer, Paper presented at Second Symposium on Protection Against Radiation Hazards in Space, Gatlinburg, Tennessee, October 12-14, 1964. From NASA SP-71.

3. W. Wayne Scott, NASA TND-2659.

4. H. A. Kramers, Phil. Mag. $\underline{46}$, 836 (1923).

5. J. W. Motz, Phys. Rev. $\underline{100}$, 1560 (1955).

Part 2.

ELECTRON SCATTERING IN ALUMINUM

by David H. Rester and Walter J. Rainwater, Jr.

ELECTRON SCATTERING IN ALUMINUM

INTRODUCTION

The first twelve-month period of an experimental program to study the
interaction of electrons with matter by the measurement of electron spectra
has been completed under NASA contract NASw-948. This study consisted of mea-
surements of electron scattering from thin aluminum foils and of electron
penetration through aluminum slabs. Of the two types of measurements the
electron scattering measurements are more fundamentally descriptive of the
interaction of electrons with the atom. The results of these measurements
are given as cross sections for Coulomb scattering of electrons from the alumi-
num atom as a function of scattering angle and incident electron energy. The
electron penetration measurements consisted of the determination of electron
energy spectra as a function of exit angle and slab thickness.

The cross section for Coulomb scattering of electrons by aluminum without
atomic excitation are reported for incident electron energies of 0.1, 0.2,
0.5, 0.7, 1.0, 1.25, 1.5, 2.0, 2.5 and 3.0 MeV at scattering angles from 30
to 150 deg. The cross section for these energies and angles have been com-
pared to the Mott cross section calculated by Spencer and Doggett[1]. The Mott
cross section calculations were carried out for a point, unscreened nucleus.
In the energy range from 0.1 to 3.0 MeV for scattering angles from 30 to 150
deg the effects of finite nuclear size and atomic electron screening are
assumed to be negligible. The criteria for this judgment are based on the

range of momentum transfer values q of .34 to 13 (in units of $m_o c$) for which measurements have been made. It is predicted that screening effects become important in aluminum for q < 0.1. This has been verified by the calculations of Lin[2] for copper (Z = 29) which predict only about a 1% reduction of the cross section at 0.1 MeV and a scattering angle of 30 deg (q = .34). On the other hand finite nuclear size is not expected to be significant except at large values of momentum transfer. In the present experiment the largest value of momentum transfer occurs for an incident energy of 3 MeV and a scattering angle of 150 deg. Here the value of q = 13 is still considered to be small enough for aluminum that the effect on the cross section due to the nuclear charge distribution is small.

The study of the transmission of electrons through aluminum slabs has been concentrated on measurements for 1-MeV electrons with normal incidence to the slab. Pulse height distributions of transmitted electrons were taken at various observation angles from 0 to 90 deg for slab thicknesses equivalent to 0.2, 0.4, and 0.6 the range of 1-MeV electrons in aluminum. Electron energy distributions above 100 keV have been reduced from the pulse height distributions by removing the response of the electron spectrometer system to monoenergetic electrons. These spectra have been compared to the electron energy distributions calculated by M. J. Berger[3] of the National Bureau of Standards, using Monte Carlo techniques. The comparisons of the experimental and the calculated electron spectra for three scattering angles for each thickness are presented. Additional comparisons are a plot of the electron yield integrated over energy as a function of angle and a plot of the most probable energy loss at each angle for each thickness as a function of angle.

EXPERIMENTAL PROCEDURE

The arrangement of the experimental apparatus is shown in Fig. 1. The scattering chamber was made of aluminum with an inside diameter of ten inches. The electron detectors were mounted on cooling manifolds suspended from the top of the chamber, which could be rotated through 360 deg. A target holder for remotely positioning a viewing quartz and a target, either a thin aluminum foil or an aluminum slab, was provided. The LTV 3-MeV Van de Graaff accelerator provided the beam of monoenergetic electrons for incident energies from 0.5 to 3 MeV. In the energy range from 0.1 to 0.3 MeV the electrons were accelerated by a 300-kV Texas Nuclear accelerator. The total number of electrons entering the chamber was determined by use of a current integrator. As shown in Fig. 1 the electron beam was collected in a carbon Faraday cup for the case of targets consisting of thin aluminum foils. For the case of aluminum slabs the entire scattering chamber was electrically insulated and used to collect the beam.

Electrons leaving the target at a given angle passed through a detector collimator-aperture system which subtended a solid angle of about 10^{-4} sr from the target center. Measurements of electron yields were made at scattering angles ranging from 30 to 150 deg in 15-deg increments for the case of single scattering, or scattering by thin foils, and from 0 to 90 deg for the case of multiply scattered electrons. Alignment procedures throughout the experiment insured positioning of the detectors to within 0.2 deg. The energy spectra of the scattered electrons were determined by means of solid state detector spectrometers employing lithium-ion-drift silicon crystals, low noise amplifier systems, and a multichannel pulse height analyzer. Since the
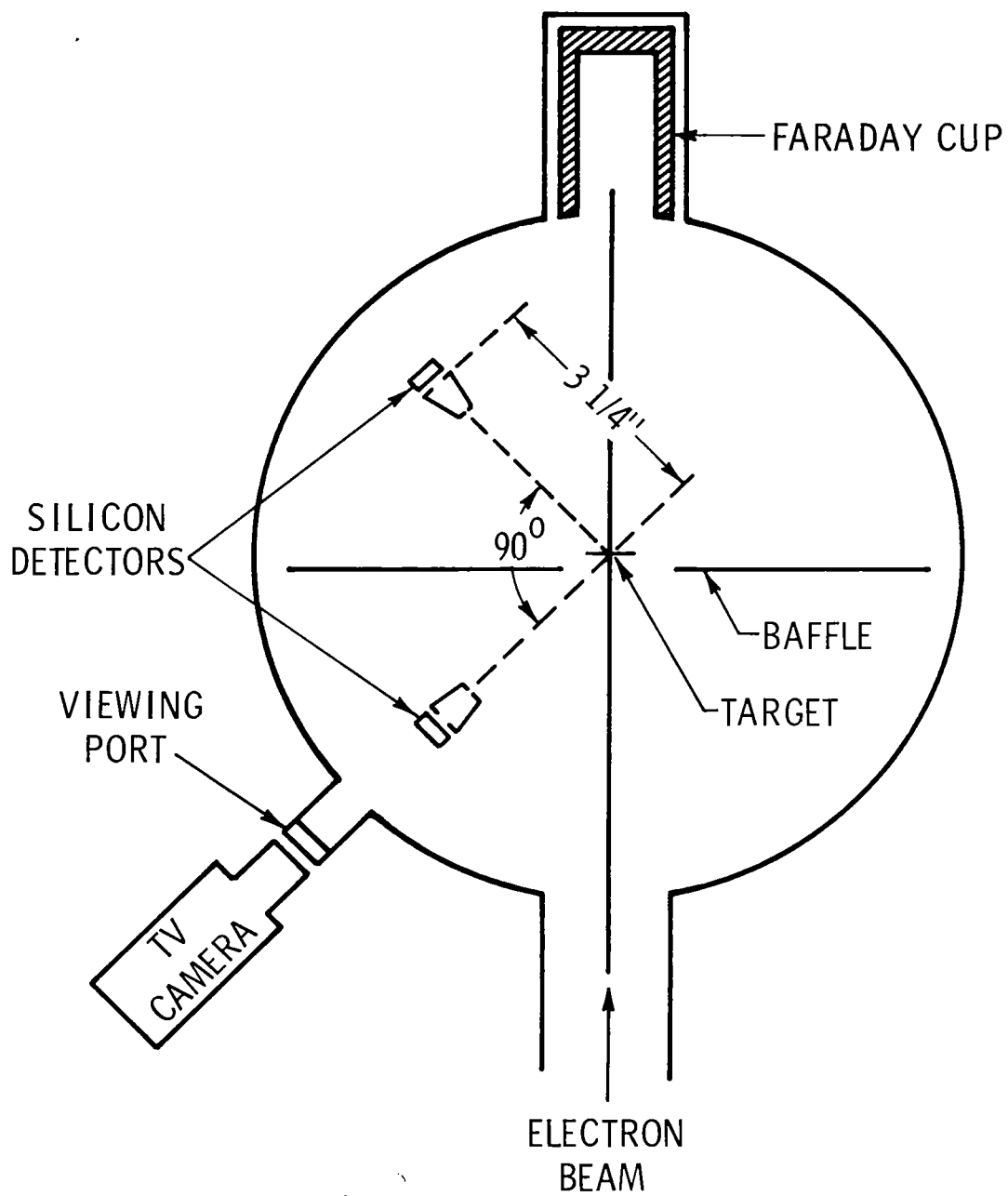
FIGURE 1   EXPERIMENTAL ARRANGEMENT

incident energy was varied from 0.1 to 3 MeV, it was necessary to employ different thicknesses of crystals to obtain usable pulse height spectra. Lithium-ion-drift wafers of 1-, 2-, and 3-mm thicknesses were used to measure spectra for incident energies up to 2 MeV. The appropriate thickness was chosen to maximize the signal to background while stopping the electrons completely for incident energies up to 1.5 MeV. In order to reduce detector penetration effects at higher energies single wafers of various thicknesses were stacked to obtain thicknesses greater than the range of the incident electrons. As examples of the differences in pulse height distributions obtained for various stacked-wafer configurations, pulse height distributions are shown in Figures 2 and 3. Figure 2 illustrates the response obtained with a stacked configuration of a 1-mm and a 3-mm wafer, while Fig. 3 shows a response obtained with a stacked configuration of a 2-mm and a 3-mm wafer, both for 2.5-MeV electrons. The range in silicon predicted for 2.5-MeV electrons is less than 4.9 mm. In the case of the stacked-wafer configuration of 4 mm, the effect of electron penetration can be seen by a reduction of the full energy peak and a sizable broad peak between the full energy peak and the electron-electron peak. In the case of the 5-mm configuration it can be seen that the full energy peak is relatively larger with a reduction in the number of pulses between it and the electron-electron peak. Its response is more nearly like that of a single wafer detector. A diagram of the detector-collimator system showing the typical arrangement of the stacked wafers is shown in Fig. 4.

At each energy, spectra were accumulated with the detectors at room temperature except at 100 keV. At this energy 1-mm detectors were employed which
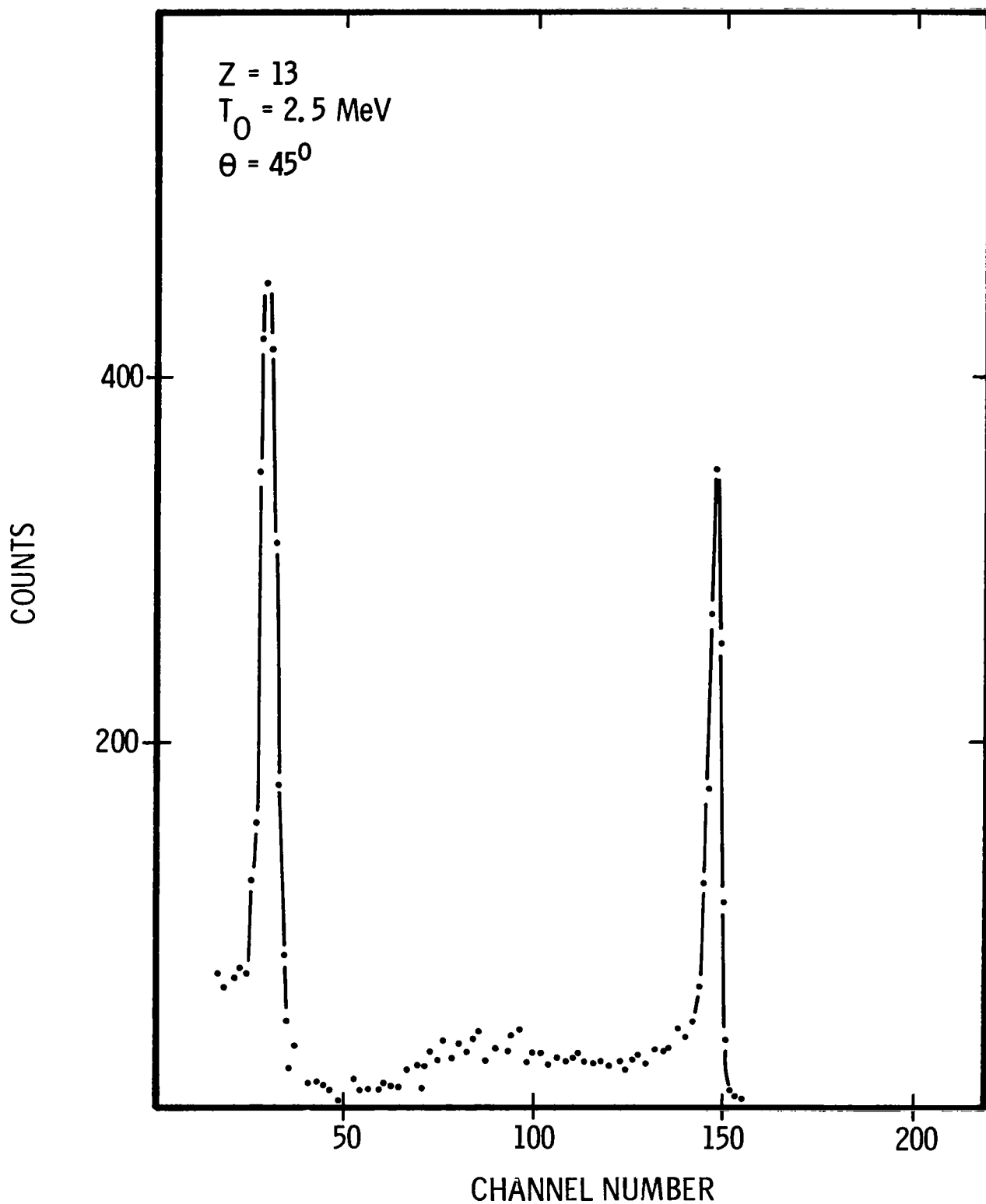
51

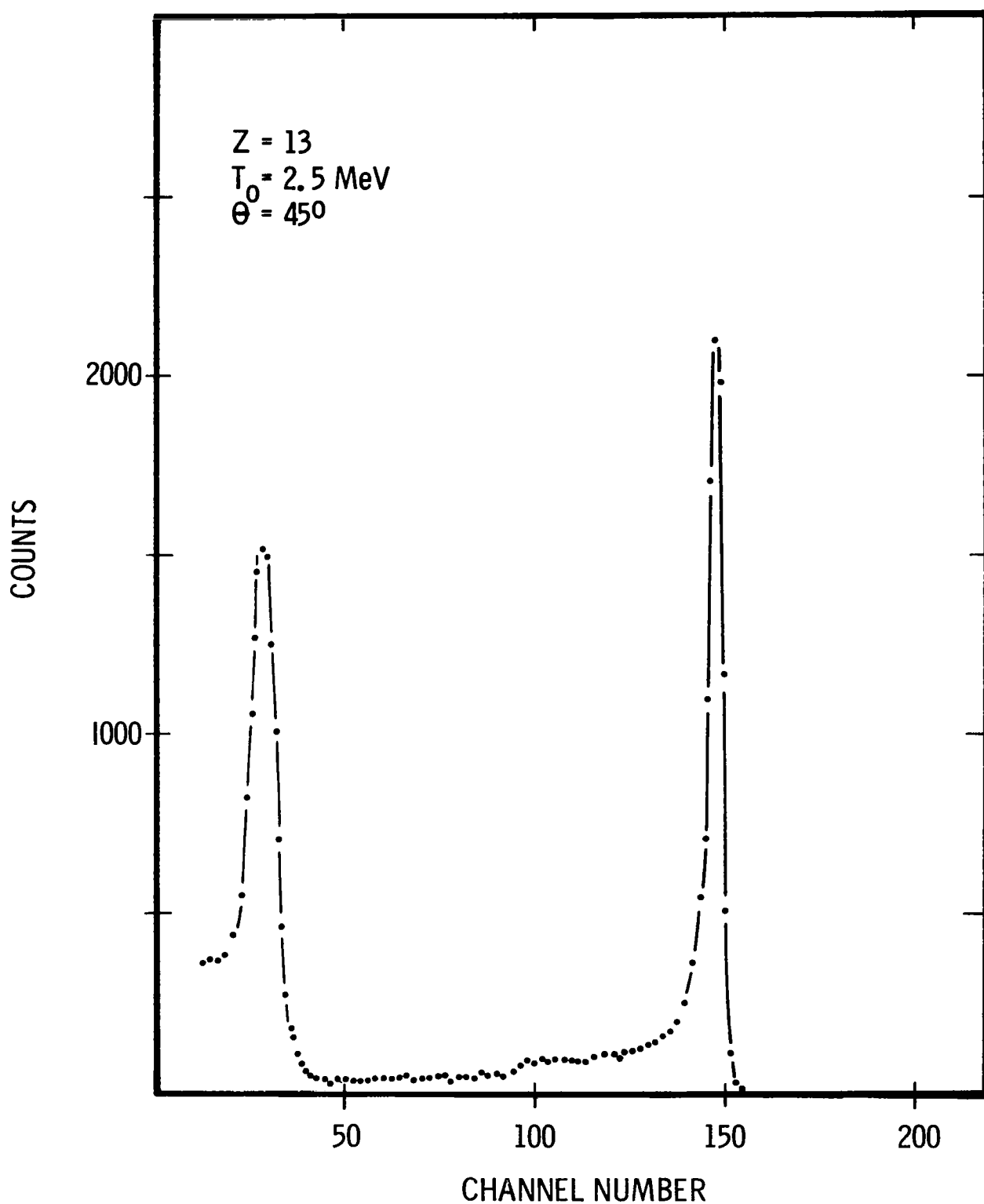FIGURE 2   PULSE HEIGHT DISTRIBUTION TAKEN WITH 4MM STACKED—WAFER
DETECTOR

FIGURE 3   PULSE HEIGHT DISTRIBUTION TAKEN WITH 5MM STACKED—WAFER DETECTOR
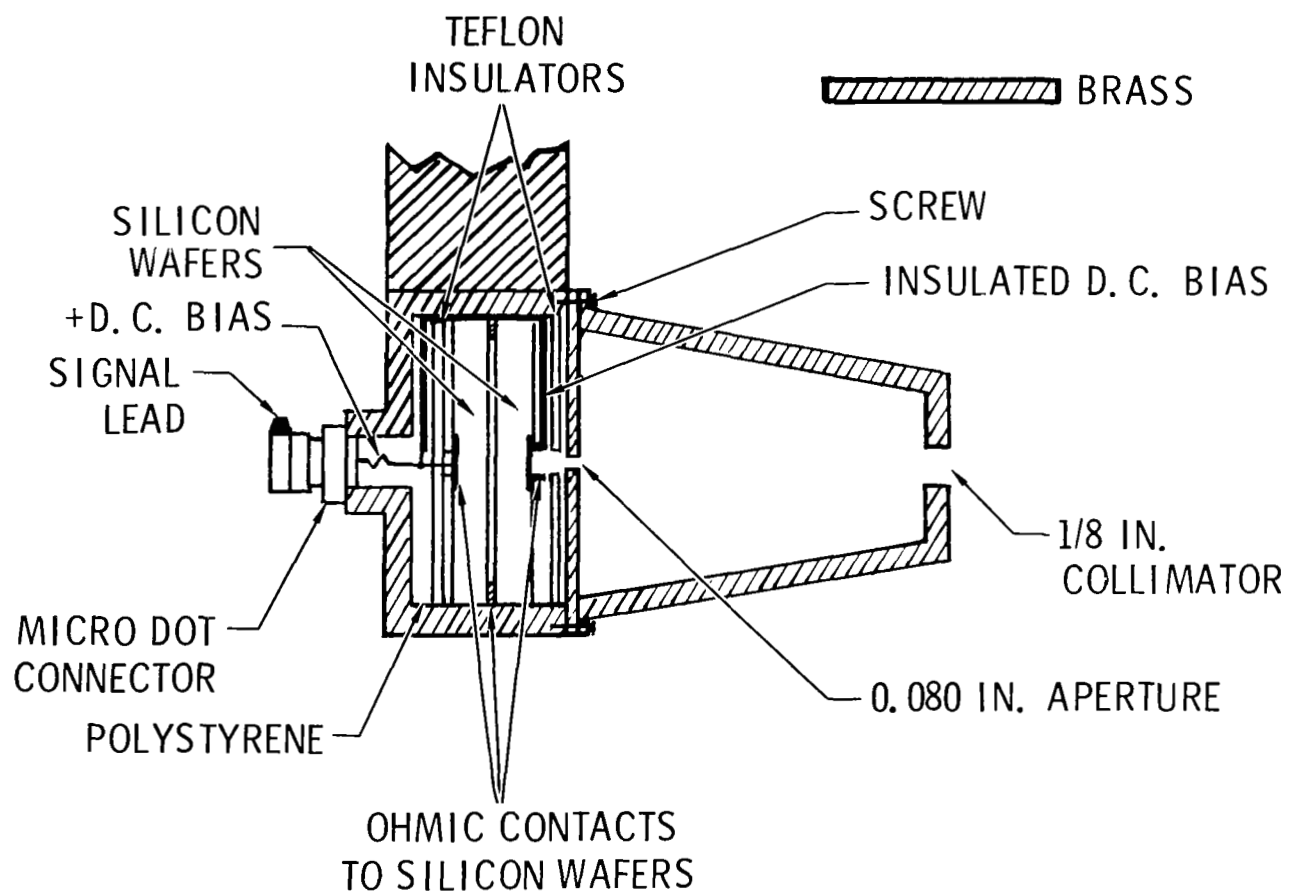
FIGURE 4   DETECTOR—COLLIMATOR SYSTEM CONTAINING STACKED WAFERS

exhibited room temperature f.w.h.m. of 22 keV. A resolution of 22% at 100 keV rendered the electron-electron peak unresolvable at the smaller forward angles. By cooling the wafer to -25°C, energy resolutions were obtained down to 6%, and the electron-electron peak could be resolved and its energy determined. A spectrum accumulated at a scattering angle of 30 deg for an incident energy of 100 keV is shown in Fig. 5. Typical pulse height distributions obtained for an incident energy of 1 MeV with a 2-mm detector are shown in Figures 6 and 7. These spectra are characteristic of the spectra observed at all bombarding energies. Fig. 6 shows a spectrum accumulated at a scattering angle of 45 deg. Two peaks in the distribution are visible. The peak at higher pulse height is due to the Coulomb scattering of electrons by the atom, which is left in its ground state after the interaction. This peak occurs at a pulse height corresponding to the incident energy. The peak at lower pulse height is due to electron-electron scattering. The energy of electrons scattered by target electrons is determined by the simple kinematics of the collision and therefore depends on the scattering angle. At angles greater than 90 deg, as illustrated by Fig. 7, this peak does not occur.

Thin self-supporting aluminum targets ranging in thickness from 11 to 271 $\mu g/cm^2$ were used in the thin target experiments. These targets were fabricated by vacuum evaporation of aluminum onto glass slides which had been previously coated with a thin film of soap. The slides were placed in a tray into which distilled water was slowly introduced until the entire perimeter of the slide was in contact with the water. At this point the aluminum foil was gradually separated from the slide as the soap film dissolved. Aluminum rings were used to lift the foils from the water and to provide supporting frames for placement in the scattering chamber. Target thicknesses were determined by weighing a known area of aluminum deposited on a surface adjacent to
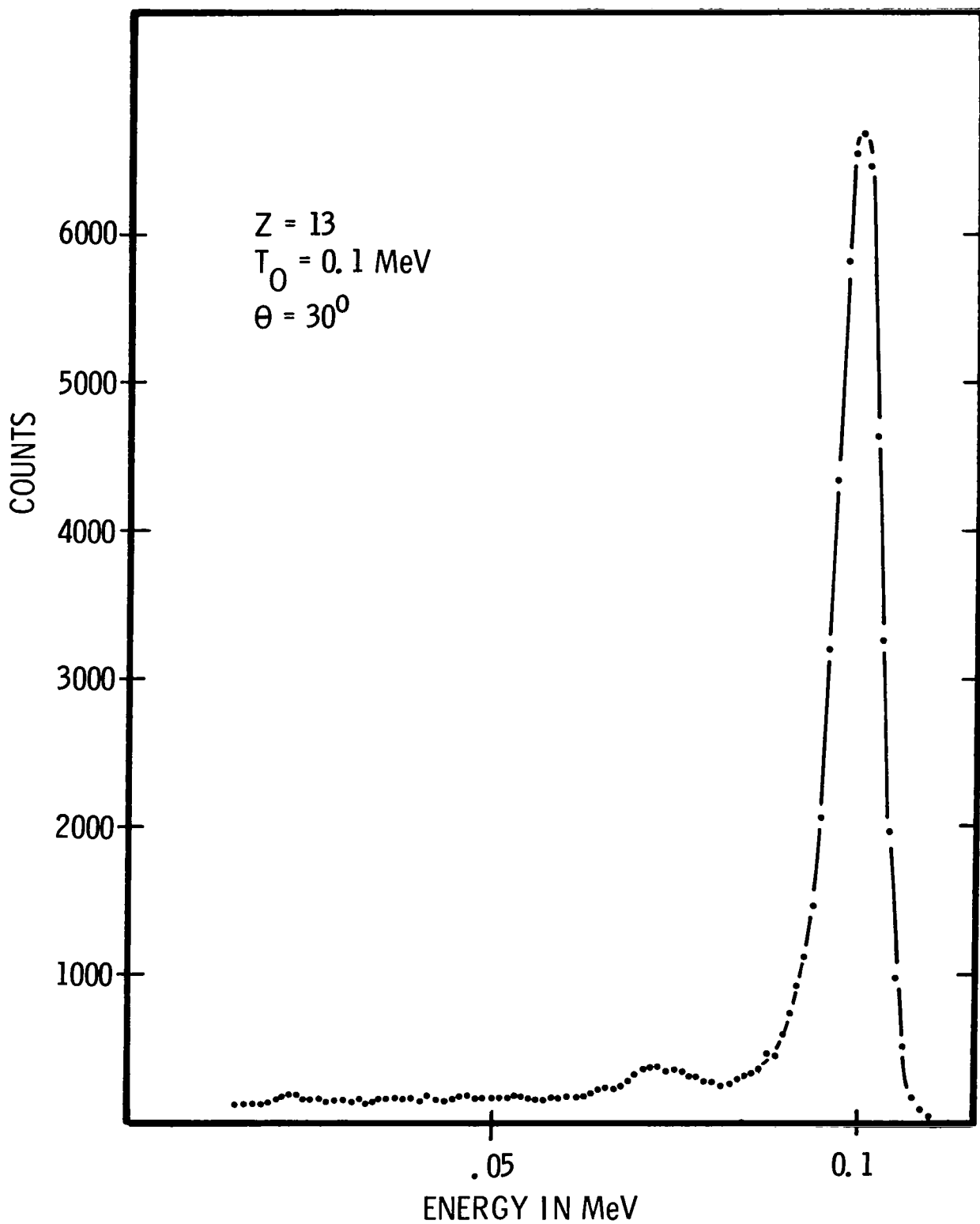
55

FIGURE 5   PULSE HEIGHT DISTRIBUTION TAKEN WITH 1MM LITHIUM—
ION—DRIFT SILICON WAFER AT —25°C

56

Z = 13
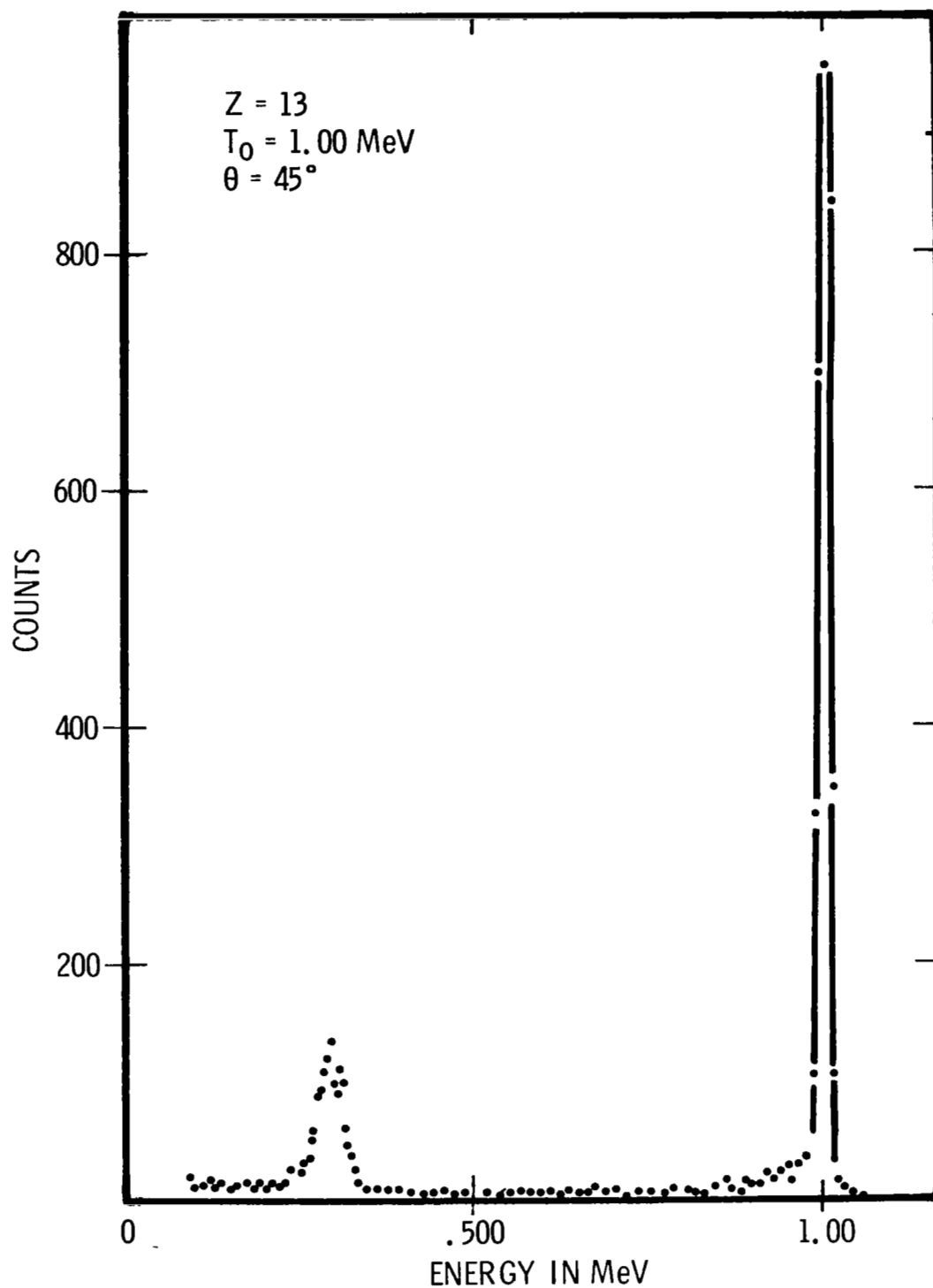T_0 = 1. 00 MeV
θ = 45°

COUNTS

ENERGY IN MeV

FIGURE 6   PULSE HEIGHT DISTRIBUTION TAKEN AT 45° FOR AN INCIDENT
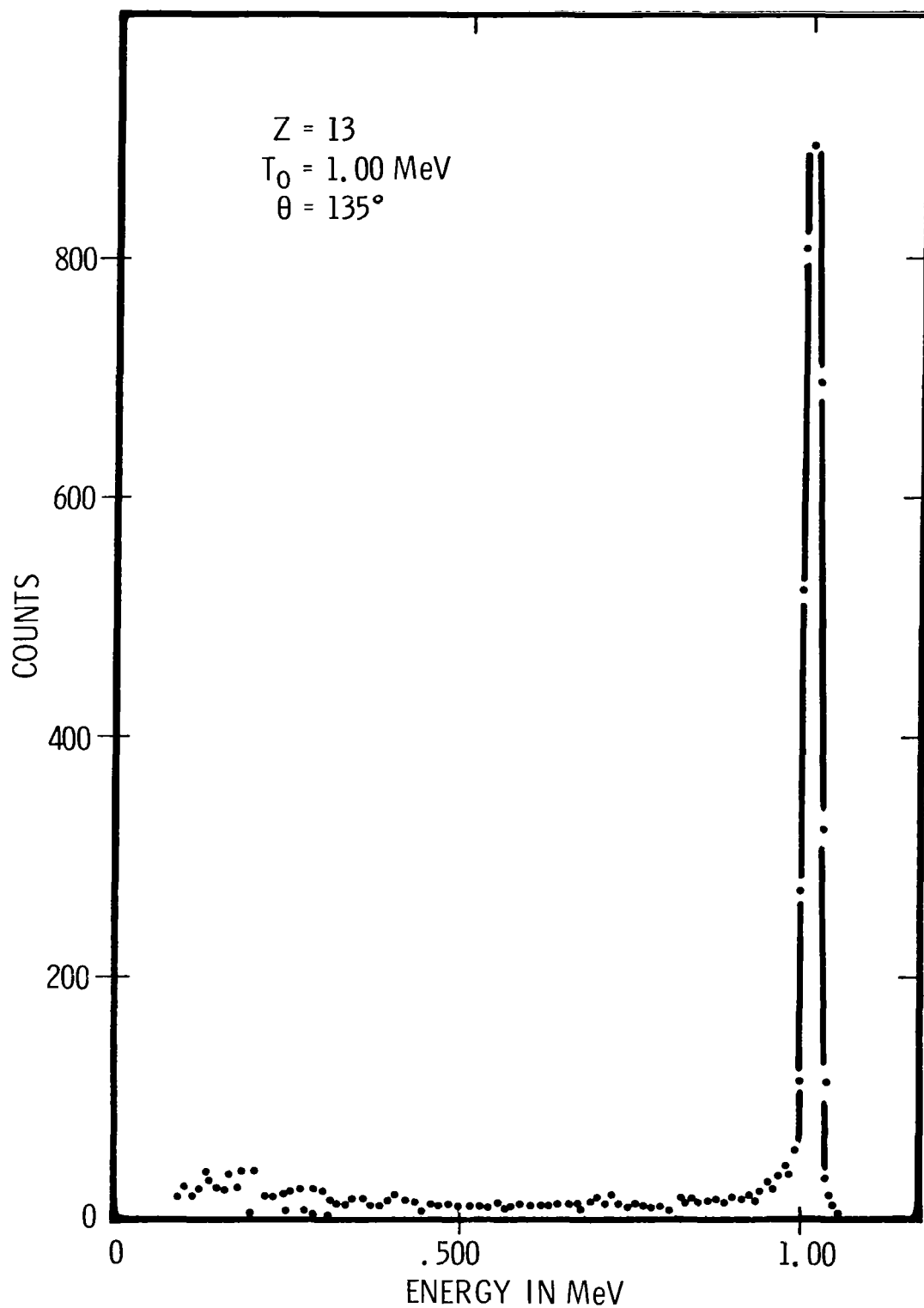ELECTRON ENERGY OF 1 MEV

57

FIGURE 7   PULSE HEIGHT DISTRIBUTION TAKEN AT 135° FOR AN INCIDENT
ELECTRON ENERGY OF 1 MeV

the target slides. Additional determinations of the target thickness were made by measuring the energy loss of the 5.3-MeV alpha particles from a PO-210 source. Relative thicknesses of the foils were obtained, of course, by comparing the experimental cross sections reduced from measurements from various foils. Agreement within experimental error was found between the various types of determinations. Targets of 99.99% purity for use in the transmission experiment were obtained from Reynolds Aluminum Company to specified thicknesses corresponding to 0.2, 0.4 and 0.6, the range of 1-MeV electrons in aluminum.

In order to eliminate possible multiple scattering effects in the thin target measurements, various thicknesses of foils were used. In addition the target was rotated for the scattering angles of 75, 90, and 105 deg so that the path length of the electron in the foil was minimized. The contribution from electrons which were scattered from the chamber walls into the detectors was reduced to negligible levels by means of a thick aluminum baffle placed across the center of the chamber parallel to the plane of the target. x-ray backgrounds were significantly reduced through optimally placed shielding at each scattering angle. These backgrounds were determined by removing the target from the beam and accumulating spectra at each angle. In the thick target measurements x-ray backgrounds were accumulated at each angle by covering the entrance aperture of the detector with a 0.1-inch aluminum disk. These background subtractions ranged from a few percent to a 20% correction.

The solid state detector spectrometers were energy calibrated by measurements of the internal conversion electron lines from the Th (B+C+C") emanating source, Cs-137, and Bi-207. These sources provide well resolved electron lines

of energies from 0.148 to 1.68 MeV and allow the energy calibration of the spectrometer to be carried out to within 1%.

EXPERIMENTAL RESULTS

Single Scattering

The yields of scattered electrons at each scattering angle and incident energy were obtained by removing the response of the electron spectrometer to monoenergetic electrons from the pulse height distributions. The response of the lithium-ion-drift single wafer detectors to monoenergetic electrons was found by two methods. One method was to extract the response from the pulse height distribution obtained by observing the electrons scattered from the scattering foil at a forward scattering angle such as 30 deg. Below 1.5 MeV the contribution to the spectrum from "inelastic" electrons at less than the full pulse height peak is very small. In addition the electron-electron peak is well resolved and can be easily removed from the distribution. The other method was by use of a 180-deg magnetic beta-ray spectrometer, which provided monoenergetic electrons with normal incidence at the detector position in the spectrometer. Detectors used in the experiment were placed in the magnetic spectrometer and their responses were obtained for incident energies from 0.2 to 1.0 MeV. These responses were found to agree with the responses reduced from the pulse height distributions due to scattered electrons. Fig. 8 shows quantitatively the results of the response measurements from 0.2 to 1 MeV for a 2-mm and a 3-mm detector by both of these methods. In the figure the fraction of the response corresponding to pulse height resulting from less than the full energy deposition in the detector is plotted as a function of incident

NUMBER LOSING $<T_0$/NUMBER INCIDENT

□ VAN DE GRAAFF

○
● } β-RAY SPECTROMETER

2MM DETECTOR
WITH 0. 08 IN. APERTURE

3MM DETECTOR
WITH 0. 14 IN. APERTURE

.35
.30
.25
.20
.15
.10
.5
0

0   0.1   0.2   0.3   0.4   0.5   0.6   0.7   0.8   0.9   1.0
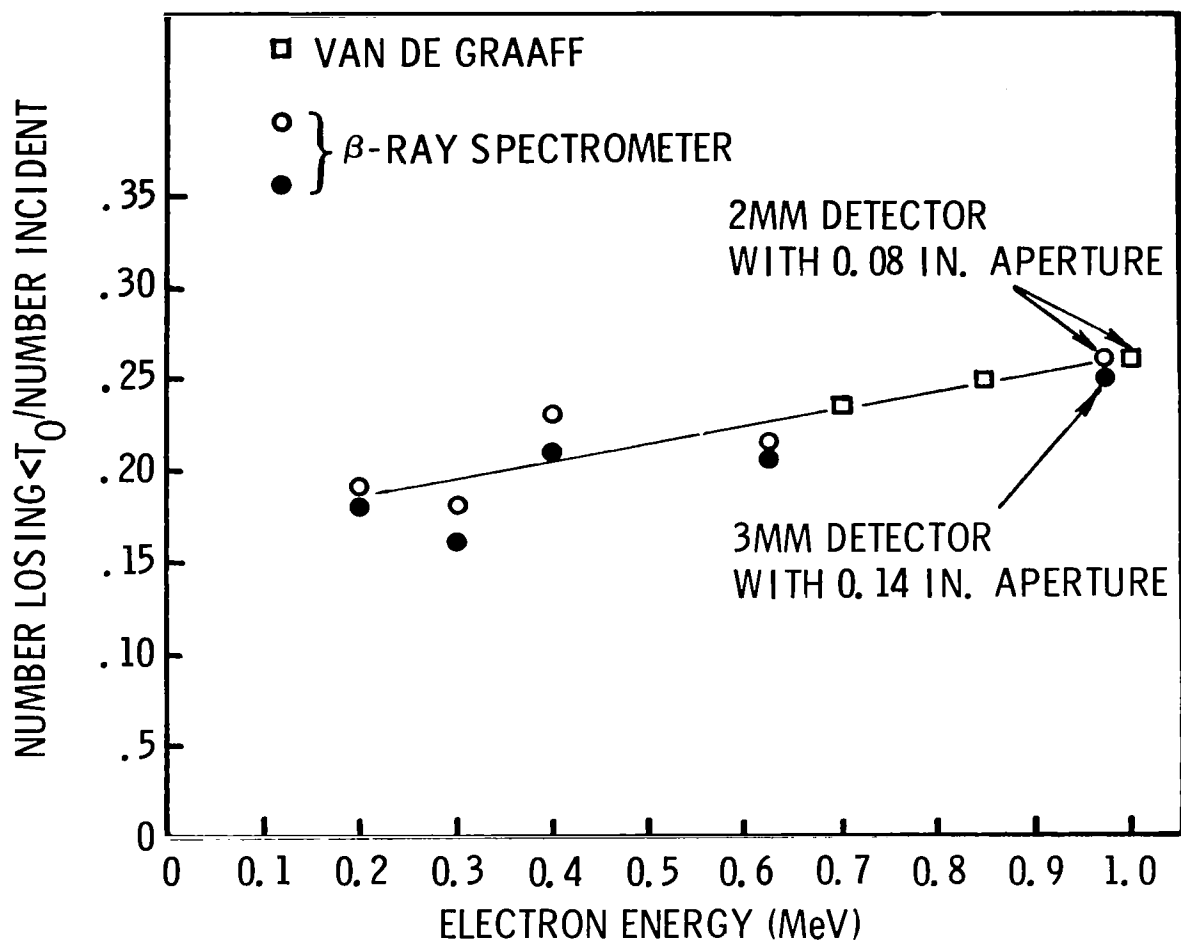
ELECTRON ENERGY (MeV)

FIGURE 8   FRACTION OF DETECTOR RESPONSE WITH PULSE HEIGHT
LESS THAN GAUSSIAN PEAK

energy. In the determination of the yield of scattered electrons, from which cross section values were obtained, the number of electrons corresponding to the full energy pulse height were obtained and corrected for the number of electrons registering less than the pulse height corresponding to the full energy. At the energies above 1.0 MeV all corrections of this type were obtained from the pulse height distributions of the scattered electron spectrum at 30 deg. Thus, the correction to the yield in the full energy line above 1.0 MeV has been obtained by integrating the pulse height spectrum at 30 deg for a given incident energy after removing the peak due to electron-electron scattering and applying this correction to the peaks at all the scattering angles for the same bombarding energy.

The experimental cross sections $d\sigma/d\Omega$ were reduced from the measured yields by use of the following relation:

$$d\sigma/d\Omega = \frac{N}{t \, \Delta\Omega \, q}$$

The quantity N is the yield of electrons measured in a known solid angle $\Delta\Omega$ at a given scattering angle. The quantity t is the number of target atoms per square centimeter normal to the beam direction and is determined by the target thickness. The quantity q is the number of electrons incident on the target.

The experimental cross sections were compared to the Mott cross section for a point, unscreened nucleus which has been calculated by Doggett and Spencer.[1] These comparisons are shown in Fig. 9. The figure consists of a plot of the experimental cross sections normalized to the Mott cross section
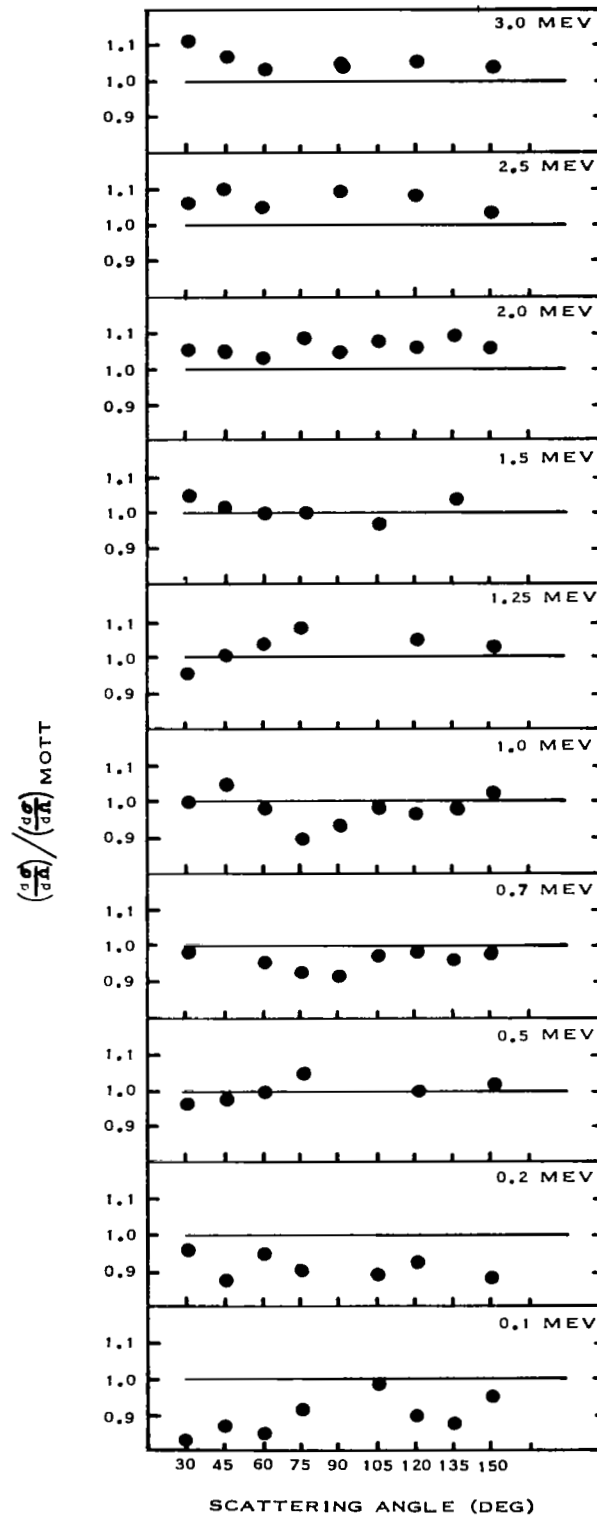
FIGURE 9   EXPERIMENTAL CROSS SECTION NORMALIZED TO THE MOTT
CROSS SECTION

as a function of scattering angle. While the experimental results agree within the experimental error at all energies, it is apparent that the experiment is closer to the theory at energies from 0.5 to 1.5 MeV. The experimental values at 0.1 and 0.2 MeV are below the theoretical predictions while the experimental values at 2.0, 2.5, and 3.0 MeV are above the theoretical predictions.

A conservative estimated error in the experimental values of the cross sections is 10%. The largest contribution to the estimated error is in the target thickness determination, which has an average error estimated to be 4% for the various thicknesses used in this experiment. Since the cross section is very dependent on the scattering angle, considerable error can be introduced by uncertainties in setting the scattering angle. However, in the region of scattering angle from 20 to 60 deg at all energies it was possible to monitor the energy of the electron-electron peak. The energy of this peak is a very sensitive measure of the angle and thus provides a precise means of setting the scattering angle at which measurements are to be made. Additional uncertainties arose from current integration, detector response, energy calibration, and the effective solid angle.

Transmission Measurements

Energy spectra of transmitted electrons with an incident energy of 1.0 MeV were obtained at scattering angles from 0 to 90 deg for aluminum slabs of 0.11, 0.22, and 0.33 g/cm^2. Experimental energy spectra are shown in Figures 10 through 18 along with the calculated spectra of Berger at three angles for each slab thickness. These spectra were derived from the measured pulse height spectra by stripping the detector response to monoenergetic electrons from the latter. The response was determined from 0.2 to 1.0 MeV
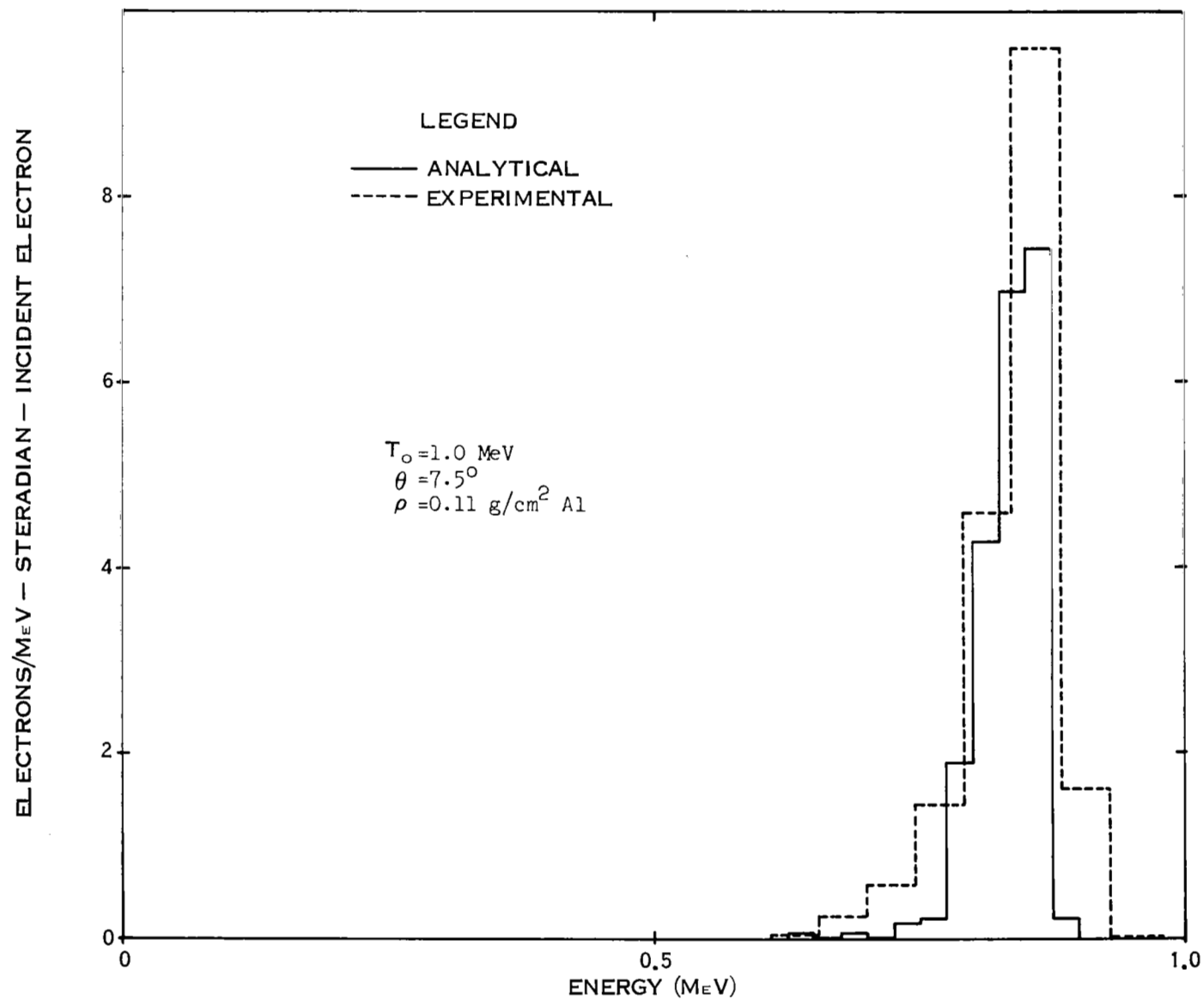
64

FIGURE 10   ENERGY SPECTRA OF TRANSMITTED ELECTRONS FOR 0.2 THE
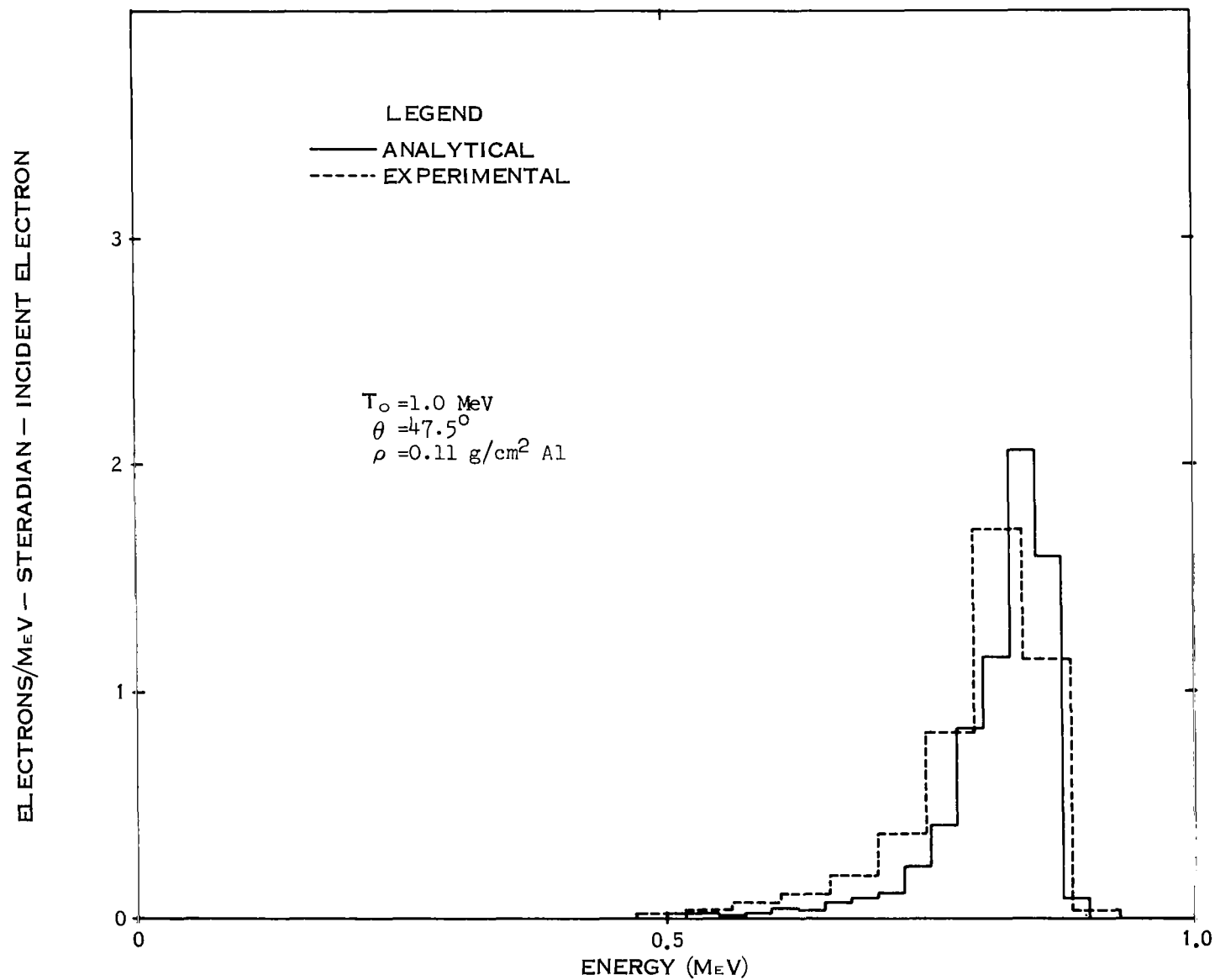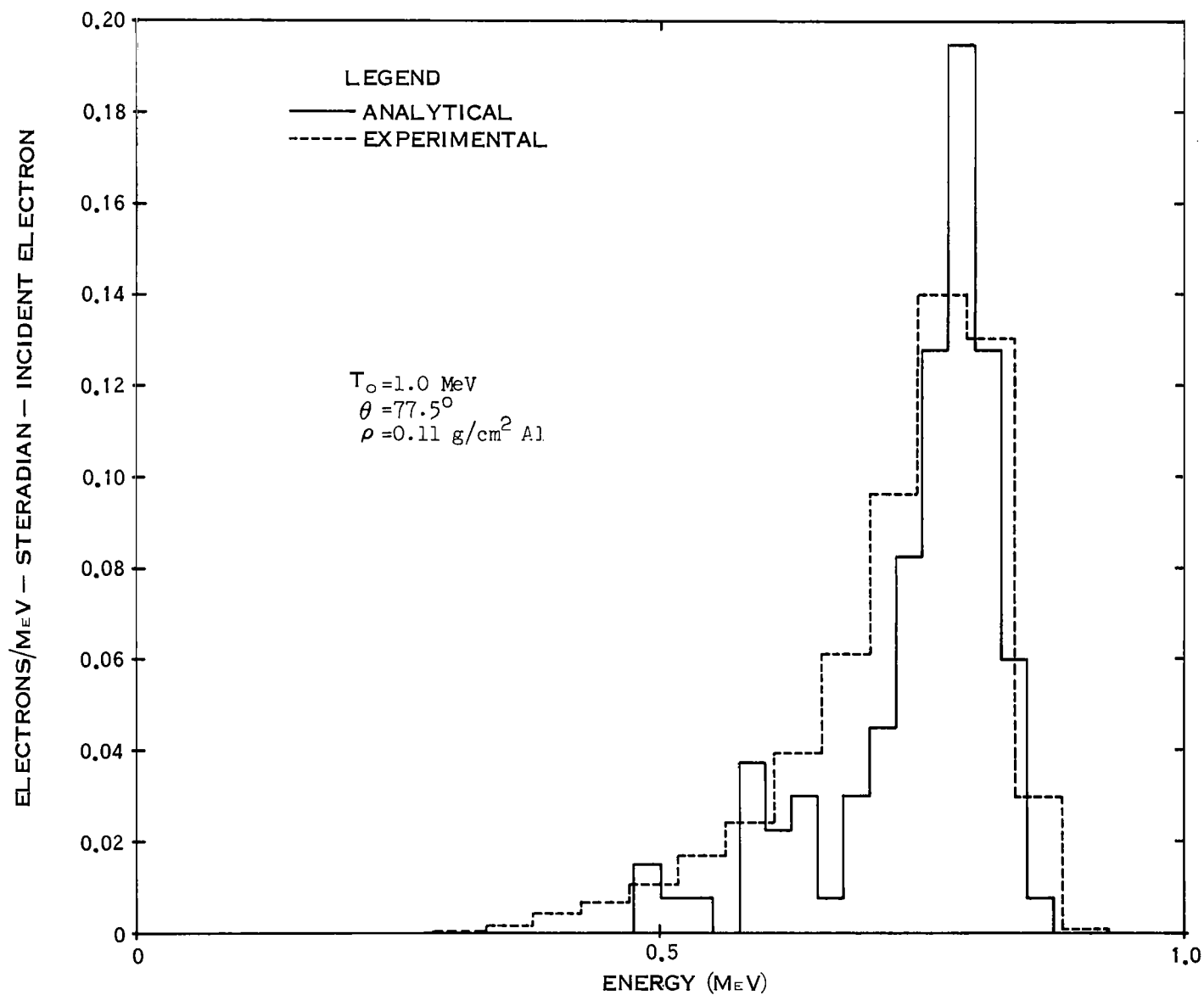RANGE OF 1 MeV ELECTRONS IN ALUMINUM; θ = 7.5°

FIGURE 11   ENERGY SPECTRA OF TRANSMITTED ELECTRONS FOR 0.2 THE
RANGE OF 1 MₑV ELECTRONS IN ALUMINUM; θ = 47.5°

FIGURE 12   ENERGY SPECTRA OF TRANSMITTED ELECTRONS FOR 0.2 THE
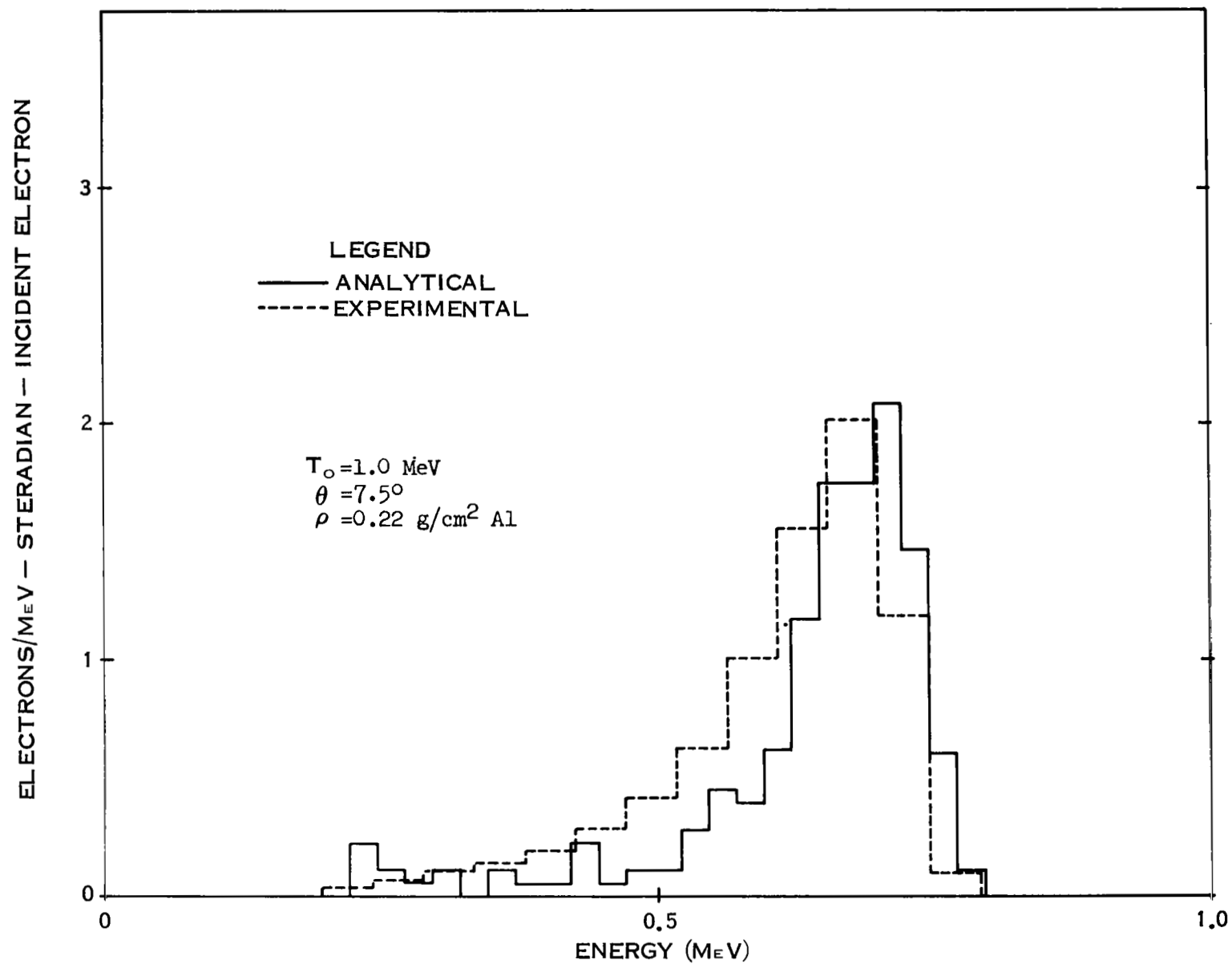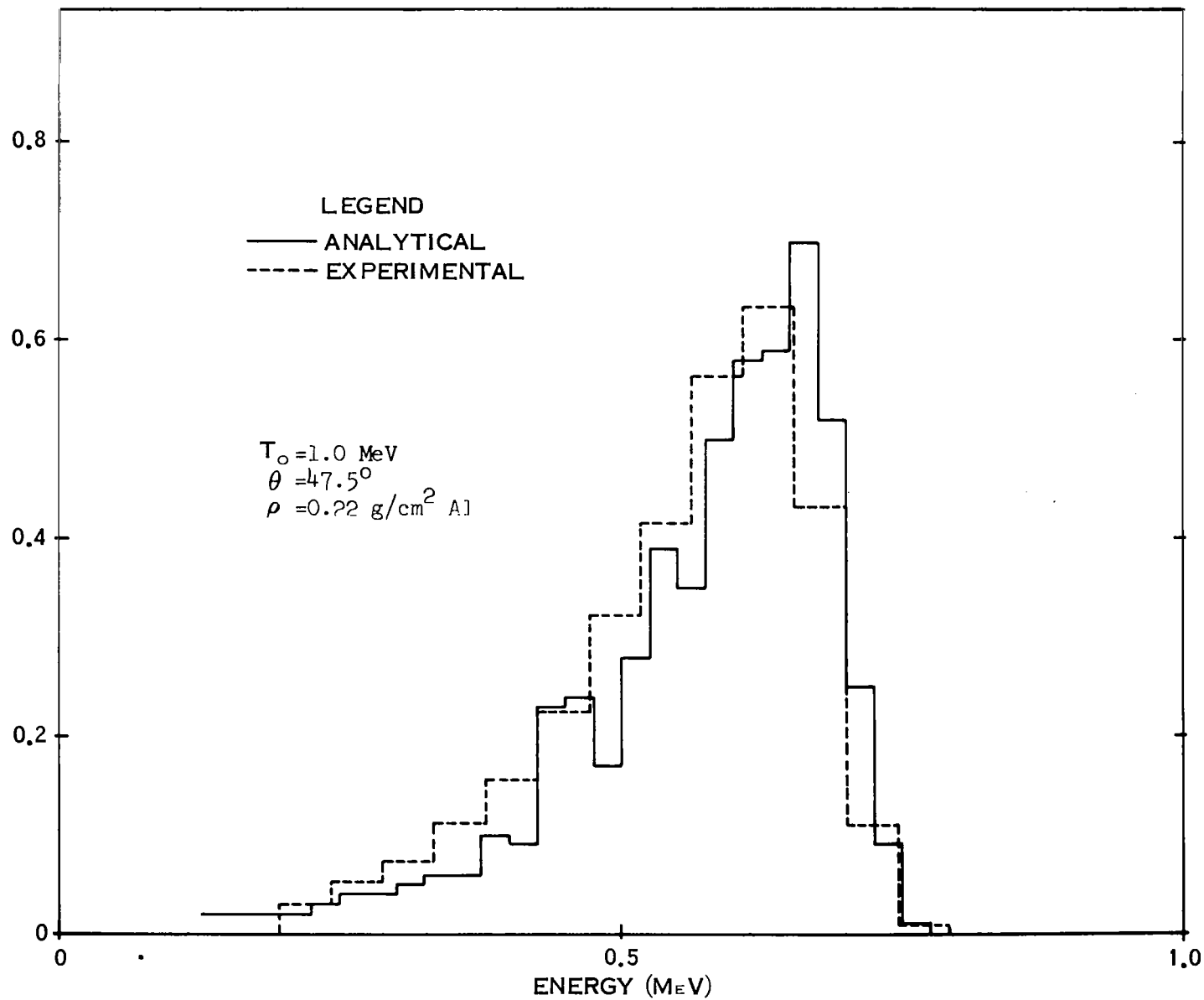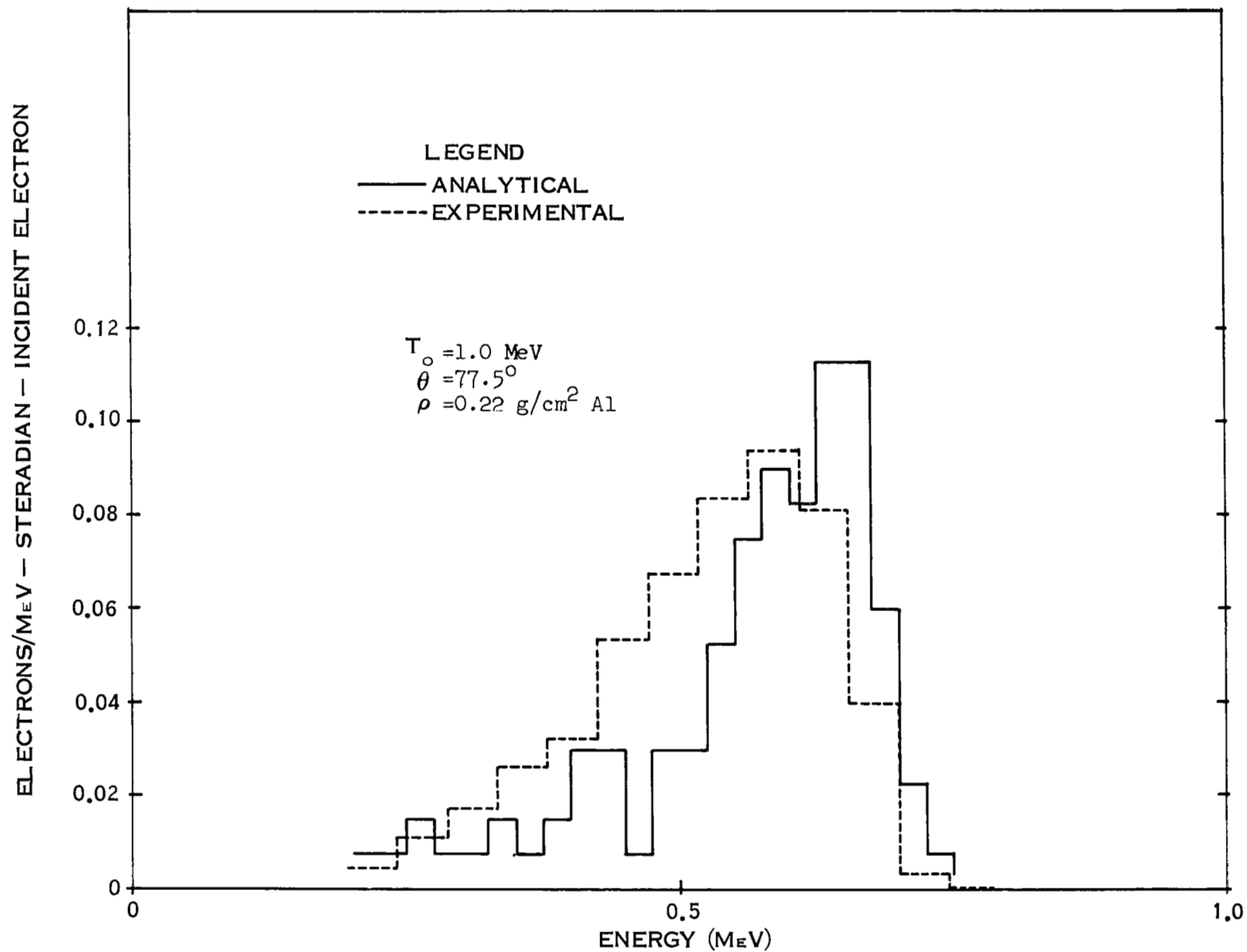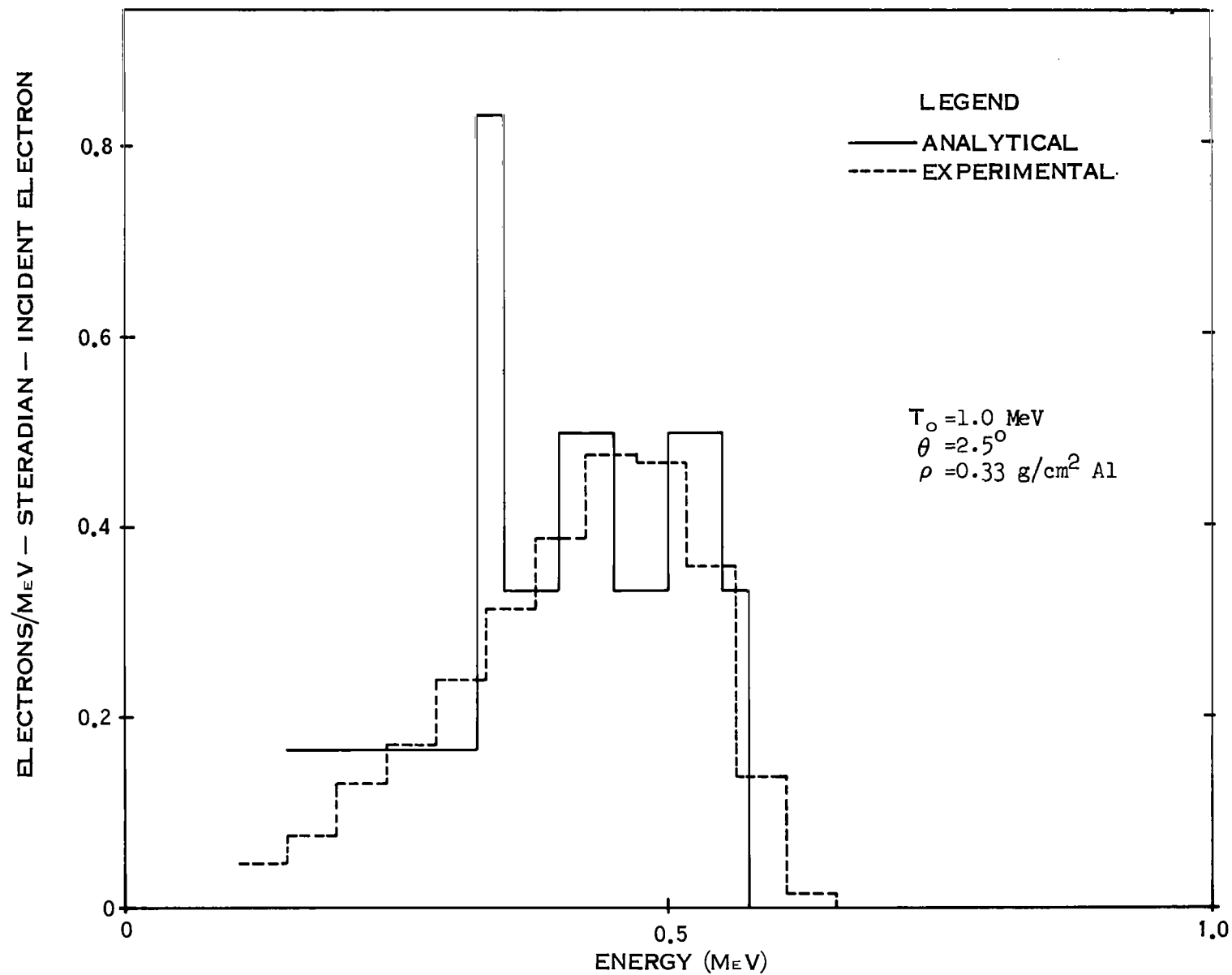RANGE OF 1 MₑV ELECTRONS IN ALUMINUM; θ = 77.5°

FIGURE 13   ENERGY SPECTRA OF TRANSMITTED ELECTRONS FOR 0.4 THE
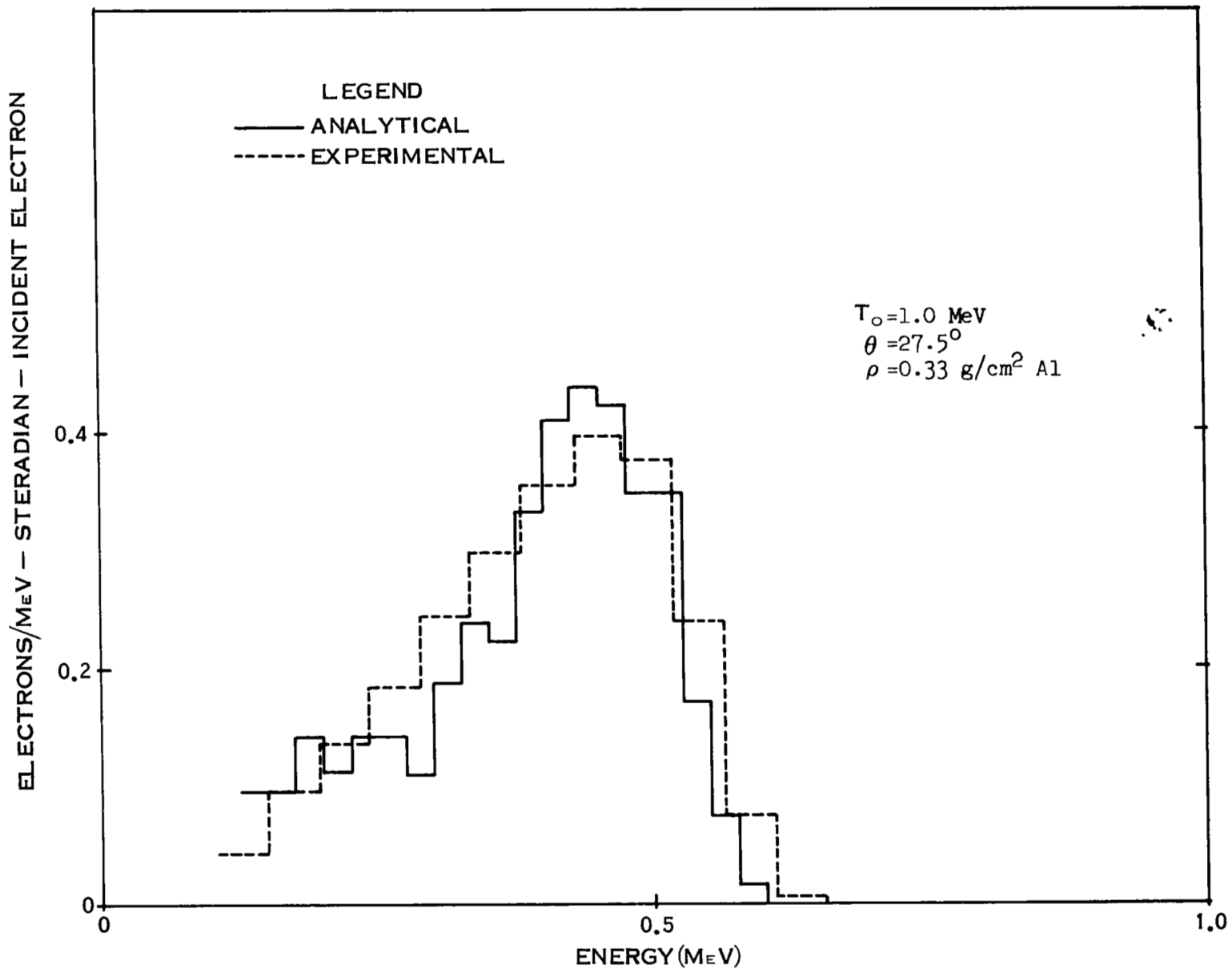RANGE OF 1 MₑV ELECTRONS IN ALUMINUM; θ = 7.5°

FIGURE 14   ENERGY SPECTRA OF TRANSMITTED ELECTRONS FOR 0.4 THE
RANGE OF 1 MᴇV ELECTRONS IN ALUMINUM; θ = 47.5°

FIGURE 15   ENERGY SPECTRA OF TRANSMITTED ELECTRONS FOR 0.4 THE
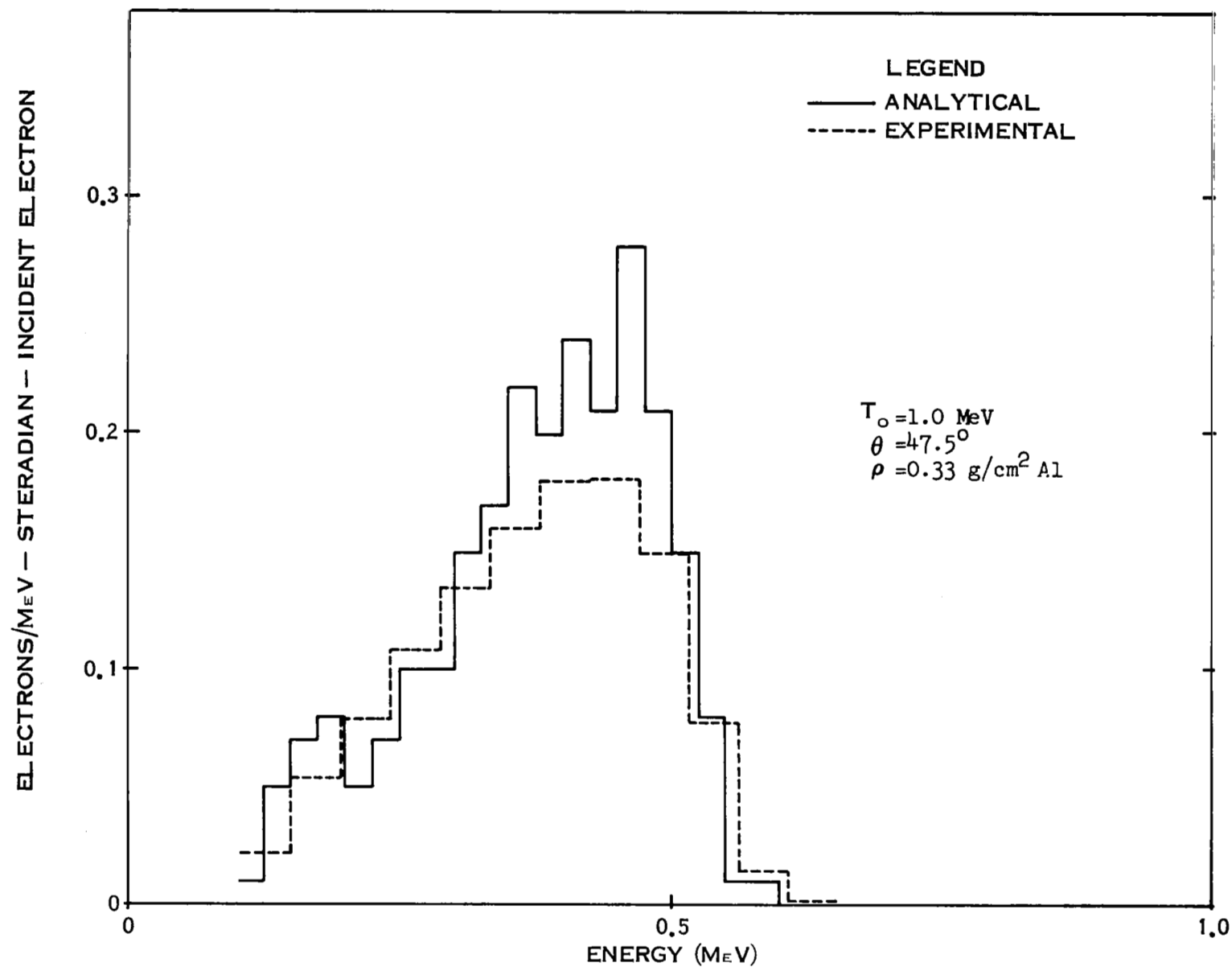RANGE OF 1 M$_E$V ELECTRONS IN ALUMINUM; θ = 77.5°

ELECTRONS/MₑV – STERADIAN – INCIDENT ELECTRON

0.8

0.6

0.4

0.2

0

LEGEND

—— ANALYTICAL

----- EXPERIMENTAL

T_o =1.0 MeV
θ =2.5°
ρ =0.33 g/cm² Al

0   0.5   1.0

ENERGY (MₑV)

FIGURE 16   ENERGY SPECTRA OF TRANSMITTED ELECTRONS FOR 0.6 THE
RANGE OF 1 MₑV ELECTRONS IN ALUMINUM; θ = 2.5°

FIGURE 17   ENERGY SPECTRA OF TRANSMITTED ELECTRONS FOR 0.6 THE RANGE OF 1 MᴇV ELECTRONS IN ALUMINUM; $\theta = 27.5^{\circ}$

FIGURE 18   ENERGY SPECTRA OF TRANSMITTED ELECTRONS FOR 0.6 THE
RANGE OF 1 MᴇV ELECTRONS IN ALUMINUM; θ = 47.5°

by use of the previously described techniques. The stripping technique consisted of fitting the detector response to monoenergetic electrons with a histogram of a width equivalent to the f.w.h.m. of the Gaussian peak. Each pulse height distribution was then divided into energy groups corresponding to the width of the detector response histogram and converted to a spectrum in histogram form by averaging the counts per channel over each energy group. The starting point for this energy group division was always taken with the midpoint of the response histogram at 1.0 MeV. The yield in the highest energy group, or bin, in which counts appeared was increased by the percentage of counts that appeared in the low energy tail of the detector response corresponding to the midpoint energy of that bin. The number of counts by which this bin was increased was divided by the remaining number of bins back to zero energy. This quotient was subtracted from each of the remaining bins since the low energy tail is nearly constant in yield back to zero energy. This stripping operation was then repeated on the second highest energy bin, etc., until a bin yield became insignificant or the bin including 0.1 MeV was reached. This operation increased the number of electrons in the higher energy portion of the spectrum and reduced the number in the lower energy end. This effect was most prominent where large energy degradation occurred as is illustrated by Figures 19 through 27.

The Monte Carlo analysis was carried out for 12,000 incident electrons, and transmission spectra were calculated above 100 keV for eighteen 5-deg angular increments. Since each spectrum was divided into 25-keV energy bins, as shown in Figures 10 through 18, the bins with the maximum number of electrons in the energy distributions contained counts ranging from 208 at 47.5 deg
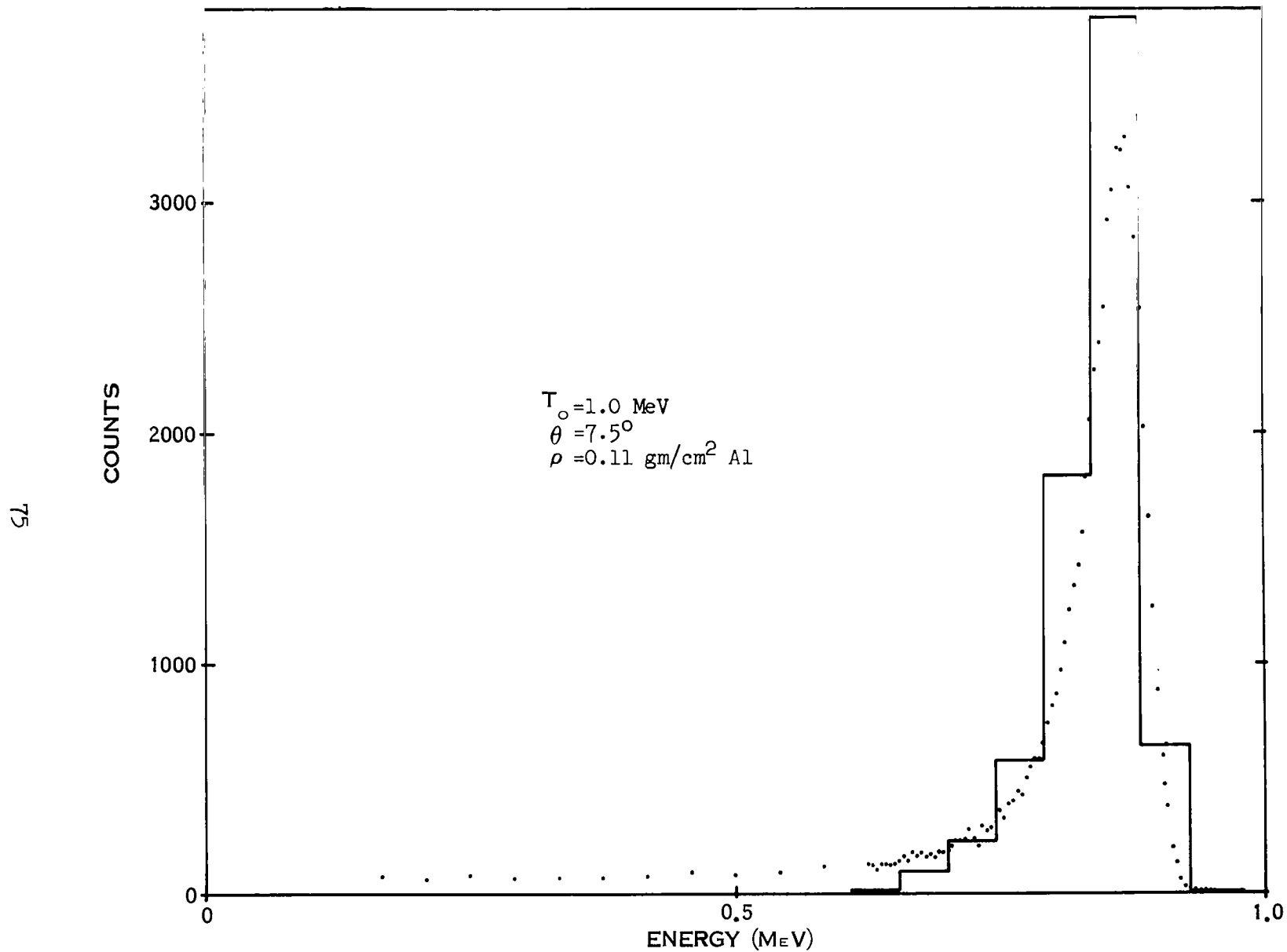
FIGURE 19   COMPARISON OF PULSE HEIGHT AND ENERGY SPECTRA FOR
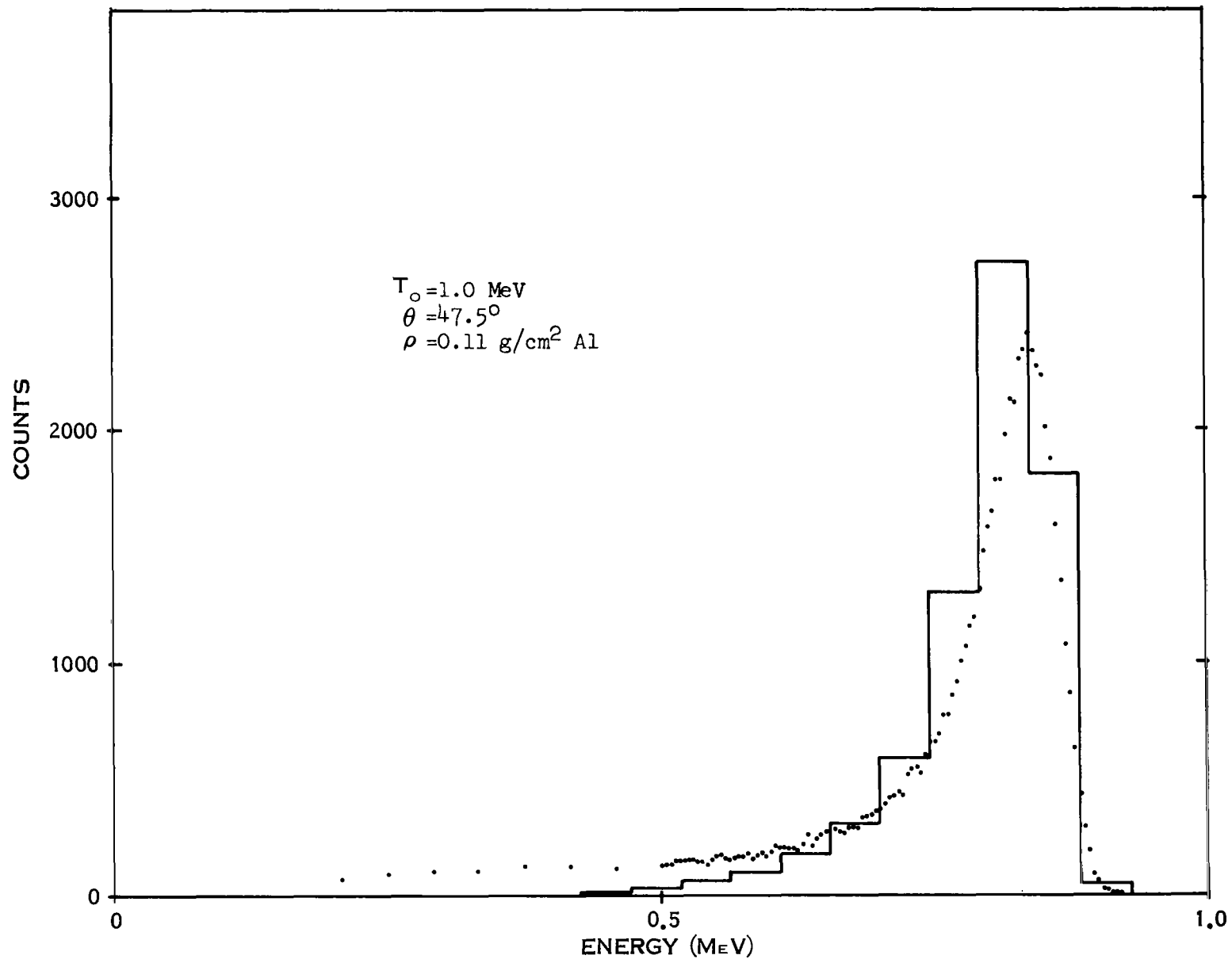0.2 THE RANGE OF 1 MₑV ELECTRONS IN ALUMINUM; θ = 7.5°

$T_o = 1.0$ MeV
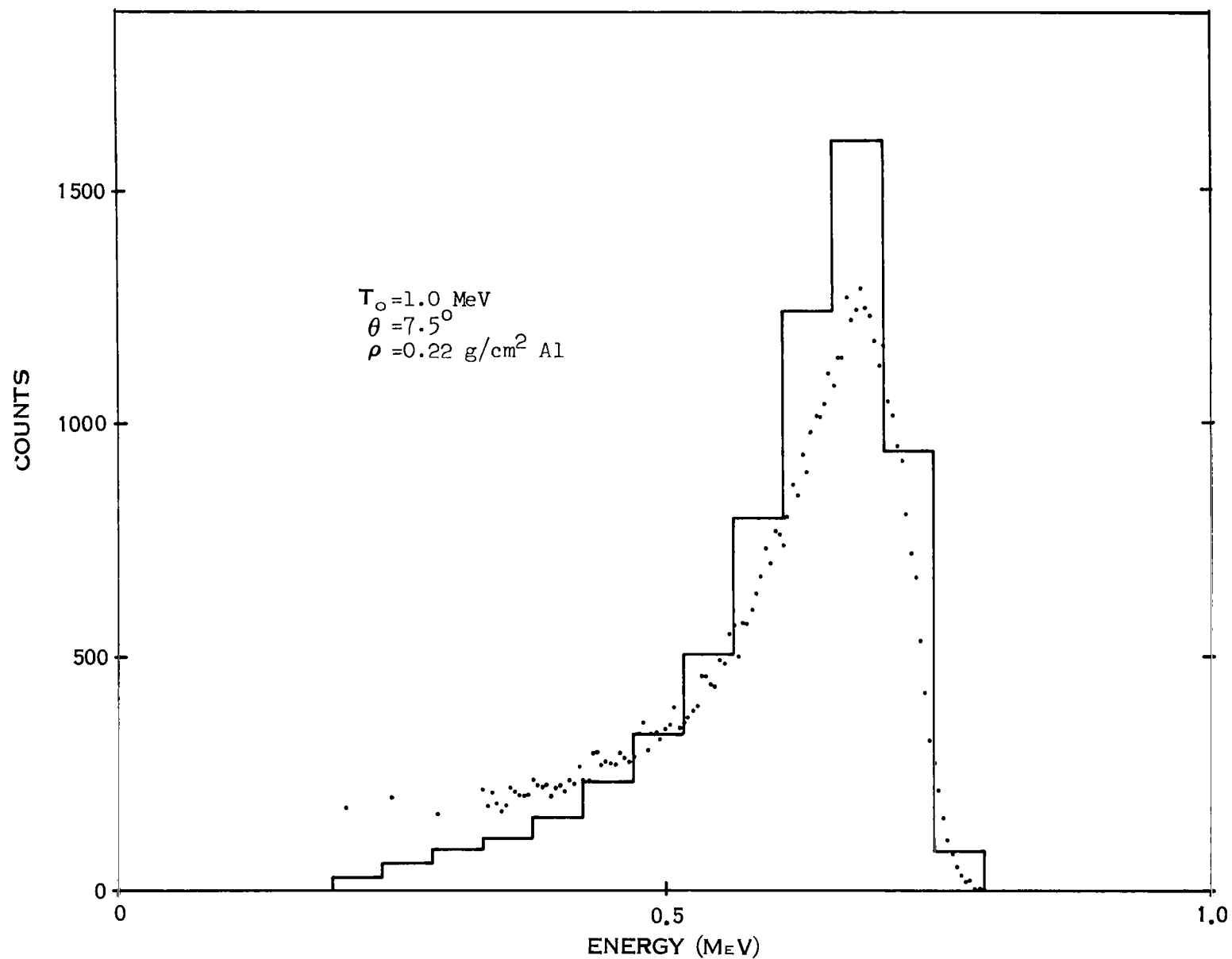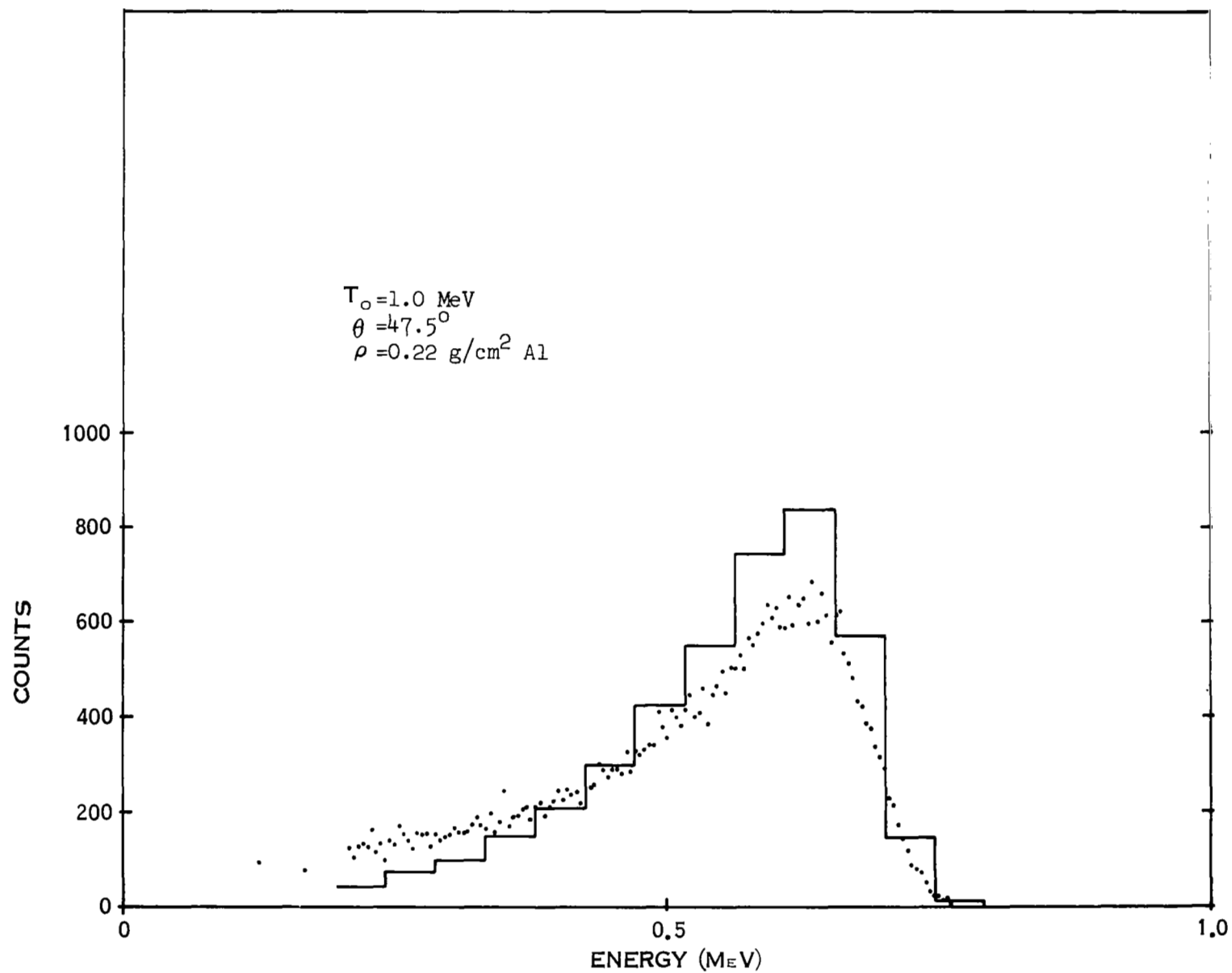$\theta = 47.5^{\circ}$
$\rho = 0.11$ g/cm^2 Al

FIGURE 20   COMPARISON OF PULSE HEIGHT AND ENERGY SPECTRA FOR
0.2 THE RANGE OF 1 M$_E$V ELECTRONS IN ALUMINUM; $\theta = 47.5^{\circ}$
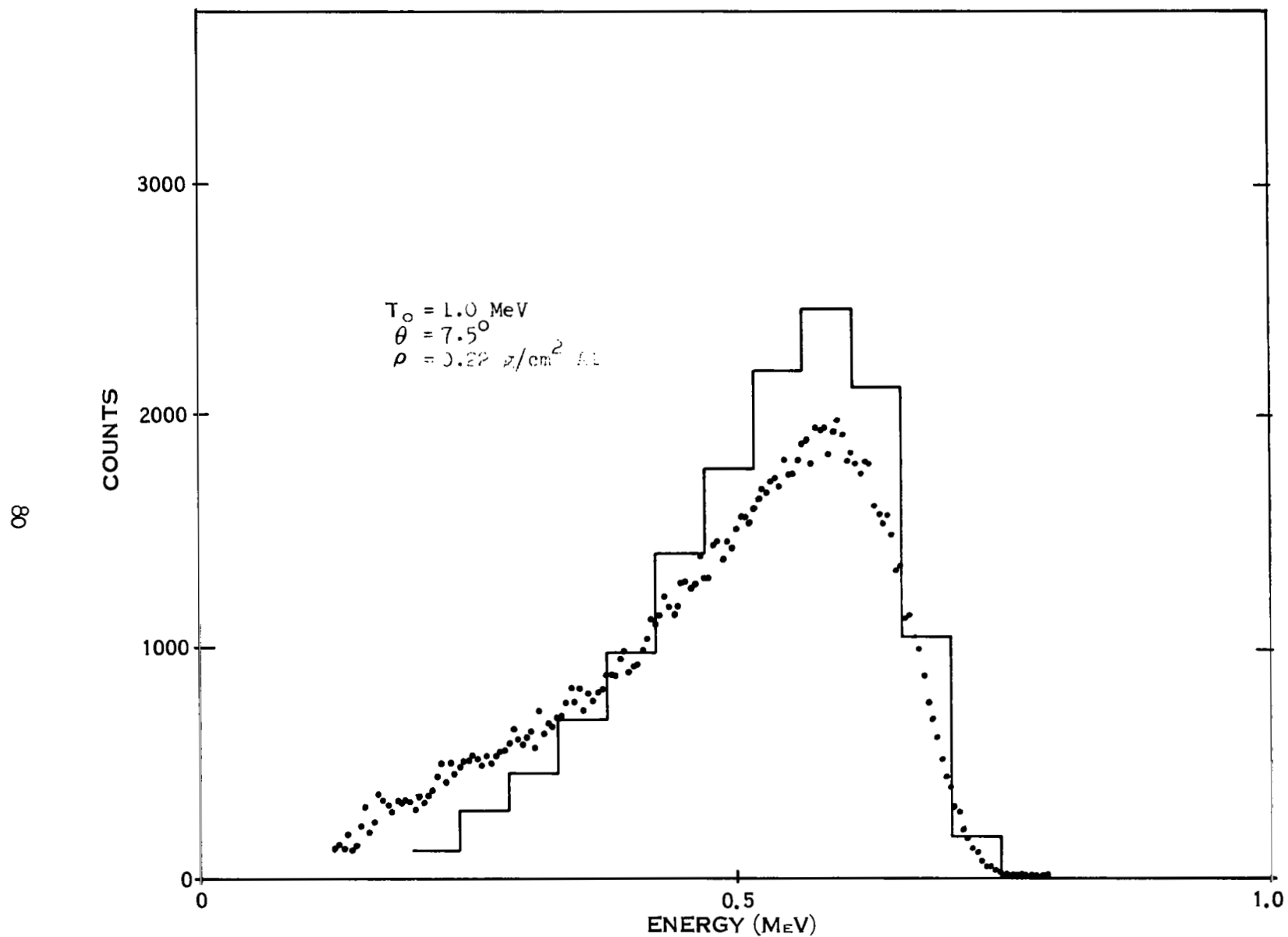
FIGURE 21   COMPARISON OF PULSE HEIGHT AND ENERGY SPECTRA FOR 0.2
THE RANGE OF 1 M$_E$V ELECTRONS IN ALUMINUM; θ = 77.5°

FIGURE 22   COMPARISON OF PULSE HEIGHT AND ENERGY SPECTRA FOR 0.4
THE RANGE OF 1 M$_E$V ELECTRONS IN ALUMINUM; θ = 7.5°

$T_o = 1.0$ MeV
$\theta = 47.5^o$
$\rho = 0.22$ g/cm^2 Al
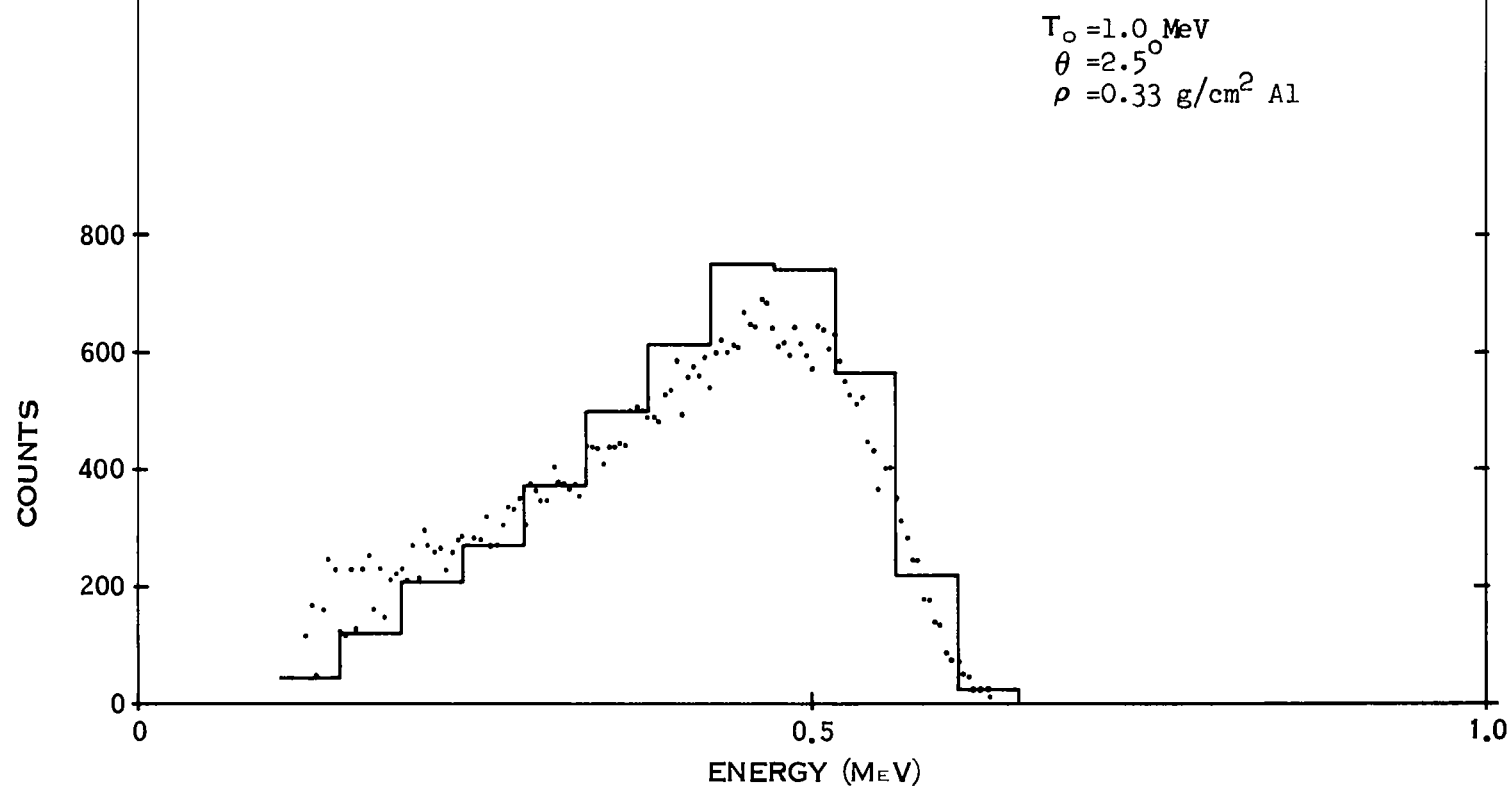
FIGURE 23   COMPARISON OF PULSE HEIGHT AND ENERGY SPECTRA FOR 0.4
THE RANGE OF 1 MeV ELECTRONS IN ALUMINUM; $\theta = 47.5^o$

FIGURE 24   COMPARISON OF PULSE HEIGHT AND ENERGY SPECTRA FOR 0.4
THE RANGE OF 1 MₑV ELECTRONS IN ALUMINUM; θ = 77.5°

FIGURE 25   COMPARISON OF PULSE HEIGHT AND ENERGY SPECTRA FOR 0.6
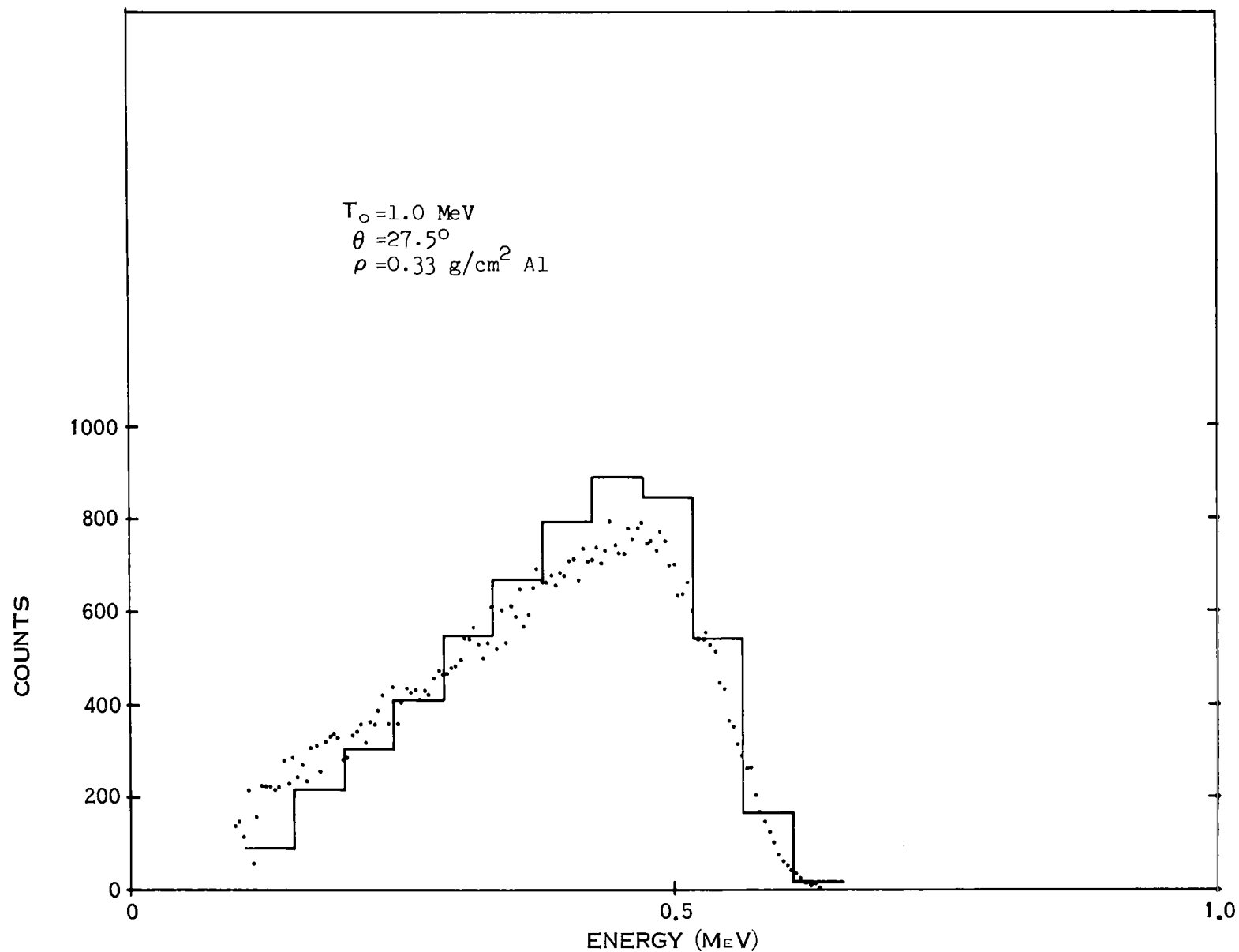THE RANGE OF 1 MₑV ELECTRONS IN ALUMINUM; θ = 2.5°

FIGURE 26   COMPARISON OF PULSE HEIGHT AND ENERGY SPECTRA FOR 0.6
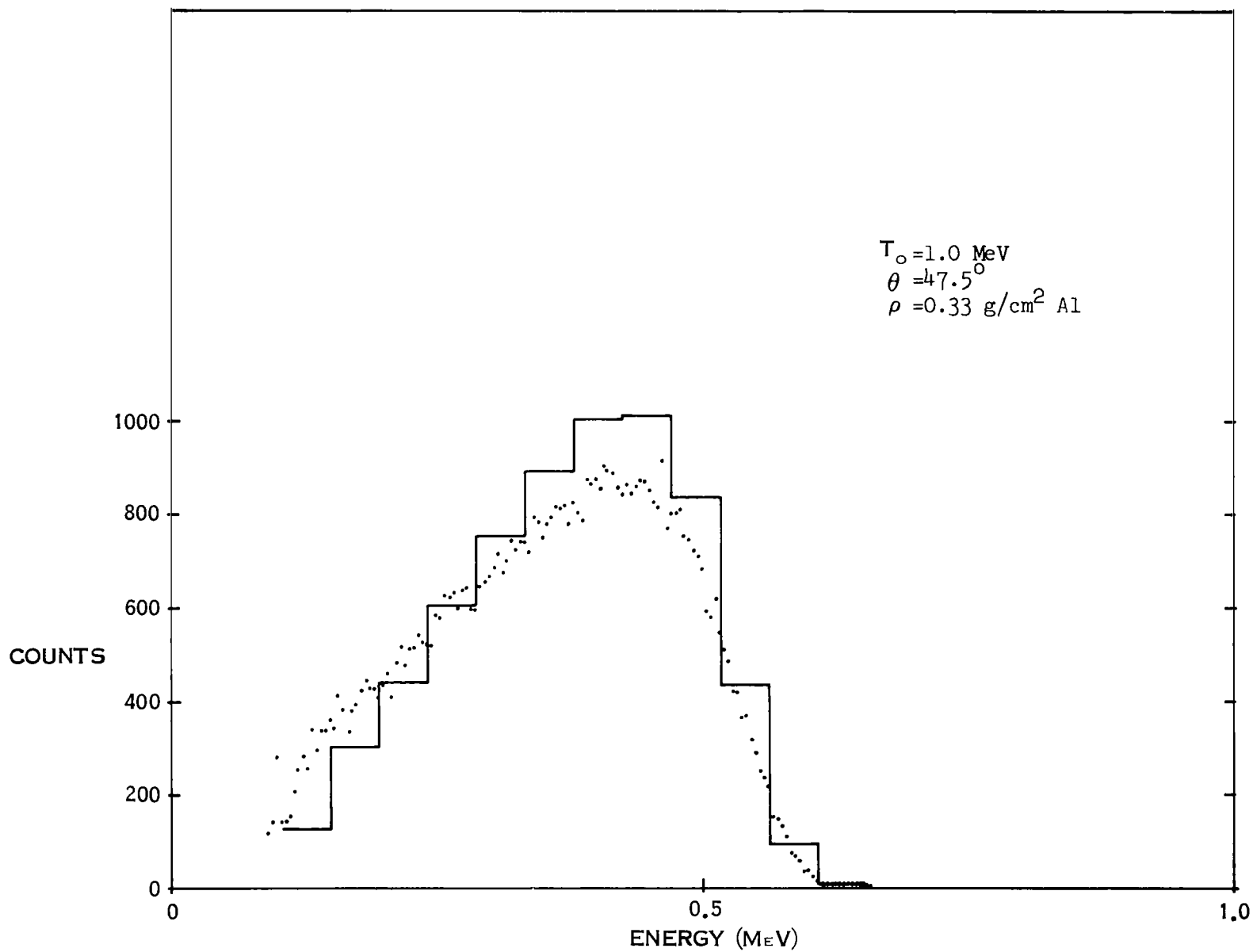THE RANGE OF 1 MₑV ELECTRONS IN ALUMINUM; θ = 27.5°

FIGURE 27   COMPARISON OF PULSE HEIGHT AND ENERGY SPECTRA FOR 0.6
THE RANGE OF 1 MᴇV ELECTRONS IN ALUMINUM; θ = 47.5°

for the 0.11 g/cm^2 slab to only 3 at 2.5 deg for the 0.33 g/cm^2 slab. There-fore, the fluctuations in the calculated spectra arise from the limited number of electron histories which were analyzed. Even so the agreement between the shapes of the Monte Carlo calculated and the measured spectra is generally good.

A comparison of the most probable energy loss of the transmitted electrons is shown by the plot in Fig. 28. Here the most probable energy loss is plotted as a function of scattering angle for each slab thickness. The limitations in making a comparison of this type arise from the fact that the peaks of these energy distributions are broad. The 25-keV bin width of the calculated spectra sets the minimum uncertainty with which it is possible to determine the energy loss.

Also of interest are the comparative yields at each angle for a given thick-ness. Inspection of the areas under the histograms in Figures 10 through 18 reveals close agreement for most of the nine spectra shown. A more sensitive comparison of these respective yields is shown in Figures 29 through 31. Here the angular distributions, or the total number of electrons per steradian per incident electron versus scattering angle, are plotted for each slab thickness. These graphs show the results of an integration over energy of each of the twenty measured spectra along with an integration over energy of each of the calculated spectra from 0.1 to 1.0 MeV. The measured and calculated yields agree to within the limits of both techniques, the estimated experimental error being 10%, except possibly at the 0.11 gm/cm^2 slab thickness. Here, for the forward angles, the analytical yields fall about 35% below the measured values. This difference may be partly due to the additional error introduced
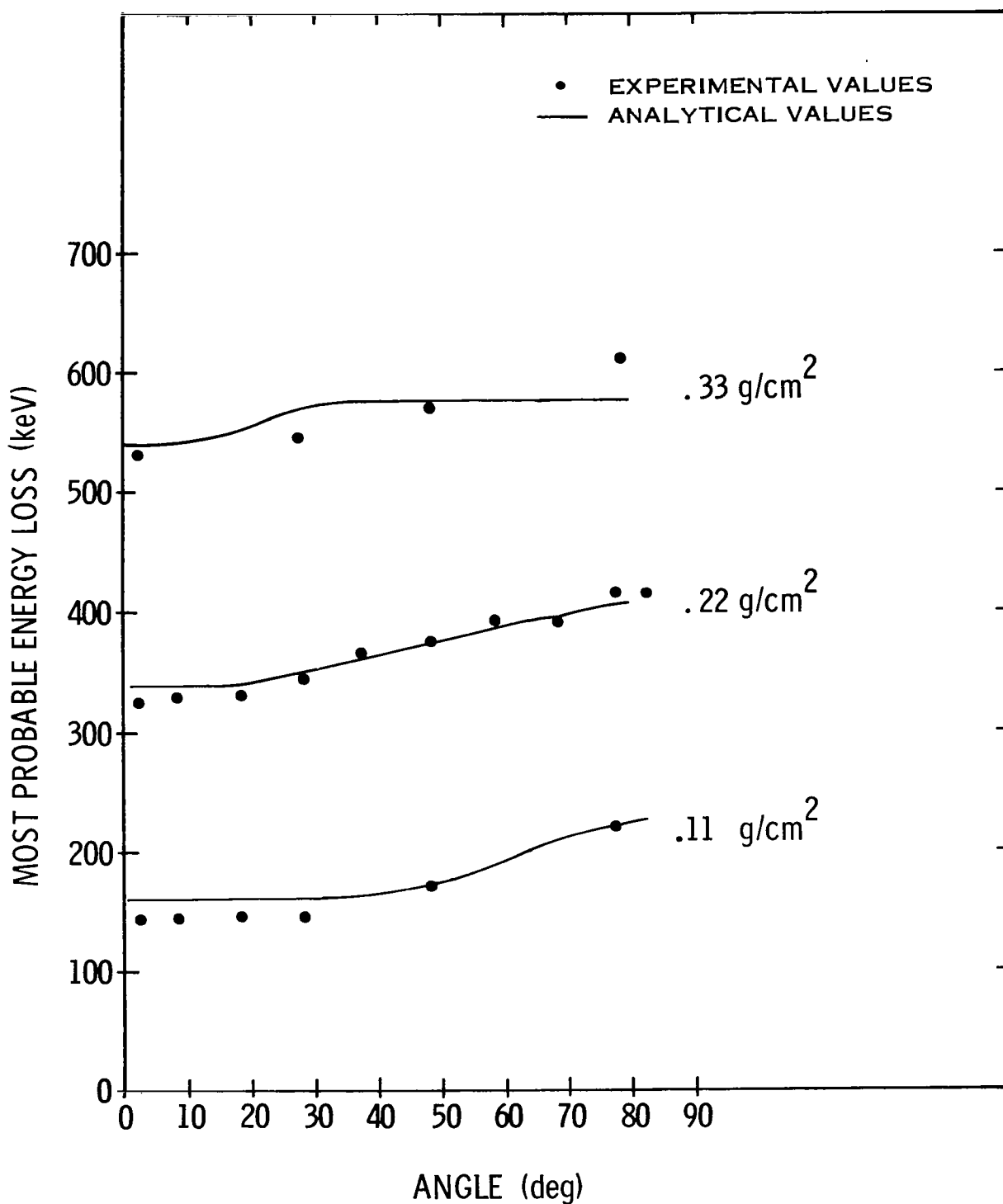
FIGURE 28   MOST PROBABLE ENERGY LOSS IN ALUMINUM OF ELECTRONS
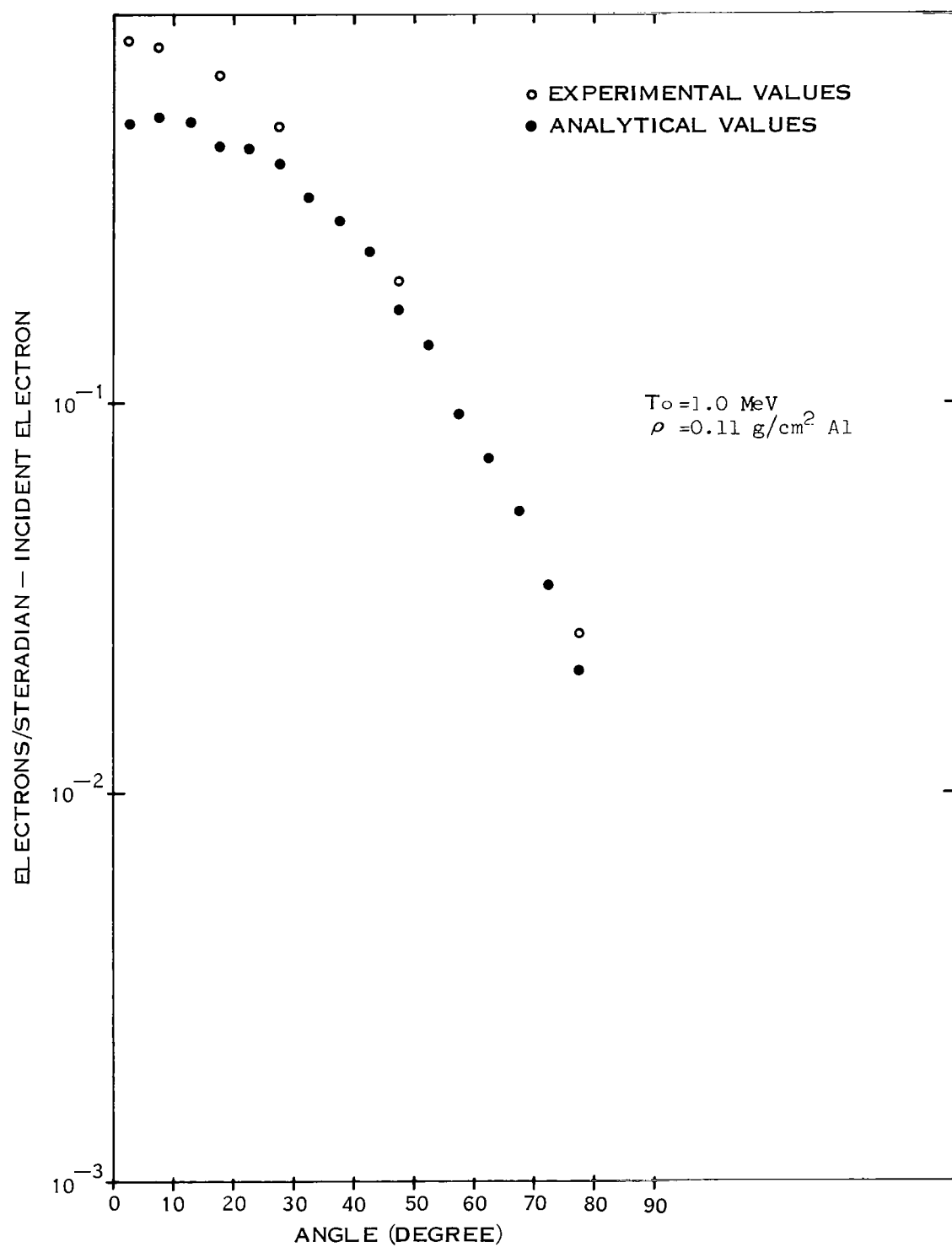WITH AN INCIDENT ENERGY OF 1 MεV

85

FIGURE 29   COMPARISON OF EXPERIMENTAL AND ANALYTICAL ANGULAR
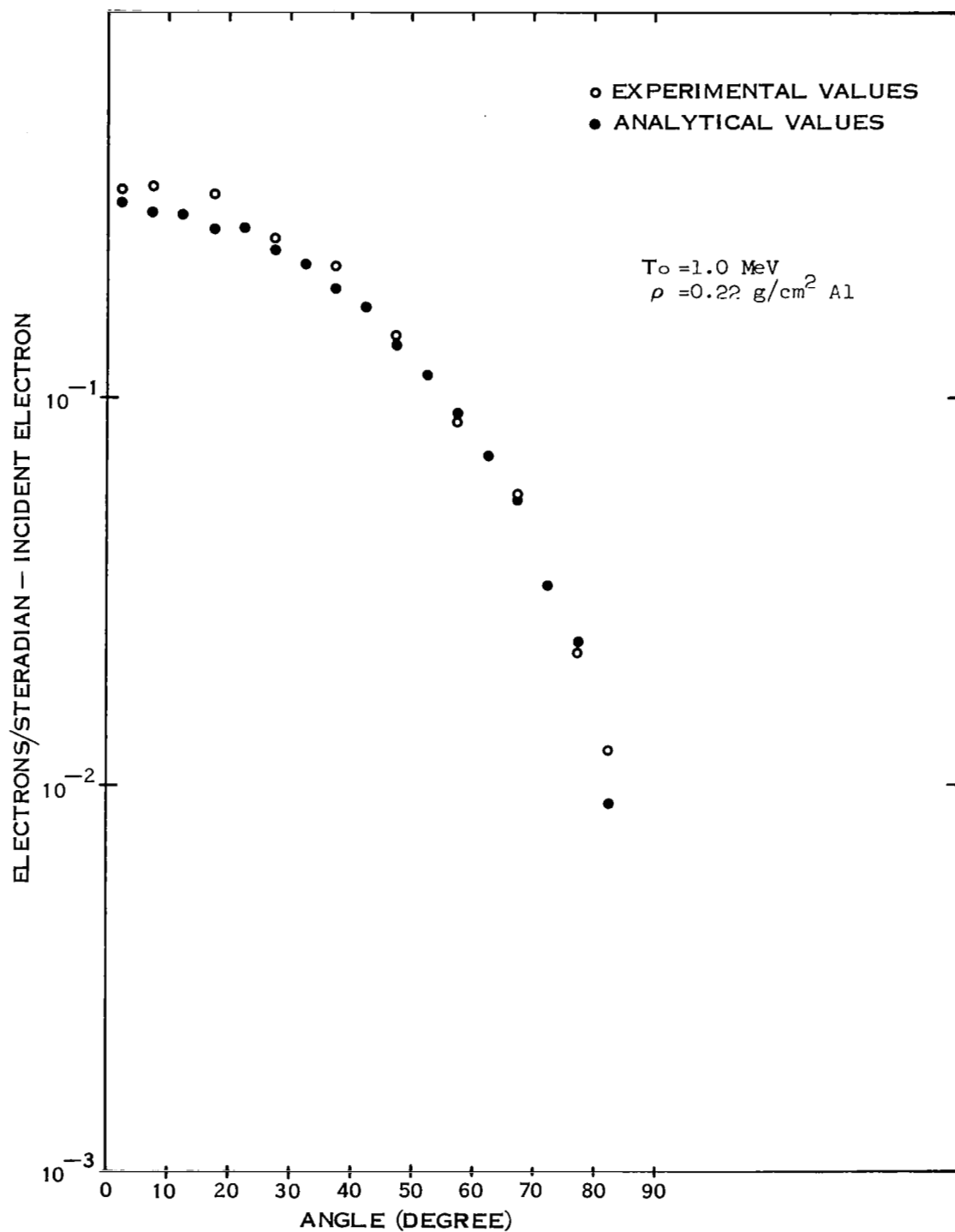DISTRIBUTIONS; ρ = 0.11 G/CM^2 AL

FIGURE 30   COMPARISON OF EXPERIMENTAL AND ANALYTICAL ANGULAR
DISTRIBUTIONS; ρ = 0.22 G/CM^2 AL
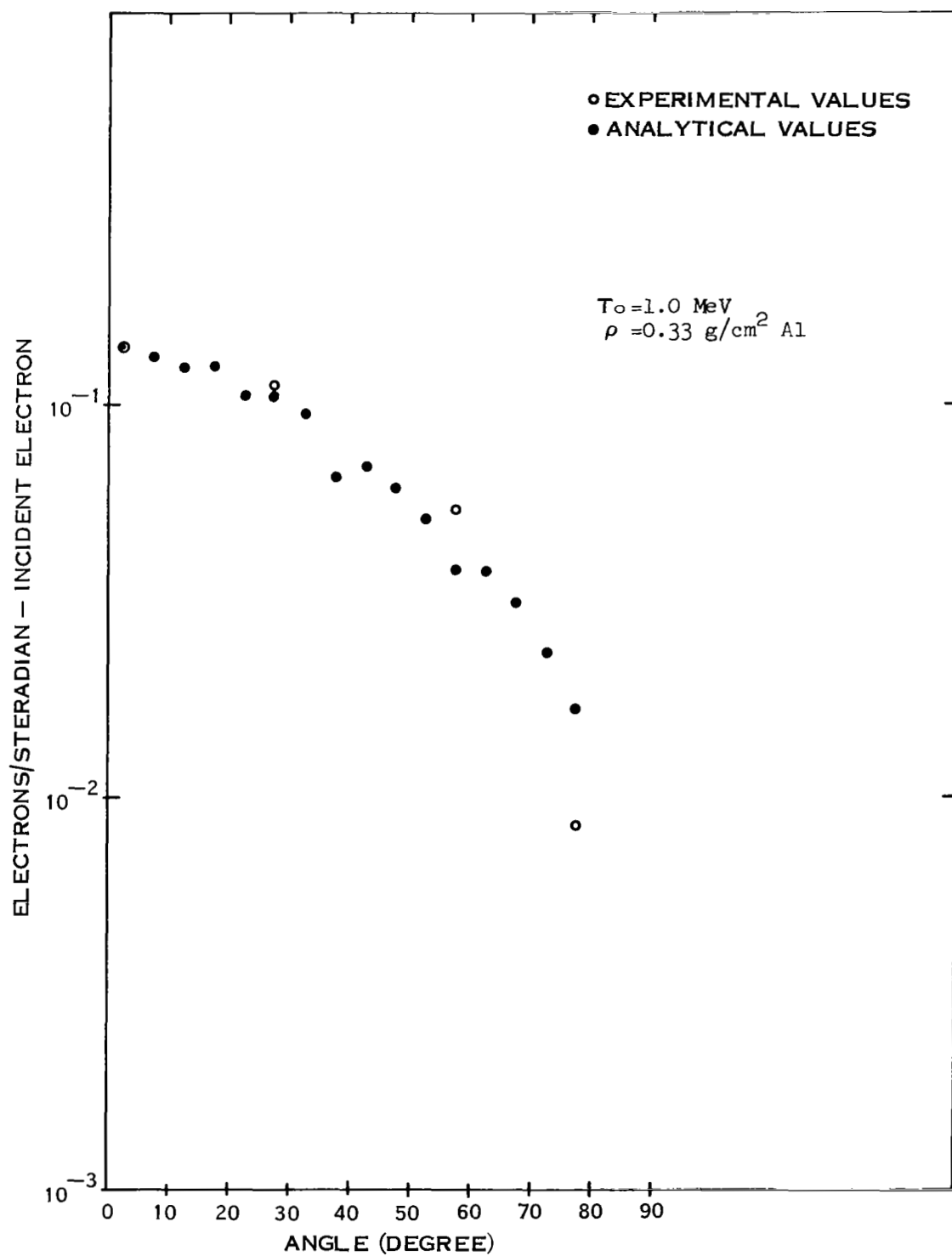
FIGURE 31   COMPARISON OF EXPERIMENTAL AND ANALYTICAL ANGULAR
DISTRIBUTIONS; ρ = 0.33 G/CM^2 AL

in integrating the lower beam currents (of the order of 10^{-11} amps) necessary to prevent saturation of the counting system. The experimental error at these angles could be twice that where beam currents of an order of magnitude higher were possible. At larger angles, for all three slab thicknesses, the analytical yields become more uncertain due to the decreasing number of electrons in a spectrum. The statistical error alone at these angles approaches 15%.

REFERENCES

1. J. A. Doggett and L. V. Spencer, Phys. Rev. <u>103</u>, 1597 (1956).

2. Shin-R Lin, Phys. Rev. <u>133</u>, A965 (1964).

3. Private communications.